

VOL. 9 NO. 2 FEBRUARY 1965

PUBLISHED MONTHLY

Journal of

ELECTROANALYTICAL CHEMISTRY

*International Journal Dealing with all Aspects
of Electroanalytical Chemistry,
Including Fundamental Electrochemistry*

EDITORIAL BOARD:

J. O'M. BOCKRIS (Philadelphia, Pa.)
B. BREYER (Sydney)
G. CHARLOT (Paris)
B. E. CONWAY (Ottawa)
P. DELAHAY (Baton Rouge, La.)
A. N. FRUMKIN (Moscow)
L. GIERST (Brussels)
M. ISHIBASHI (Kyoto)
W. KEMULA (Warsaw)
H. L. KIES (Delft)
J. J. LINGANE (Cambridge, Mass.)
G. W. C. MILNER (Harwell)
J. E. PAGE (London)
R. PARSONS (Bristol)
C. N. REILLEY (Chapel Hill, N.C.)
G. SEMERANO (Padua)
M. VON STACKELBERG (Bonn)
I. TACHI (Kyoto)
P. ZUMAN (Prague)

E L S E V I E R

GENERAL INFORMATION

See also Suggestions and Instructions to Authors which will be sent free, on request to the Publishers.

Types of contributions

- (a) Original research work not previously published in other periodicals.
- (b) Reviews on recent developments in various fields.
- (c) Short communications.
- (d) Bibliographical notes and book reviews.

Languages

Papers will be published in English, French or German.

Submission of papers

Papers should be sent to one of the following Editors:

Professor J. O'M. BOCKRIS, John Harrison Laboratory of Chemistry,
University of Pennsylvania, Philadelphia 4, Pa., U.S.A.

Dr. R. PARSONS, Department of Chemistry,
The University, Bristol 8, England.

Professor C. N. REILLEY, Department of Chemistry,
University of North Carolina, Chapel Hill, N.C., U.S.A.

Authors should preferably submit two copies in double-spaced typing on pages of uniform size. Legends for figures should be typed on a separate page. The figures should be in a form suitable for reproduction, drawn in Indian ink on drawing paper or tracing paper, with lettering etc. in thin pencil. The sheets of drawing or tracing paper should preferably be of the same dimensions as those on which the article is typed. Photographs should be submitted as clear black and white prints on glossy paper.

All references should be given at the end of the paper. They should be numbered and the numbers should appear in the text at the appropriate places.

A summary of 50 to 200 words should be included.

Reprints

Twenty-five reprints will be supplied free of charge. Additional reprints can be ordered at quoted prices. They must be ordered on order forms which are sent together with the proofs.

Publication

The *Journal of Electroanalytical Chemistry* appears monthly and has six issues per volume and two volumes per year, each of approx. 500 pages.

Subscription price (post free): £ 12.12.0 or \$ 35.00 or Dfl. 126.00 per year; £ 6.6.0 or \$ 17.50 or Dfl. 63.00 per volume.

Additional cost for copies by air mail available on request.

For advertising rates apply to the publishers.

Subscriptions

Subscriptions should be sent to:

ELSEVIER PUBLISHING COMPANY, P.O. Box 221, Amsterdam, The Netherlands.

SUMMARIES OF PAPERS PUBLISHED IN JOURNAL OF ELECTROANALYTICAL CHEMISTRY

Vol. 9, No. 2, February 1965

THE MECHANISM OF STEP PROPAGATION AND PYRAMID FORMATION ON THE (100) PLANE OF COPPER FROM *IN SITU* NOMARSKI-OPTICAL STUDIES

In situ observations of copper electrodeposits on to the (100) plane of copper from highly purified solutions of CuSO_4 , and from highly purified solutions to which *n*-decylamine was added to concentrations of 10^{-4} – 10^{-10} mole/l, have been made using Nomarski interference contrast and polarized interferometry. In pure solutions, at current densities of 5 and 10 mA/cm² pyramids form, which, at higher current densities, easily truncate and gradually transform into blocks and cubic layers. Truncation is facilitated by addition of small amounts ($< 10^{-7}$ mole/l) of *n*-decylamine. Layers, which develop along with pyramids, have their origin in misorientation of substrate. In the presence of *n*-decylamine ($\geq 10^{-7}$ mole/l), a ridge type of deposit forms. Mechanism of the formation of various types of deposit, the rates of their growth, and the role of surface-active agents in the formation of layers with macro-steps are discussed.

A. DAMJANOVIC, M. PAUNOVIC AND J. O'M. BOCKRIS,
J. Electroanal. Chem., 9 (1965) 93–111

TRACE ANALYSIS BY ANODIC STRIPPING VOLTAMMETRY

IV. THE DETERMINATION OF COPPER IN STEELS

A generally applicable, rapid method for the determination of low concentrations of copper (0.1–0.0005%) in iron and steels is proposed. Copper is electrodeposited from an alkaline triethanolamine solution on a HMDE, and determined, after medium exchange, from the anodic stripping voltogram. None of the usual alloying metals present in steels interferes with the copper determination.

S. GOTTESFELD AND M. ARIEL,
J. Electroanal. Chem., 9 (1965) 112–116

CAPILLARY RESPONSE AT A DROPPING MERCURY ELECTRODE

A solution film inside the capillary is the principal locus of shielding at a D.M.E. A graphical method for obtaining the true double-layer capacitance is presented, and a model is given which represents the electrical characteristics of the solution film.

R. DE LEVIE,
J. Electroanal. Chem., 9 (1965) 117–127

A STUDY OF THE ANOMALOUS BEHAVIOUR OF THE GLASS ELECTRODE IN SOLUTIONS CONTAINING HYDROFLUORIC ACID

A defined surface hydration of the glass electrode is secured by pre-treatment with 0.1 *N* HF followed by rinsing with pure 0.1 *N* HCl for a few minutes. On subsequent contact with 0.1 *N* HCl containing HF, the electrode potential shows a change which is determined by the [HF].

The immediate reaction is an adsorption of HF by the glass surface. This is followed, at [HF] higher than 0.01 *N*, by the substitution of two F⁻ for OH⁻ per Si atom.

With increasing HF the attack on the Si-O-Si bonds becomes severe, but it can be tolerated to a considerable degree because the newly formed surface is identical with the previous one.

Some applications of the glass electrode in titrations with HF are suggested in an appendix.

E. SØRENSEN AND T. LUNDGAARD,
J. Electroanal. Chem., 9 (1965) 128-133

POLAROGRAPHIC REDUCTION OF NITRATE IONS IN THE PRESENCE OF ZIRCONIUM SALTS

The present study has shown that the irreversible polarographic reduction of the nitrate ion in the presence of 0.1 *M* zirconium as supporting electrolyte is not catalytic, but rather involves the reduction of distinct Zr-NO₃ complexes. The nature of the reducible species is dependent on the relative and absolute concentrations of the zirconium and nitrate ions. It is also apparent that the age of the solution of zirconium used as supporting electrolyte affects the character of the nitrate polarographic wave. Freshly prepared solutions of zirconium give nitrate waves which are poorly resolved from the hydrogen discharge wave of the supporting electrolyte. Zirconium solutions aged for at least two weeks give well-defined, completely resolved waves ideally suited for analytical use. Using aged 0.1 *M* zirconyl chloride solutions as supporting electrolyte, a constant i_d/C_{NO_3} ratio is obtained over a wide range of nitrate ion concentration ($2.4 \cdot 10^{-5}$ to $2 \cdot 10^{-2}$ *M*).

H. W. WHARTON,
J. Electroanal. Chem., 9 (1965) 134-139

POLAROGRAPHIC BEHAVIOUR OF CHROMIUM AROMATIC COMPOUNDS: CYCLOPENTADIENYL-CYCLOHEPTATRIENYL CHROMIUM(0) AND (1+)

The couple, $(C_5H_5)Cr^0(C_7H_7)/[(C_5H_5)Cr(C_7H_7)]^+$, exhibits in non-aqueous medium (benzene: methanol 1:4) a cathodic-anodic polarographic wave at about -0.7 V vs. *N*/2 C.E. and correspondingly a single diffusion-controlled oscillopolarographic peak. $[(C_5H_5)Cr(C_7H_7)]^+$ in aqueous alkaline solutions has a diffusion-controlled, one-electron main reduction wave, preceded and followed by adsorption waves. This behaviour reveals a close analogy to the polarographic and oscillopolarographic behaviour of the dibenzenechromium couple, the only relevant difference being a positive shift of about 0.1 V in the redox potentials of the C₅-C₇-Cr system.

C. FURLANI, A. FURLANI AND L. SESTILI,
J. Electroanal. Chem., 9 (1965) 140-148

THE ELECTRICAL DOUBLE LAYER ON THALLIUM AMALGAM ELECTRODES

Measurements of double-layer capacity and zero-charge potential have been made on 10, 30 and 40% thallium amalgams. These results have been compared with existing literature data. The integrated capacity curves agree with literature values for experimental electrocapillary curves. The surface concentration of thallium, at potentials where overvoltage measurements have been made, is one-half to three-fourths of the bulk concentration. In contrast to results reported in the literature, the double-layer capacity of 40% thallium amalgam shows no dependence on frequency, within experimental error in the range from 0.5–10 kc.

J. N. BUTLER,
J. Electroanal. Chem., 9 (1965) 149–162

THIN-LAYER CHRONOPOTENTIOMETRIC DETERMINATION OF REACTANTS ADSORBED ON PLATINUM ELECTRODES

(Short Communication)

A. T. HUBBARD AND F. C. ANSON,
J. Electroanal. Chem., 9 (1965) 163–164

FORMATION OF THICK OXIDES ON PLATINUM ELECTRODES

(Short Communication)

A thick coherent platinum oxide film can be deposited on a platinum electrode from molten KNO_3 with or without electrolysis. The thickness of the film and the ratio of PtO to PtO_2 in the film can be varied according to treatment.

R. L. EVERY AND R. L. GRIMSLEY,
J. Electroanal. Chem., 9 (1965) 165–166

A CONTRIBUTION TO THE THEORY OF THE CHANGE OF ELECTRODE REACTION RATE BY ADSORPTION OF AN ELECTRO-INACTIVE SUBSTANCE

(Short Communication)

J. KORYTA AND K. HOLUB,
J. Electroanal. Chem., 9 (1965) 167–169

VOLTAMMETRIC STUDIES USING VARIOUS ELECTRODE SYSTEMS

(Short Communication)

V. T. ATHAVALE, S. V. BURANGEY AND R. G. DHANESHWAR,
J. Electroanal. Chem., 9 (1965) 169–171

THE MECHANISM OF STEP PROPAGATION AND PYRAMID FORMATION ON THE (100) PLANE OF COPPER FROM *IN SITU* NOMARSKI-OPTICAL STUDIES

A. DAMJANOVIC, M. PAUNOVIC AND J. O'M. BOCKRIS

The Electrochemistry Laboratory, The University of Pennsylvania, Philadelphia, Pa. 19104 (U.S.A.)

(Received October 27th, 1964)

INTRODUCTION

CONWAY AND BOCKRIS^{1,2}, in an analysis of alternative paths taken by an ion in the process of deposition and arrival at growth sites, concluded that transfer of an ion to a surface plane, and the subsequent surface migration of the ion through the adsorbed water layer to a growth site, is a more probable path than the direct transfer of an ion to a given growth site from which it migrates no further. MEHL AND BOCKRIS^{3,4} experimentally distinguished between these two alternative paths (at least as far as an early stage of deposition goes), and concluded that, in silver electrodeposition at low current densities, the path is *via* surface diffusion of partially dehydrated adions (and this surface diffusion controls the overall rate of the reaction at least in the early stages of the process of deposition). GERISCHER⁵ independently arrived at a similar conclusion. Subsequent work has accumulated further evidence in support of the proposed mechanism⁶⁻⁹ and the theory (under ideal experimental conditions) was elaborated⁶⁻¹⁰ and includes particularly the dependence of the kinetics of the aggregation of adions to growth sites on the imperfections of the substrate^{7,8,10}.

This analysis was based on studies of short time transients, mostly galvanostatic, in which the total amount of deposited (or dissolved) metal atoms is less than that corresponding to a monolayer evenly distributed over the whole surface. In contrast to this "monolayer deposition" study, long time deposition, or study of electrochemical crystal growth, is less understood, although many papers have been published concerning the morphology of the deposit under a variety of conditions (*e.g.*, refs. 11-15). The methodology of the examination of the mechanism by which crystals grow as a result of the electrodeposition of ions on to planar surfaces is more difficult than that of the elementary processes which occur in the examination of the kinetics of the transfer of ions to growth sites. The crystal growth occurs after the ions in solution have undergone charge exchange, *via* various subsequent steps, and consequently, different methods must be evolved from those which involve interpretation of the passage of charge across the interface as a function of time, potential, concentration in solution, etc.

In the present study, electron optics, interference contrast microscopy, interferometry, and superimposed transients over a constant current density have been

used for an examination of the growth on the (100) plane of copper single crystals. A special cell was used which allows observation *in situ* under the condition of maintaining relatively high purity in the solution¹⁶.

EXPERIMENTAL

Traces of surface active agents may seriously affect electrochemical crystal growth and change the type of the deposit¹¹. Hence, extreme care has been taken to control the purity of solutions and to prepare and maintain a clean crystal surface and cell prior to, and during, deposition. To prevent air oxidation of the copper surface,

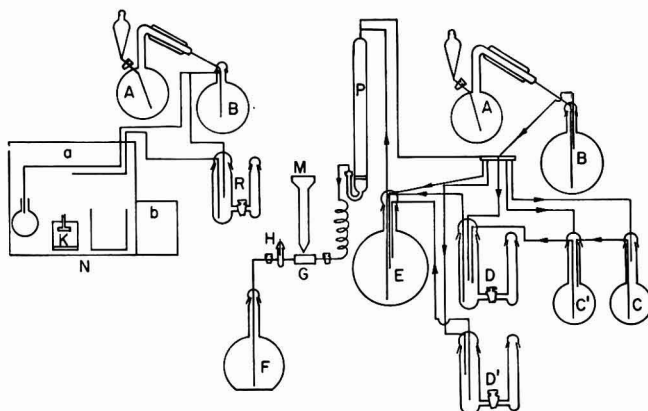


Fig. 1. A schematic representation of the experimental set-up for the electrodeposition study. A, distillation vessels; B, reservoirs for conductivity water; C and C', recrystallization vessels; D and D', pre-electrolysis vessels for CuSO_4 and H_2SO_4 solutions, respectively; E, main vessel for solution; P, activated alumina and charcoal column; M, microscope; G, main Teflon cell; H, reference electrode; F, outlet reservoir, R, pre-electrolysis vessel for H_3PO_4 solution; N, argon (dry) box; K, cell for electropolishing; a and b, main chamber and forechamber of the dry box, respectively.

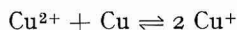
or its contamination with dust particles, pre-treatment of the single crystal electrode in an argon-filled dry box and its transfer in an inert atmosphere in a closed cell under a microscope has been arranged. A block scheme of the system is given in Fig. 1.

Solution preparation

All operations for the preparation and purification of solutions, including transfer of solutions and water from one vessel to another, were carried out in closed, all-glass systems, under an atmosphere of pure nitrogen. CuSO_4 crystals were recrystallized twice, first in an auxiliary vessel (C, Fig. 1) from conductance water, and then in the main vessel (C', Fig. 1) from redistilled (vessel B, Fig. 1) conductance water under a pressure of nitrogen *highly purified* by passing through a train of silica gel, hopcalite, soda lime, platinized asbestos and activated charcoal traps at

liquid nitrogen temperature. Twice-recrystallized copper sulphate crystals were first quickly washed, and then dissolved in freshly redistilled conductance water. The solution was then passed in a closed system under the pressure of purified nitrogen into a two-compartment pre-electrolysis vessel (D, Fig. 1). The saturated solution was pre-electrolyzed cathodically for about 10 h at a constant current density (~ 10 mA/cm²; size of the electrode ~ 10 cm²). Similarly, in another two-compartment vessel (D', Fig. 1), 50% H₂SO₄ was pre-electrolyzed at a current density of 10 mA/cm² for about 10 h (on an electrode about 10 cm² in area).

The final solution was prepared in a main, 10-l solution reservoir (E, Fig. 1), by adding the required amount of redistilled conductance water to a known amount of CuSO₄ solution and H₂SO₄. Before introducing solutions and water into the reservoir, spectrographically pure copper wire (surface area > 100 cm²) was introduced into the main reservoir which was freed of air by passing purified nitrogen through it for some time (~ 1 h). Copper wire served to equilibrate the solution¹⁷, according to:



The solution was in contact with metallic copper for about 24 h. During this time, and after, the solution was stirred by a magnetic stirrer, whilst purified nitrogen was slowly bubbled through it.

In preliminary work, electrodeposition was carried out with solution which had been purified as described. The main experiments reported here, however, were carried out with solutions which were still further purified by passage through a column (P, Fig. 1) of activated charcoal and alumina¹⁸⁻²⁰. A column, 90 cm high and 6 cm wide, with a medium-porosity frit at the bottom, was filled with neutral alumina (80-200 mesh), to a height of about 50 cm, and with activated charcoal (6-14 mesh), 10 cm in height²⁰. Before use, the column was continuously washed for about 20 days with fresh 1 M H₂SO₄, and then with redistilled conductance water (see ref. 20); the column was under a small excess pressure of purified nitrogen all the time. The solutions were passed through the column just before the deposition experiment started. The first solution to pass through the column and system of tubes connecting the column to the cell (but not over the crystal itself) was discarded. After each run the column was washed with 1 M H₂SO₄ and freshly redistilled conductance water.

Pre-treatment of the copper substrate

In all experiments the metal substrate was a cylindrical ($d = 8$ mm, $l = 7$ mm) copper single crystal*, cut to expose a (100) plane. The crystal was mounted in a Teflon cell, described in a separate publication¹⁶. Copper, mounted in the cell body, was polished first mechanically (with 0.3 μ alumina) outside the dry box, and then electrochemically at a constant potential inside the dry box. After mechanical polishing, the crystal (and the cell body) was washed with conductance water, a mixture of ethanol and ether, and finally with ethanol²¹. Electropolishing was done in an atmosphere of purified argon under a small overpressure. ($\sim 5-10$ cm of water). Phosphoric acid, 50% by volume, was first pre-electrolyzed for about 10 h at 10 mA/cm² at a platinum electrode of area about 4 cm² outside the dry box in an all-

* Purity better than 99.995%

glass closed vessel (R, Fig. 1). Oxygen evolved during this time was removed by heating the anodic compartment of the pre-electrolysis vessel for some time while slowly bubbling purified nitrogen through it. Phosphoric acid, and redistilled conductance water for washing, were passed into the main chamber (a, Fig. 1) of a dry box *via* a system of separated closed tubings. Since the copper crystal underwent polishing more satisfactorily in an already used polishing solution than in a fresh solution of 50% phosphoric acid, a high-purity copper sheet ($\sim 5 \text{ cm}^2$) was placed as an anode ($\sim 2 \text{ mA/cm}^2$ for 2 h in about 200 cm^3 of the solution) in each freshly prepared solution prior to electropolishing. Current-potential relations were determined for each solution, and the working potential was chosen for the bright polishing²². An all-Teflon cell for electropolishing (Fig. 2), in the form of a hollow cylinder

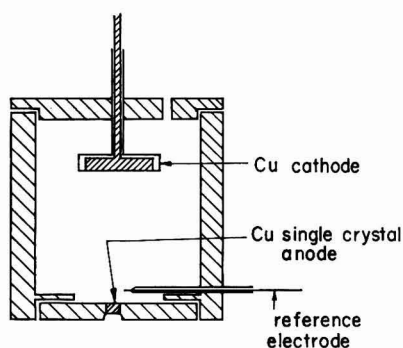


Fig. 2. All Teflon cell for electropolishing.

with two lids, one of which was the main body of the electrodeposition cell containing the crystal, insured the same position of the crystal in respect to the cathode fixed to the second lid. A copper single crystal in the Teflon body was oriented so that its (100) plane was (closely) parallel to the base of the main Teflon body. Close to the crystal face, a platinum bead sealed in a thin glass tube served as the reference electrode in electropolishing. After electropolishing for 20 min, the crystal was washed inside the dry box first with 10% phosphoric acid²³, and then with redistilled conductance water. The amount of water required for washing was determined by controlling the conductivity of the wash water.

Light microscopy

Light microscopy is desirable in the study of the kinetics of metal deposition for continuous measurements of the rate of crystal growth, where, if electron microscopy only is used, it is impossible (with any practical electron microscope) to follow the changes during the course of deposition. A further disadvantage of the application of electron microscopy in metal deposition studies is associated with the fact that after cessation of the net current, further crystal growth and dissolution (or surface rearrangement) under the influence of local currents may occur.

It is desirable to measure both the velocity of lateral displacement of a segment of the growing crystal and the velocity of growth in a vertical direction. To achieve the former with a magnification of up to 1000 times needs a distance from objective to substrate of < 0.3 mm so that solution, cover glass and symmetrical anode grid must be kept very thin¹⁶. An optical system is at present available which allows measurement both of lateral displacement and vertical growth *in situ* with the same instrument, namely the interference contrast microscope and polarized interferometry (Reichert) which utilize NOMARSKI optics²⁴. Apart from the possibility of studying with one instrument the rate of lateral and vertical growth, the principal advantages of the Nomarski optics applied here are:

(i) the resolution in depth of $1/100$ wavelength, or better²⁴, compares with phase contrast microscopy and is far better than that in normal dark field microscopy;

(ii) in interferometry, performance compares with that of the Tolanski double beam method but does not require the reference reflecting surface over the crystal.

The heights of steps were measured by observing the displacement of fringes. The height of a pyramid was measured by counting the number of extra fringes over the pyramid.

Electron microscopy

When the substrate had large areas which appeared to be flat in the Nomarski microscope, electron microscopy (Hitachi HS-6) was used.

After removing the cover glass and anode, and replacing the solution with water, and then with alcohol, replicas were made by applying parlodion to the electrode. The usual technique of shadowing by platinum-palladium alloy and then with carbon was followed.

Superimposed galvanostatic transients

In work on short time deposition, the characteristics of the potential behavior with time at constant current density in the time region 10^{-5} – 10^{-3} sec are mechanism-indicating. In order to obtain analogous information during the deposition of copper, constant current transients were superimposed on the steady-state current associated with crystal growth.

The circuit used has been described elsewhere^{3,6,7,25}. In comparison with previously used arrangements for transient recording, the transient technique was improved in several ways.

(a) Fast switch and galvanostatic circuit were designed in such a way as to provide pulses of rise time less than $2 \mu\text{sec}$ and to allow control of pulse length between $100 \mu\text{sec}$ and 400msec . Short range ($10 \mu\text{sec/cm}$) and long range (0.2 – 1msec/cm) transients were taken in each run.

(b) The overvoltage recording system was improved in order to obtain noiseless recording of fast varying signals of 1mV in the presence of slowly varying signals of about 100mV .

General procedure

The cell for electrodeposition, which consisted of the main Teflon body with crystal, the Teflon lid, a thin sheet (thickness $\sim 0.05 \text{mm}$) of copper anode, the cover glass (thickness $\sim 0.06 \text{mm}$), the solution inlet with a three-way stopcock, and out-

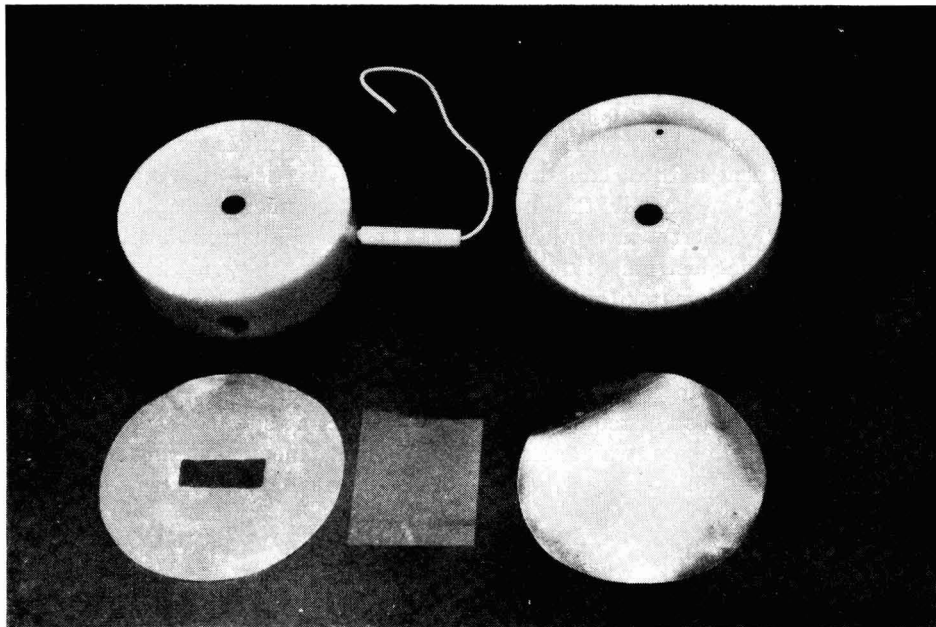


Fig. 3. Components of the electrodeposition cell.

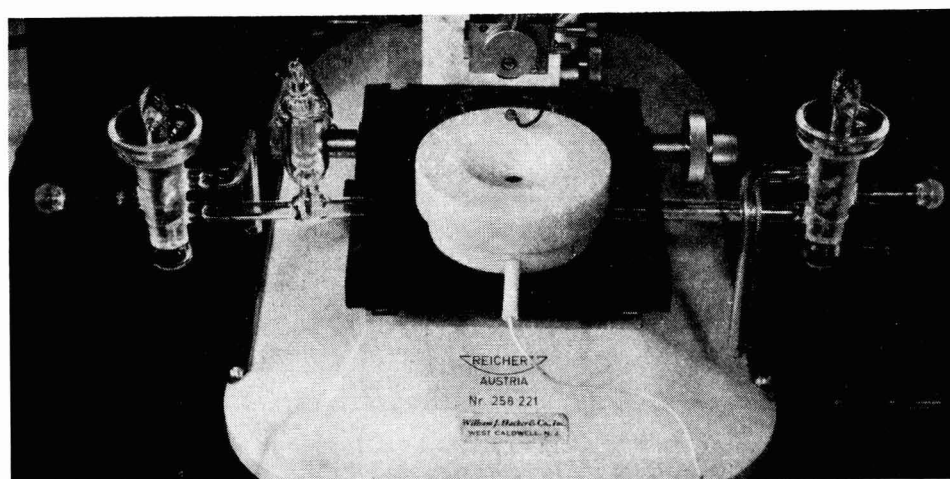


Fig. 4. Assembled cell under the microscope. The reference electrode compartment is seen on the outlet tubing (left).

let with the reference electrode compartment and a stopcock (Figs. 3 and 4), was assembled inside the dry box. The assembled cell with closed stopcocks on inlet and outlet leads was taken out from the main chamber of the dry box, *via* the forechamber (b, Fig. 1) which is separated from the main chamber by a vacuum-tight door. The forechamber could be evacuated and filled with purified argon several times in succession so that the main chamber was always protected from being contaminated. The assembled cell with crystal was placed on a microscope stage and connected with the solution purification column outlet (P, Fig. 1). Under pressure of purified nitrogen, a solution was forced to pass from the solution reservoir (E, Fig. 1) to the purification column, and finally through the column and the cell. Flow of solution was adjusted to about 0.3 ml/sec, and for the given cell dimensions this corresponds to a velocity of solution flow over the electrode of about 30 cm/sec. This rate of flow, and the concentration of solution (0.25 M CuSO₄ + 0.1 M H₂SO₄) allow electro-deposition to be carried out up to about 50 mA/cm² without having diffusion control. The limiting current was calculated from the equation²⁶

$$i_l = \frac{nFc^0 2l^{\frac{1}{2}} w D^{\frac{1}{2}} v^{\frac{1}{2}}}{3\mu^{\frac{1}{2}}}$$

where c^0 is the bulk concentration of copper sulphate, l the length and w the width passed by solution with a velocity v , μ is the kinematic viscosity, n the valency, and D and F have the usual meanings. Immediately after introducing solution into the cell, a Polaroid microphotograph of the substrate was taken, and a chosen constant current was switched on. Registration of the potential of the cathode was made with respect to the reference electrode (H, Fig. 1). This was formed by electro-deposition of Cu on Pt foil at 10 mA/cm² and was placed in the outlet tubing of the electro-deposition cell. The cell allowed continuous observations of the substrate (cathode) through a pinhole in the copper anode, placed below a thin cover glass (0.05 mm). The cover glass is pressed to the main Teflon body by a Teflon lid, and this prevents any leak of the solution and contact of the solution with either microscope objective or atmosphere. Although observation was made through the cover glass, and a thin (< 0.2 mm) layer of solution, it was possible to use objectives with numerical apertures 0.65 and to obtain useful magnifications of 600 ×. Microphotographs were taken at regular intervals (after each 0.5 C/cm² had passed). In some experiments, constant short current pulses were superimposed over the (constant) deposition current. The voltage-time relationship during these pulses was photographed on an oscilloscope. From these photographs, the capacity of the electrode, the rise time of the potential for the superimposed pulse, and the increase in over-potential during the pulse were determined. The current density of the superimposed pulse was always 1 mA/cm². The duration of the superimposed pulses and the superimposed current chosen, corresponded to less than 0.1 monolayer of (evenly distributed) "extra" ions deposited.

Deposition was carried out up to a total thickness of deposit corresponding to 10 C/cm², *i.e.*, 3.7×10^{-4} cm. Current densities ranged from 1–50 mA/cm². After electro-deposition had been completed, a replica was taken for electron microscopy. The heights of various growth forms on the cathode were determined by the polarized interferometric technique described above.

TABLE 1

TYPES OF DEPOSITS FROM HIGHLY PURIFIED SOLUTIONS AT VARIOUS CURRENT DENSITIES

<i>Current density</i> (mA/cm ²)	<i>Type of deposit</i>	<i>Overpotential</i> at 10 C/cm ² (mV)
5	layer type of deposit	40-60
5	pyramids	60-80
7.5	layers + pyramidal growth	110
10	layers + pyramidal growth	130-140
15	layers + pyramidal growth + truncated pyramids	140-160
20	(layers) + truncated pyramids + blocks	165
30	truncated pyramids + blocks	225
40	polycrystalline (?) + truncated pyramids + blocks	230
50	polycrystalline	240

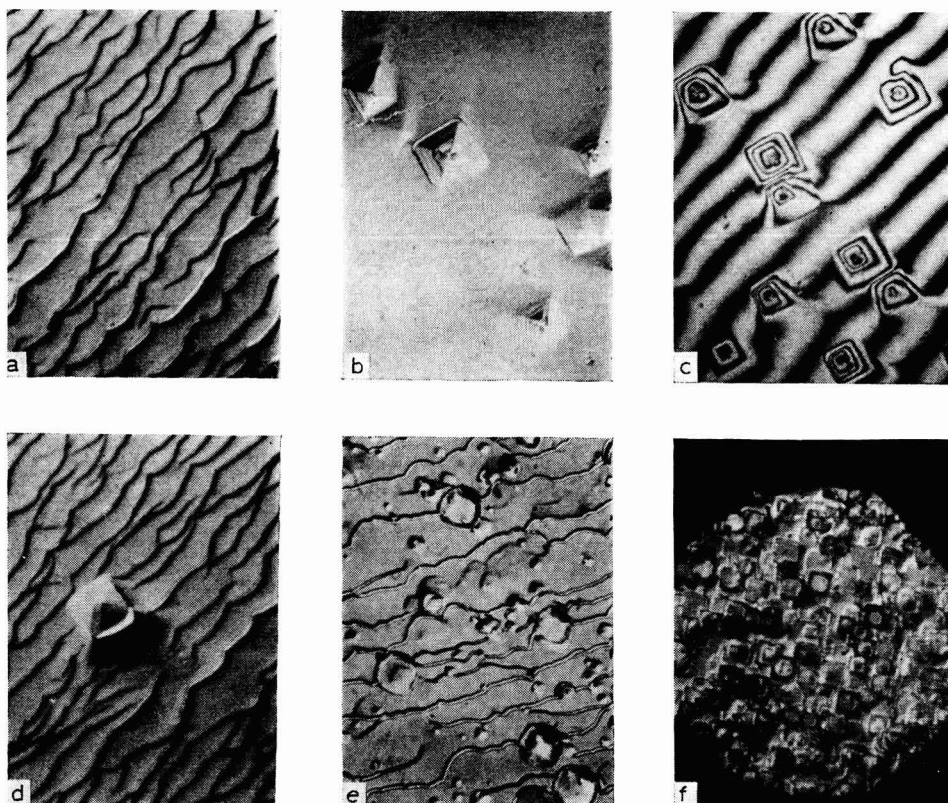


Fig. 5. Types of deposit on the (100) plane of copper crystal: (a), layer type of growth with macrosteps all running in one direction (5 mA/cm²); (b), pyramids on a smooth substrate (5 mA/cm²); (c), pyramids on smooth substrate as observed by interferometry; (d), layers with pyramids (7.5 mA/cm²); (e), layers with pyramidal growth (10 mA/cm²); (f), truncated pyramids and blocks (30 mA/cm²).

RESULTS

1.1 Types of crystal growth as a function of current density

A description of the crystal growth forms observed in the steady state at different current densities from highly purified 0.25 M CuSO₄, 0.1 M H₂SO₄ solutions at room temperature is given in Table 1. At a constant rate of crystal growth, the overpotential decreased with time. The average value of overpotential at the termination of growth (10 C/cm²), at a particular rate, is also given. At 5 mA/cm², a *layer type* of deposit usually forms with side faces, or *macro-steps*, all running in one direction (Fig. 5, a). However, *pyramids*, with well-developed faces, often grow on the substrate on which (except for a slight waviness) no layers, or any other type of deposit, is observed either by interference contrast (Fig. 5, b), or by polarized interferometry (Fig. 5, c). When pyramids form, the overpotential is higher than that for the layer formation. Occasionally, pyramids grow over a substrate covered by layers, and then the deposit resembles that obtained at 7.5 mA/cm² (Fig. 5, d). At higher current densities (10–15 mA/cm²), layers persist, the density of pyramidal outgrowths increases, and a number of pyramids becomes truncated (Fig. 5, e). At still higher current densities (20–30 mA/cm²), blocks start to form (Fig. 5, f). At rates of crystal growth above about 40 mA/cm², a polycrystalline deposit forms even at an early stage of deposition corresponding to 1 C/cm².

1.2 Crystal growth inhibited by adsorbed n-decylamine

(a) *Dependence of type of growth at constant current density on the surface occupancy by inhibitor.* In choosing a substance to introduce into the electrode surface, the principal criterion is knowledge of the isotherm. Such relations are little known for solid–solution interfaces. However, BOCKRIS AND SWINKELS²⁷ have recently reported a radio-tracer study of the adsorption of *n*-decylamine from aqueous solutions on to a number of metals, as a function of potential. This substance was chosen so that its coverage, θ , in the crystal growth experiments could be known. The extrapolated function of the dependence of coverage, θ , on concentration of *n*-decylamine in the studied potential region given in Fig. 6, can be obtained approximately from the data of BOCKRIS AND SWINKELS^{27,28} on the adsorption of *n*-decylamine on copper in 1 N NaClO₄. Since it seems probable that only adsorbed molecules of inhibitor are responsible for a change of deposit with the addition of inhibitor, in the following the coverage corresponding to the concentration of inhibitor in the bulk of the solution is given.

A known amount of *n*-decylamine was added to a highly purified solution in a reservoir (2 l) placed between the purification column (P, Fig. 1) and the cell (G, Fig. 1). Experiments were carried out at various values of coverage of *n*-decylamine, θ , from 0.57 to 10⁻⁷ (bulk concentration from 10⁻⁴ mole/l to 10⁻¹² mole/l) at current densities of 5 mA/cm². Effects on the crystal growth were observed when the *n*-decylamine had a fractional coverage of $\theta = 10^{-4}$ (a concentration of only 10⁻⁹ mole/l). It was observed that distances between steps in the layer type of deposit at the same average thickness of the deposit decreased as the amount of surface active agents in the solution increased. It appears that the overpotential also increases with the increasing concentration of *n*-decylamine (Table 2). For coverage between 0.03 and 0.57 (concentrations of the organic substance between 10⁻⁴ and 10⁻⁶ mole/l), the

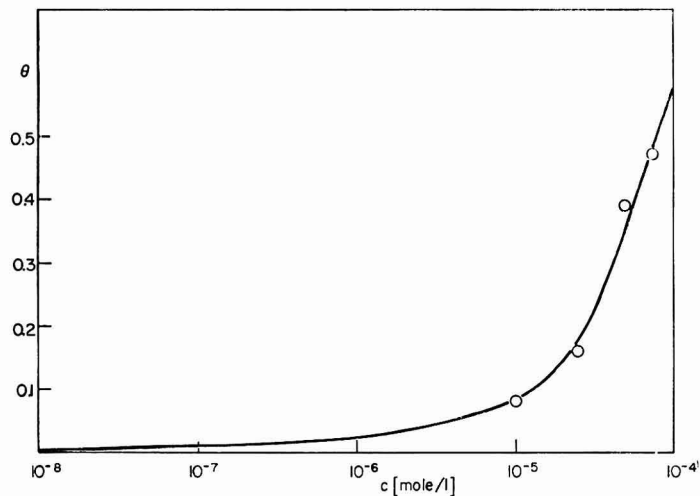


Fig. 6. Adsorption isotherm for *n*-decylamine on copper in 1 *N* NaClO₄ from the data of Bockris and Swinkels^{27,28}.

TABLE 2

TYPES OF DEPOSITS AT 5 mA/cm² AND VARYING CONCENTRATION OF *n*-DECYLAMINE IN A SERIES OF CONSECUTIVE EXPERIMENTS

Estimated coverage	<i>n</i> -Decylamine bulk concn. (mole/l)	Type of deposit	Av. distance between steps or ridges at 10 C/cm ² (10 ⁻⁴ cm)	Overvoltage at 10 C/cm ² (mV)
10 ⁻⁷	10 ⁻¹²	layers	10	50
10 ⁻⁵	10 ⁻¹⁰	layers	10	50
10 ⁻³	10 ⁻⁸	layers	8	65
10 ⁻²	10 ⁻⁷	ridges	3	65
5.7 × 10 ⁻¹	10 ⁻⁴	ridges	3	80



Fig. 7. Ridge-type deposit at 5 mA/cm² from a solution containing 10⁻⁷ mole/l of *n*-decylamine.

deposit was of an entirely different type from that obtained in highly purified solutions. Thus, at $\theta < 10^{-2}$ (at concentrations of *n*-decylamine $< 10^{-7}$ mole/l) the crystal growth form was of layers with a distance between steps of about 10^{-3} cm. At $\theta > 10^{-2}$, the deposit observed already after the passage of 0.5 C/cm^2 was of the ridge type (Fig. 7). This deposit has been described in the literature¹³.

(b) *Dependence of type of growth at constant surface occupancy of inhibitor upon the current density.* In a third series of experiments, deposition was studied at a constant coverage, $\theta = 10^{-3}$ (constant, 10^{-8} mole/l, concentration of *n*-decylamine) and various current densities. Results are given in Table 3. With the introduction

TABLE 3

TYPE OF DEPOSIT AS A FUNCTION OF CURRENT DENSITY IN THE PRESENCE OF *n*-DECYLAMINE, $\theta = 10^{-3}$ (CONCENTRATION 10^{-8} M/l)

Current density (mA/cm ²)	Appearance of crystal growth at magnification 600 ×	
	In the presence of <i>n</i> -decylamine	Absence of <i>n</i> -decylamine
5	layers (truncated pyramids)	layers (pyramids), larger (up to 50%) distances between steps.
10	layers + truncated pyramids	layers + pyramids, larger distances between steps, low tendency to form truncated pyramids.
15	layers + truncated pyramids + blocks	layers, larger distances between steps, lower tendency to form truncated pyramids.
20	polycrystalline	layers, truncated pyramids, blocks

of surface active agents in the solution, there are changes in the deposits at each current density. In general, if the distances between steps on a layer type of deposit are considered, they decrease, at the same current and thickness of the deposit, when *n*-decylamine is added to the solution. Pyramids tend to become more readily truncated (at lower current densities) and to transform to blocks. In a series of photographs of the same area, a pyramid formed at an early stage of deposition ($\sim 2 \text{ C/cm}^2$), is seen to become truncated at a latter stage ($\sim 5 \text{ C/cm}^2$) of deposition, and eventually it transforms into a block ($\sim 8 \text{ C/cm}^2$) which grows sidewise into a large square layer. A polycrystalline deposit, which resembles that formed in the presence of pure solutions, develops at current densities (ca. 20 mA/cm^2) lower than that (ca. 40 mA/cm^2) at which a similar crystal growth occurs in the absence of adsorbed *n*-decylamine.

When the purification of the solution includes only crystallization and pre-electrolysis processes, the distances between steps on layer-types of structures are shorter than if activated alumina and charcoal are used in solution purification. The same trend is observable both at 5 and at 10 mA/cm^2 (Table 4).

2. Formation and growth of layers

From a series of *in situ* photographs of the same cathode area, taken after the passage of a successive series of numbers of coulombs, analysis of the crystal growth can be made. The growth of layers was followed by observing lateral movement of layers (interference contrast microscopy) and measuring the height of the steps (polarization interferometry).

2.1. *Direction of propagation of steps.* All steps propagate in the same direction. Displacement of the steps was measured with respect to the apex of some pyramid, when pyramidal outgrowth was observed, or with respect to some small irregularity on the surface (small pit, etc.), or with respect to the coordinate drawn through one of the above reference points. The direction of step propagation was observed for two different positions of the crystal axis with respect to the direction of the solution flow. The result of these observations was that the direction of step propagation does not depend on the direction of the solution flow.

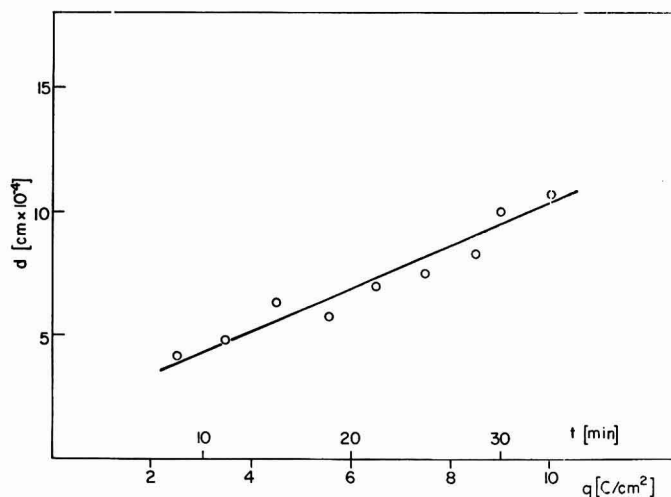


Fig. 8. Average distance, d , between macro-steps at various times of deposition (or average thickness of the deposit). Current density 5 mA/cm².

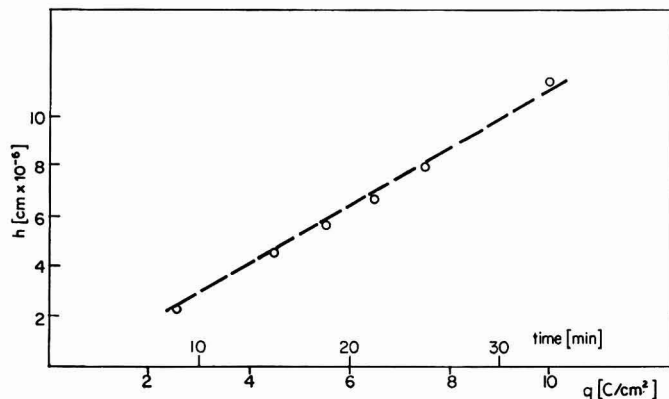


Fig. 9. Average height, h , of macro-steps at various times of deposition (or average thickness of the deposit) as obtained by interferometry. Current density 5 mA/cm².

2.2 Distance between steps. The average distance between steps to the first approximation, in the region studied, increases linearly with the thickness of the deposit (Fig. 8). If deposition is carried out from a solution which is not highly purified, *e.g.*, from one in which the solution does not pass through an alumina-charcoal purification column, the linear dependence of the distance between steps upon thickness ceases at larger (about $3 \cdot 10^{-4}$ cm) thickness of the deposit. The distance between steps becomes independent of the thickness of the deposit.

2.3 Height of the steps. The heights of the steps at different thicknesses of deposit was measured at regular intervals by the interferometric method described above. Measurements showed that in the region studied, the average height of steps increases linearly with the thickness of the deposit (Fig. 9).

2.4 Rate of horizontal and vertical motion of steps. This work reports the first direct measurement of the rate of propagation of steps on electrolytically growing crystal faces. Analysis has shown that the velocity of the horizontal motion of steps of average length is constant with time at a given current density (Fig. 10). The average velocity of the step motion is about $2 \cdot 10^{-6}$ cm/sec for the rate of deposition of 5 mA/cm². Some steps, however, propagate with a non-uniform velocity (*cf.* Fig. 11).

The lateral rate of advance of visible steps appears to be independent of the thickness of the deposit (up to about 10 C/cm²), the density of the steps (which decreases as the thickness of the deposit increases) and of the heights of the steps. Addition of surface active agents appears not to affect this rate.

To account for the lateral rate of advance of macro-steps and taking into account the step heights and the density of steps, less than a few per cent of the amount of the deposited metal ions (per unit time) would be sufficient. Hence, the main outward growth of the deposit occurs between the macro-steps. The lateral rate of advance of visible steps is somewhat higher (about 5–10 times) than the calculated

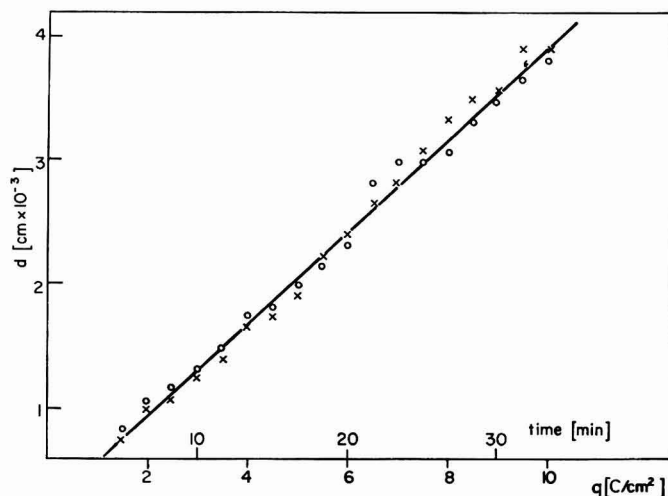


Fig. 10. Position of a macro-step with respect to a fixed reference point on the crystal. Current density 5 mA/cm².

average outward growth of layers (between steps). The total amount of metal ions deposited per unit time of the surface between two macro-steps of unit length and at a distance l apart is equivalent to

$$g = i \cdot l$$

If all metal adions are deposited at the macro-step the rate of advance of the step would be given by

$$v = \frac{i \cdot l}{500 \cdot 10^{-6}} \cdot \frac{a}{2} \cdot \frac{1}{h}$$

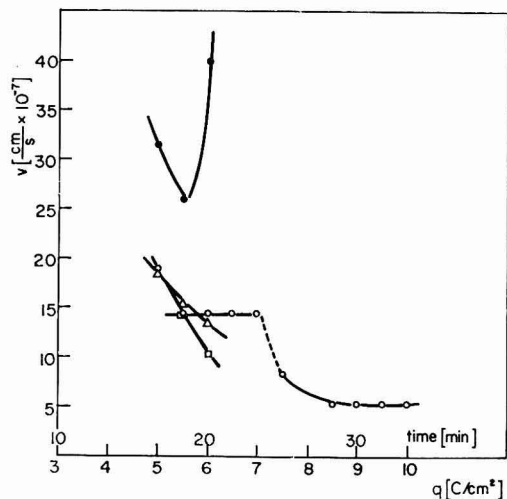


Fig. 11. Non-uniform rate of advance of some macro-steps. Current density 5 mA/cm².

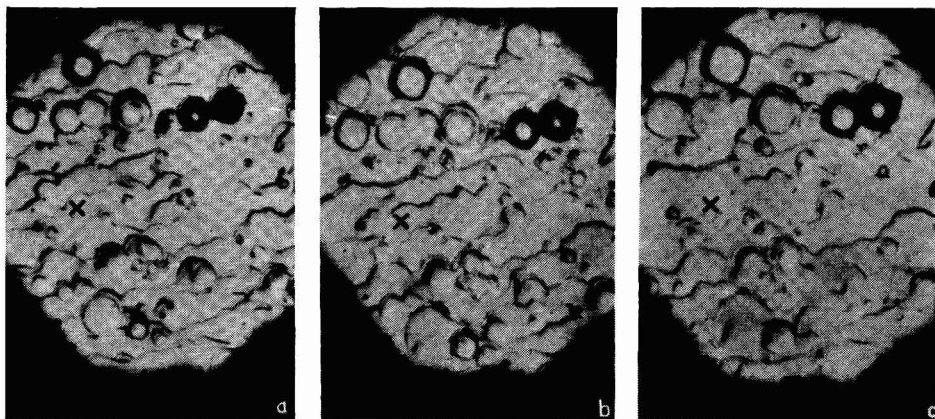


Fig. 12. Joining and fading out of macro-steps (\times), as observed during deposition: (a), 8 C/cm²; (b), 9 C/cm²; (c), 10 C/cm².

where $500 \cdot 10^{-6}$ (C/cm²) is the equivalent in coulombs for a full monolayer, h is the height of the step, and $a/2$ is half the length of the unit cell and is thus equivalent to the thickness of a monolayer. This calculated rate of advance of macro-step is about 10–20 times larger than the observed rate.

2.5 Fading out of steps. Many of the steps in the viewing field originated and ended in the middle of the surface. Points where these macro-steps "emerged" on the "flat" surface also moved as the steps propagated. Two steps were observed to join by their ends (points of emergence) thus producing longer steps.

A step may fade away (starting from one end), thus diminishing the length of the step. In this way, layers between steps become larger, and the density of steps decreases with the increasing thickness of the deposit. Both phenomena are illustrated in Fig. 12, at places marked by \times .

3. Formation of pyramids, truncated pyramids and blocks

3.1 Influence of current density and presence of inhibitor. The number of pyramidal outgrowths increased with increase of current density. Pyramids were formed randomly (in time) during observation at constant current density. Pyramidal faces were stepped particularly near the base, and became truncated at a higher current density. At the same current density more truncated pyramids are formed when the *n*-decylamine occupies part of the surface than when it is absent. Once a pyramid becomes truncated, it may grow sidewise and transform into a block type of deposit. No block type of deposit was observed in these experiments to form initially as such.

3.2 Rate of horizontal growth of pyramids. The change of position of the growing side of a pyramidal outgrowth was measured with respect to a chosen reference point. In a run, twenty photographs (*in situ*) were taken at regular time intervals corresponding to 0.5 C/cm² irrespective of current density.

From a series of measurements, it was concluded that the rate of horizontal growth is uniform with time. It appears that this rate is not affected much by current density and is about $1 \cdot 10^{-6}$ cm/sec and thus somewhat lower than the rate of step propagations at the same current density. Also, it appears that this rate is not appreciably affected by the addition of *n*-decylamine. The density of pyramidal outgrowths, including block type of structure, increases with increasing current density. At about 15 mA/cm², there are about 10^5 such outgrowths per cm² compared to 10^6 at 20 mA/cm².

4. Superimposed galvanostatic transients

The superimposed current density was in all cases 1 mA/cm². In the presence of *n*-decylamine at $\theta = 10^{-3}$, superimposed overvoltage was between 6 and 10 mV for current density from 5–20 mA/cm². Rise time in msec was from 0.5–1 msec showing the tendency of decreasing rise time with increasing current density of deposition for the same superimposed current density. The capacity of the double layer had values from 12–16 μ F/cm².

For the second set of experiments, carried out holding current density constant, 5 mA/cm², and varying coverage, θ , from 10^{-5} – $5 \cdot 10^{-1}$, the superimposed overvoltage had values from 6–10 mV, the capacity of the double layer 16–18 μ F/cm² and rise time 0.25–1.9 msec.

DISCUSSION

1. *Formation of layers*

It was observed that all macro-steps advance during deposition in the same direction, and also that in a given experiment the ratio between the average step height and the average distance between steps at each thickness of the deposit is unchanged during the deposition*. This suggested that the macro-steps form from micro-steps which are initially present on the substrate and originate from misorientation of the substrate in respect to the (100) plane of the single crystal for, if the micro-steps originate from screw dislocations, they would propagate in various directions. A misorientation of only a few minutes will result, in an ideal case, in numerous monatomic steps on a flat substrate**.

To test the hypothesis of misorientation of the substrate as the origin of micro-steps, the orientation of the crystal was changed by cutting it so that the [100] axis of the crystal became now slightly inclined in a direction opposite to that in earlier experiments, in respect to the axis perpendicular to the substrate. At a rate of deposition of 5 mA/cm², and an average thickness of deposit of 3.5×10^{-4} cm, the distance between steps, d , is measured to be 10^{-3} cm, and the height of steps, h , determined by the interferometric measurement for this experiment to be 1.2×10^{-5} cm (*cf.* Figs. 8 and 9). The misorientation of the substrate was calculated to be about 36 min of a degree (angle) using the equation

$$\alpha = \frac{h}{d} \cdot \frac{180}{\pi}$$

Thus, after cutting, the direction of propagation of the macro-steps should be opposite to that of the former motion (with respect to the same axis in the surface) if the micro-steps originate in misorientation. This prediction of propagation of macro-steps was experimentally confirmed.

2. *The mechanism of propagation of macro-steps*

(a) *Dependence of distance between steps on the rate of growth.* The fact that the average distance between visible or macro-steps is larger at high current density than at low current density can be explained as follows. When a micro-step is stopped (or slowed) by meeting with an impurity, the micro-step on which it rests can grow twice as far per unit time at 10 mA/cm² at as 5 mA/cm². Hence, a given point on the surface of a plane will be exposed to the solution impurities for a shorter time at the higher current density, and has a lesser chance of possessing impurity atoms on the surface, and the probability of the initiation of bunching, *i.e.*, initial macro-step formation, is reduced. Thus, the average frequency of macro-steps is correspondingly diminished.

The amount of adsorption on a fresh surface before it is again covered by a new layer may be calculated as follows. It can be shown that, in the presence of agitation, the dependence of the coverage upon time is given by³⁰:

$$\theta_t = \theta_e [1 - e^{-Dt/\delta K}],$$

* This ratio can, however, change from one experiment to another.

** A similar idea has been suggested by HOWES²⁹.

where θ_t is the coverage after time t , θ_e is the coverage at $t = \infty$, D the diffusion coefficient, δ the diffusion layer thickness, and K the equilibrium constant for adsorption on the metal. Taking the values for n -decylamine from BOCKRIS AND SWINKELS (see Fig. 6), $\theta_e = 10^{-5}$ when c_0 is 10^{-10} mole/l, *i.e.*, 10^{-13} mole/cm³, $K = 10^8$ cm³/mole*, and with $D = 10^{-5}$ cm²/sec and taking δ as 0.01 cm, $\theta_{10^{-2} \text{ sec}} \approx 10^{-9}$, *e.g.*, θ in time of 10^{-2} sec, which is the time required for a full monolayer deposition at 5 mA/cm², is 10^{-9} . In this region of t in the equation for the rate of adsorption, θ_t is simply proportional to t so that when the current density is halved, the number of impurity atoms is doubled, and the frequency of initial bunches increases.

(b) *Dependence of distance between steps on the purity of solution.* If the hypothesis that distances between stable bunches depend on the occupation of the surface with impurities is accepted, then it should be possible to influence the distance between the steps by augmenting intentionally the concentration of the adsorbed entity. The results of doing this are shown in Table 4. It is indeed seen that the

TABLE 4

AVERAGE DISTANCE BETWEEN MACRO-STEPS IN A SERIES OF CONSECUTIVE EXPERIMENTS AT TWO CURRENT DENSITIES AND TWO DEGREES OF SOLUTION PURIFICATION

Current density (mA/cm ²)	Av. distance between steps at 10 C/cm ² (10 ⁻⁴ cm)	Remarks on soln. purification
5	5	Pre-electrolysis (P.E.) only.
5	10	P.E. + adsorption on charcoal and alumina
10	10	P.E. only
10	20	P.E. + adsorption on charcoal and alumina

distance between steps decreases with increasing amount of adsorbed entity. For highly purified solutions, $\theta_e (=Kc_0)$ in the former equation becomes smaller, and the time required to reach the same coverage with surface active agents increases. Monatomic steps can thus propagate longer distances in purer solutions before encountering the same density of obstacles and are slowed. Distances between bunches initially formed will increase with increasing purity of solution. On this basis, greater distances between macro-steps are expected in solutions of higher purity.

(c) *Rate of propagation of macro-steps.* Soon after bunches become stable and the first macro-steps form, their further propagation does not depend on the density of macro-steps. The rate with which they propagate is constant and about $2 \cdot 10^{-6}$ cm/sec for a net current density for the whole surface of 5 mA/cm². Were the deposition to occur on side faces of macro-steps only, the rate would be some twenty times larger. Thus, crystal growth occurs mainly between macro-steps on the "flat" layers.

3. Mechanism of fading of macro-steps

The increase in the distances between macro-steps which took place with increasing time was found to occur often by fading out of some macro-steps rather than by one macro-step travelling faster than another and catching it up. This fading of macro-steps resembles the fading of bunches discussed in the theory of step propagation³⁴, but differs from the predictions of the theory in that the macro-

* $K = k\Gamma_{\text{max}}$, and it is assumed that $\Gamma_{\text{max}} = 10^{-9}$ mole/cm².

steps which fade away propagate at a rate independent of their height.

The fading (which must arise by a kind of debunching), occurs from the *end* of a step, rather than uniformly from the whole length (see Fig. 12).

4. Dependence of shape and number of pyramids (truncated pyramids and blocks) on current density

In some experiments with pure solutions, at 5 mA/cm² pyramids grow on a surface which is free from macro-steps. More usually, however, at this current density, layers form. These facts are explicable in the following way. If, in the experiments in which pyramids are observed, the initial substrate happens to be particularly close to the (100) orientation, — due, for instance, to some uncontrolled change in the condition of polishing, — then, an insufficient number of monatomic or micro-steps are present for the functioning of the step-like crystal growth mechanism. It is therefore more difficult for ions to be incorporated into the lattice, and the potential rises in agreement with the data of Table I. Conditions for the commencement of pyramid formation may then be created.

At current densities above 15 mA/cm², truncated pyramidal outgrowths and blocks appear. Thus, at higher overpotential (current densities), local exhaustion of cations may occur at the apex of the growing pyramids, and the net local current at this point decreases. A condition is then created at which impurities can compete more readily for places at the growing substrate and this will lead to the blocking of the apex of the pyramid by adsorbed impurities (*cf.* TURNER²⁰). Side faces can, however, proceed to grow and the truncated pyramid is formed which eventually ends in a block or a cube layer. The increasing tendency for the formation of truncated pyramids at higher current densities can also be accounted for in the same way. The higher the current density, the quicker the solution in the neighborhood of the growing pyramids will become exhausted and impurities may adsorb on the pyramid apex which is most probably the place of the emerging screw dislocation (see refs. 31, 32). Blocking of the dislocation will hinder the outward growth. Side faces of such truncated pyramids then constitute place at which further growth proceeds.

The stepping of the side faces of the pyramids is more pronounced close to the base of pyramids than at the apex in agreement with predictions made on the shock-wave theory³³⁻³⁵.

ACKNOWLEDGEMENTS

The authors are indebted to the American Electroplater's Society for the continued support of this work. They also wish to acknowledge the help they have derived from discussions of technique and theory in this field with Drs. KARDOS, KRÜGER, PETROCELLI, TURNER and WEIL. They are also grateful to Mr. G. RAZUMNEY for the design of a circuit for the transients and for help in some of the measurements of superimposed pulses.

SUMMARY

In situ observations of copper electrodeposits on to the (100) plane of copper from highly purified solutions of CuSO₄, and from highly purified solutions to which

n-decylamine was added to concentrations of 10^{-4} – 10^{-10} mole/l, have been made using Nomarski interference contrast and polarized interferometry. In pure solutions, at current densities of 5 and 10 mA/cm² pyramids form, which, at higher current densities, easily truncate and gradually transform into blocks and cubic layers. Truncation is facilitated by addition of small amounts ($< 10^{-7}$ mole/l) of *n*-decylamine. Layers, which develop along with pyramids, have their origin in misorientation of substrate. In the presence of *n*-decylamine ($\geq 10^{-7}$ mole/l), a ridge type of deposit forms. Mechanism of the formation of various types of deposit, the rates of their growth, and the role of surface-active agents in the formation of layers with macro-steps are discussed.

REFERENCES

- 1 B. E. CONWAY AND J. O'M. BOCKRIS, *Proc. Roy. Soc. London, Ser. A*, 248 (1958) 394.
- 2 B. E. CONWAY AND J. O'M. BOCKRIS, *Electrochim. Acta*, 3 (1960) 340.
- 3 W. MEHL AND J. O'M. BOCKRIS, *J. Chem. Phys.*, 27 (1957) 818.
- 4 W. MEHL AND J. O'M. BOCKRIS, *Can. J. Chem.*, 37 (1959) 190.
- 5 H. GERISCHER, *Z. Elektrochem.*, 62 (1958) 256.
- 6 J. O'M. BOCKRIS AND M. ENYO, *J. Electrochem. Soc.*, 109 (1962) 48.
- 7 J. O'M. BOCKRIS AND H. KITA, *J. Electrochem. Soc.*, 109 (1962) 928.
- 8 H. KITA, M. ENYO AND J. O'M. BOCKRIS, *Can. J. Chem.*, 39 (1961) 1670.
- 9 A. DESPIC AND J. O'M. BOCKRIS, *J. Chem. Phys.*, 32 (1960) 389.
- 10 A. DAMJANOVIC AND J. O'M. BOCKRIS, *J. Electrochem. Soc.*, 110 (1963) 1035.
- 11 H. FISHER, *Electrochim. Acta*, 2 (1960) 50.
- 12 H. SEITER, H. FISCHER AND L. ALBERT, *Electrochim. Acta*, 2 (1960) 97.
- 13 H. J. PICK, G. J. STOREY AND T. B. VAUGHAN, *Electrochim. Acta*, 2 (1960) 165.
- 14 T. B. VAUGHAN AND H. J. PICK, *Electrochim. Acta*, 2 (1960) 179.
- 15 G. WRANGLÉN, *Electrochim. Acta*, 2 (1960) 130.
- 16 A. DAMJANOVIC, M. PAUNOVIC AND J. O'M. BOCKRIS, *Plating*, 50 (1963) 735.
- 17 L. H. JENKINS AND J. O. STIEGLER, *J. Electrochem. Soc.*, 109 (1962) 467.
- 18 P. J. HILLSON, *Trans. Faraday Soc.*, 50 (1954) 385.
- 19 G. BARKER, *Trans. Symp. Electrode Processes, Philadelphia*, (1959) 366.
- 20 D. R. TURNER AND G. R. JOHNSON, *J. Electrochem. Soc.*, 109 (1962) 798.
- 21 J. KRUGER, *J. Electrochem. Soc.*, 106 (1959) 847.
- 22 K. F. LARKING, *Electrochim. Acta*, 7 (1962) 101.
- 23 E. C. WILLIAMS AND M. A. BARRETT, *J. Electrochem. Soc.*, 103 (1956) 363.
- 24 G. NOMARSKI AND A. R. WEIL, *Revue de Met. Paris*, 52 (1955) 121.
- 25 M. A. V. DEVANATHAN AND M. SELVARATNAM, *Trans. Faraday Soc.*, 56 (1960) 1820.
- 26 P. DELAHAY, *New Instrumental Methods in Electrochemistry*, Interscience, New York, 1954, p. 231.
- 27 J. O'M. BOCKRIS AND D. SWINKELS, *J. Electrochem. Soc.*, 111 (1964) 736.
- 28 D. A. J. SWINKELS, Thesis, University of Pennsylvania, 1963.
- 29 V. R. HOWES, *Proc. Phys. Soc. (London)*, 74 (1959) 616.
- 30 P. DELAHAY AND I. TRACHTENBERG, *J. Am. Chem. Soc.*, 79 (1957) 2355.
- 31 J. O'M. BOCKRIS AND A. DAMJANOVIC, *Modern Aspects of Electrochemistry*, Vol. III, Butterworth, London, 1964.
- 32 D. TRIVITCH AND H. FISCHER, *Electrochim. Acta*, (1960).
- 33 N. CABRERA AND D. A. VERMILYEA, *Growth and Perfection of Crystals*, Wiley, New York, 1958, p. 393.
- 34 F. C. FRANK, *Growth and Perfection of Crystals*, Wiley, New York, 1958, p. 411.
- 35 A. A. CHERNOV, *Kristallografiya*, 5 (1960) 446.

TRACE ANALYSIS BY ANODIC STRIPPING VOLTAMMETRY

IV*. THE DETERMINATION OF COPPER IN STEELS

S. GOTTESFELD** AND M. ARIEL

Laboratory of Analytical Chemistry, Department of Chemistry, Technion, Israel Institute of Technology, Haifa (Israel)

(Received October 30th, 1964)

INTRODUCTION

The object of this investigation was the evaluation of anodic stripping voltammetry, modified by medium exchange¹, as a tool for trace-metal determination in metallic samples. The particular problem chosen was the determination of low concentrations of copper in both plain carbon and alloyed steels.

Methods in current use include classical iodimetry, gravimetry and electrolysis²; spectrophotometry (employing a number of reagents and often coupled with a selective extraction step, with pH control, precipitation of macro-constituents or adjustment of their oxidation states, as indispensable preliminary steps^{3,4}); spectroscopy, and finally some polarography⁵ and cathode ray polarography^{6,7}.

Since the reduction waves of cupric and ferric ions are close together in most supporting electrolytes, the polarographic determination of copper in the dissolved steel sample usually involves the removal of most of the iron by precipitation⁵, the reduction of ferric iron to ferrous^{6,7}, or its complexation, leading to a significant shift in the polarographic half-wave potential. This last expedient has not been investigated for the analysis of steel samples, since the unfavorable proportions of iron and copper usually present render appropriate complexing rather difficult; it has, however, been suggested for the analysis of solutions containing small amounts of iron^{8,9}.

In view of this, the development of an anodic stripping method employing a small steel sample and thus facilitating iron complexation, seemed indicated. Since no preliminary separation or concentration steps were envisaged even for the lowest copper concentrations (0.0005%), minimum contamination and material loss hazards were expected. In addition, due to the modification of medium exchange, it was hoped that the method would be applicable — unchanged — to the determination of copper in high alloy steels, dispensing with the separations required by most other methods.

EXPERIMENTAL

The electrolysis cell, scanning and recording apparatus and experimental

* Part III is published elsewhere.

** Part of a M.Sc. thesis presented by S. G. to the Senate of the Technion.

procedure have been previously described^{1,10}. All reagents were of analytical-grade purity and their solutions were prepared with distilled water which had been passed through a mixed-bed de-ionizer. All the reagent solutions were carried, in appropriate amounts, through a complete blank determination, employing the longest pre-electrolysis period and the highest recorder sensitivity used in the course of this investigation. This determination resulted in a horizontal base line, in the -0.2 to -0.9 V range (*vs.* S.C.E.) thus proving copper to be absent (or any other contaminant liable to distort the voltogram in this voltage range).

Procedure

A sample of steel of approximately 100 mg is introduced into a 50-ml beaker, 5 ml of (1 : 1) HCl are added and the beaker covered and heated gently until complete solution has been achieved. 2–3 drops of concentrated HNO₃ are now added, the solution is heated to boiling and allowed to cool. 60 ml of 1 M triethanolamine (TEA) solution and 30 ml of 3 M NaOH solution are introduced into a 200-ml volumetric flask, the sample solution is added gradually, the flask shaken periodically to prevent local precipitation of ferric hydroxide, and the solution made up to volume with distilled water. 80.0 ml of this solution are measured into the lower part of the electrolysis cell and oxygen bubbled through for 2 min, followed by 5 min of nitrogen for complete de-aeration. From this point, nitrogen is kept streaming over the solution throughout the electrolysis, which is carried out at the HMDE (hanging mercury drop electrode) at -1.0 V *vs.* SCE, for 3 min. Electrolysis is stopped (by stopping the stirring), the lower part of the electrolysis cell exchanged for one containing de-aerated 0.3 M TEA solution, the solution stirred briefly, allowed to come to rest, and the anodic stripping voltogram recorded from -0.75 to -0.2 V *vs.* SCE.

At least three consecutive determinations of the copper peak are made. Nitrogen must be bubbled through the sample solution before electrolysis, and through the exchange solution before exchange, for about one minute; each determination is carried out with a fresh mercury drop. Should the standard deviation of the results obtained exceed 4%, two more determinations must be added.

After the first series of measurements has been concluded, 1 ml of standard 10^{-4} M Cu²⁺ solution is added to the solution in the cell and a second series of peak determinations carried out (both the sample weight and the standard addition recommended, are suitable for steel samples containing copper in the range of a few hundredths percent).

The copper content of the sample is calculated from the arithmetic means of the peaks obtained in the two series. A single determination may be carried out in 75 min for copper contents from 0.1–0.01% and in 2½ h for the lowest copper content determined (0.0005%).

Remarks

(1) Both the electrolysis cell and the volumetric flask should be washed with (1 : 1) HNO₃ before each determination and subsequently thoroughly rinsed with twice distilled water.

(2) For steel samples containing bismuth, 1 M KCNS solution must be employed as exchange medium¹.

RESULTS AND DISCUSSION

1. Alkaline TEA (0.3 *M* TEA–0.3 *M* NaOH) solution acts as an efficient complexing agent, keeping up to 1250 mg ferric iron/l in solution and shifting the reduction waves of many metallic ions to negative potentials (beyond the -1.0 V *vs.* SCE employed for electrolysis).

2. The problem of the presence of manganese and/or bismuth in the sample and their solution has been discussed¹.

3. Unless each current peak is obtained with a fresh mercury drop, as specified, a steady decrease in peak height is observed. This phenomenon was shown to be restricted to solutions containing NaOH and to have some relation to the electrode process; immersion of the drop in NaOH solution, without connecting the potential source, does not affect the height of the current peak subsequently obtained. Unfortunately, the presence of NaOH, because of its enhancing influence on the complexing ability of TEA¹¹, is indispensable.

4. After a thorough investigation of current–potential curves, -1.0 V *vs.* SCE was chosen as electrolysis potential. Although some simultaneous reduction of ferric iron occurs at this potential, it has been shown to have no effect on the reproducibility of the copper oxidation current peaks subsequently obtained or on the linearity of the copper concentration–peak height relation. At more negative potentials the rate of copper reduction increases, but so does the danger of interference from other constituents present in high alloy steels. At -1.0 V only lead and bismuth are reduced and amalgamated simultaneously with the copper. Both are fairly rare components of steels. Lead does not interfere with the copper determination, since its oxidation potential in 0.3 *M* TEA is sufficiently removed from that of copper, ($E_{\frac{1}{2}AS\ Cu}: -0.41$ V; $E_{\frac{1}{2}AS\ Pb}: -0.75$ V). Bismuth can be prevented from interfering with the copper oxidation current peak¹ by the use of 1 *M* KCNS as exchange medium.

5. The frequency with which manganese occurs in steels makes the modification of medium exchange indispensable. 0.03 *M* TEA (free of added NaOH) was chosen as exchange medium, since the base lines obtained with this solution were flattest. The introduction of NaOH (inevitable to some small extent during medium exchange from a NaOH-containing solution, due to carry-over by the liquid film attached to the upper part of the electrolysis cell) must be kept at a minimum. It is advisable to employ fresh exchange medium after every five transfers (or more often should the base line slope have increased considerably showing that too much NaOH has been carried over).

6. The linearity of the copper concentration–oxidation peak height relation (essential, if evaluation by standard addition is desired) was proved for the 10^{-5} – 10^{-7} *M* concentration range of Cu^{2+} ions. The standard deviation was 10%.

7. The method has been applied to a number of standard samples and in Table I the results are compared with standard certificate values. The lowest concentration determined, 0.0005%, does not appear in the standard certificate ($< 0.002\%$ is given); the result obtained, however, is in excellent agreement with that reported by SCHOLLES⁶ for the same standard sample.

The results, under “copper found” in Table 1, represent the average of 4–5 determinations; for copper concentrations in the 0.01–0.1% range, the standard

deviation did not exceed 10%; in the lower concentration range (down to 0.0005%), a standard deviation of 20% must be expected.

The lowest concentration of copper which may be determined by this method, is governed by the sensitivity of the recording instrument on one hand and by the limitation of the solubility of iron in the supporting electrolyte on the other hand. Since 0.3 *M* NaOH–0.3 *M* TEA solution is capable of keeping 1250 mg of ferric iron/l in solution, this determines the maximum copper concentration obtainable with a given steel sample. The sensitivity of the recording instrument must be sufficient for electrolysis from this solution to result in a measurable current peak during a reasonable time interval.

TABLE I
COPPER IN STANDARD IRON AND STEELS

<i>Sample</i>	<i>Sample designation</i>	<i>Certificate value for copper (%)</i>	<i>Copper found (%)</i>
Bessemer steel, 0.4% C	NBS 10F	0.032	0.032
Bessemer steel, 0.1% C (high sulfur)	NBS 129A	0.021	0.019
Ni–Mo steel	NBS 111B	0.028	0.027
Alloy steel, 13% Cr	BCS 211	0.08	0.078
Co–Mo–W steel	NBS 153	0.009	0.0097
Mo–W–Cr–V steel	NBS 132A	0.120	0.120
Pure iron granules	BCS 149	<0.002	0.0005
Lead steel	BCS 212	0.13	0.12

The determination of copper in steels containing appreciable amounts of tungsten is often tedious, due to the necessity of recovering the copper adsorbed by tungstic acid¹². The sensitivity of the proposed method is such that small steel samples can be used so that tungstic acid is not precipitated during sample solution even with steels containing 6% tungsten, and no modification of the method is required.

The maximum percentages of alloying metals present in the steels analysed for copper by this method, were: Mn, 0.8%; Ni, 1.8%; Cr, 13%; V, 2%; 8.4%; W, 6% and Pb, 0.2%. None of these metals interfered with the determination and the method can, therefore, be applied to the determination of copper in steels of varied composition.

SUMMARY

A generally applicable, rapid method for the determination of low concentrations of copper (0.1–0.0005%) in iron and steels is proposed. Copper is electrodeposited from an alkaline triethanolamine solution on a HMDE, and determined, after medium exchange, from the anodic stripping voltogram. None of the usual alloying metals present in steels interferes with the copper determination.

REFERENCES

- 1 M. ARIEL, U. EISNER AND S. GOTTESFELD, *J. Electroanal. Chem.*, 7 (1964) 307.
- 2 1960 *Book of ASTM Methods for Chemical Analysis of Metals*, American Society for Testing Materials, Philadelphia, pp. 122-124.
- 3 A. J. LEEB AND F. HECHT, *Z. Anal. Chem.*, 168 (1959) 101.
- 4 S. MEYER AND O. G. KOCH, *Arch. Eisenhüttenw.*, 32 (1961) 67.
- 5 W. C. COOPER AND P. J. MATTERN, *Anal. Chem.*, 24 (1952) 572.
- 6 P. H. SCHOLES, *The Analyst*, 86 (1961) 116.
- 7 P. H. SCHOLES, *Res. Develop. Ind.*, (1962) 38.
- 8 G. JESSOP, *Nature*, 158 (1946) 59.
- 9 I. M. ISSA AND R. M. ISSA, *Z. Anal. Chem.*, 174 (1960) 254.
- 10 M. ARIEL AND U. EISNER, *J. Electroanal. Chem.*, 5 (1963) 362.
- 11 J. F. FISHER AND J. L. HALL, *Anal. Chem.*, 34 (1962) 1094.
- 12 E. C. PIGOTT, *Ferrous Analysis*, Wiley, New York, 1953, p. 191.

J. Electroanal. Chem., 9 (1965) 112-116

CAPILLARY RESPONSE AT A DROPPING MERCURY ELECTRODE

R. DE LEVIE

Coates Chemical Laboratory, Louisiana State University, Baton Rouge, La. (U.S.A.)

(Received September 7th, 1964)

INTRODUCTION

Since the work of GRAHAME¹ many accurate measurements have been made of the capacitance of the electrical double layer between mercury and aqueous electrolyte solutions. If great care is taken to exclude reducible, oxidizable and adsorbable substances from the cell, a small frequency-dependence of the apparent double-layer impedance (or admittance) is usually still observed. GRAHAME² noted that this frequency-dependence was more pronounced with blunt capillaries than with fine-tipped capillaries, from which he concluded that the effect was due to *shading* of part of the mercury droplet by the glass at the bottom-end of the capillary. MELIK-GAIKAZYAN³ took into account also the effect of a thin film of solution between the mercury and the glass *inside* the capillary, and concluded that it had a negligible effect in his experiments in 1 M KCl at all but the lowest frequencies. From apparently unpublished calculations he estimated a film thickness of the order of 0.1 μ in his capillary. BARKER AND JENKINS⁴ observed this phenomenon at the same time, and indicated that the tendency of solution to enter the capillary could be reduced by using a capillary of which the internal radius decreased rapidly towards its orifice. VON STACKELBERG AND TOOME⁵ showed that siliconizing* of blunt capillaries significantly improved the constancy of drop time, drop weight and mass flow rate. They also reached the conclusion that solution presumably creeps up into the unsiliconized capillaries. Siliconizing of tapered capillaries did not appreciably change their characteristics. BOCKRIS AND CONWAY^{6,7} explained the observed frequency dependence of the double-layer impedance in aqueous solutions in terms of dielectric relaxation of water in the compact (Helmholz) double layer. Neglecting the abundance of GRAHAME's data in aqueous solutions which show hardly any frequency dependence of the double-layer capacitance they choose to illustrate the validity of their treatment for mercury** with results for KI solutions. According to their own standards (ref. 7, discussion, p. 713 under c), these can only be used at potentials at which there is no specific adsorption of I⁻ (which at the time was well-known³¹ to be strongly specifically adsorbed on Hg). BOCKRIS AND CONWAY however do not indicate the potential at which GRAHAME obtained his data, and GRAHAME seems never to have published them.

We want to stress that a potential-dependent reorientation of water would

* They emphasized the need for careful cleaning before siliconizing.

** For solid electrodes see ref. 8.

show in the impedance at or very close to a single well-defined potential, whereas actually the effect is observed at any potential. In a more recent paper BARKER⁹ proposed the model of a tapering* transmission line as the electrical analogue for the solution film. Such an analogue is closely akin to the one used in the description of porous electrodes, which was developed primarily by KSENZHEK AND STENDER and has been used by a great many authors since**. Recently COOKE, KELLEY AND FISCHER¹¹ carefully examined the behaviour of the solution which enters the capillary, and observed microscopically that *pockets* of solution were formed inside the capillary at some distance from its orifice. After a number of drops had been formed, these pockets of solution had grown so heavy that they combined and moved towards the orifice of the capillary, where they caused a spurious response and then left the capillary***. Siliconizing of an (uncleaned) capillary did not improve its characteristics, but using a slightly drawn-out capillary did.

These observations, which are in agreement with those of BARKER AND JENKINS⁴, explain the results of GRAHAME² although they do not substantiate his conclusion. The shading effect as assumed by GRAHAME is very unlikely to be measurable with the accuracy nowadays obtainable, see section 3(c). Indeed GRANTHAM¹³ did not observe any effect with a siliconized capillary, whereas the same, but unsiliconized capillary clearly showed the so-called *frequency dispersion*. A shading effect would not have been influenced by the siliconizing of the glass. The fact that solution creeps in between mercury and glass in a calomel reference electrode has been recognized by HILLS AND IVES^{14,15} who reported a *dramatic improvement* in electrode behaviour after siliconizing of the glass. Finally PARSONS³² cites two unpublished theses (H.A.C. MCKAY, Oxford, 1936 and M. A. V. DEVANATHAN, London, 1951) in which the tendency of electrolyte to creep up the capillary and cause irregular drop formation is mentioned, and severe creeping at negative potentials was reported by JOHNSTON AND UBBELOHDE³³ and by SOUTHWORTH³⁴.

Summarizing, the existence of a liquid film inside a normal glass capillary is well-established; this film will at least cover the inside of the capillary from the orifice up to the observed solution pockets. The subsequent treatment is closely akin to BARKER's ideas⁹, and for simplicity's sake will be restricted to the double-layer capacitance only *i.e.*, in the virtual absence of charge transfer and/or adsorption processes.

THE GRAPHICAL METHOD

The graphical method is based on the assumption that shielding (*i.e.*, non-uniformity of the current density as a result of the geometry of the electrode and its support) occurs only at a limited, well-defined part of the electrode surface, the remaining part behaving as a perfect capacitor. If this assumption is valid, we may divide the total electrode admittance, Y_{ei} , into two components, each associated with one of the above-mentioned parts of the electrode surface. Y_{ei} is most easily

* It is not clear, however, whether he has accounted properly for the effect of the solution resistance outside the electrode, *i.e.*, whether his conclusion is valid that the thickness of the liquid film decreases with increasing distance from the tip of the capillary.

** For an extensive list of references see ref. 10.

*** Recently LAFORGUE-KANTZNER AND MUXART¹² have observed irregularities in drop time which may be due to the same formation of pockets. They however give a quite different interpretation.

obtained from a cell impedance plane¹⁶ in which an accurate extrapolation to infinite frequency is possible to correct for the resistance of the capillary and the solution in the cell, R_{s01} . The resulting electrode impedance, Z_{e1} , is then transformed into the admittance Y_{e1} . The components of Y_{e1} are sketched in Fig. 1a, where Y_0 denotes the admittance of the unshielded part whereas Y_s is the admittance of the shielded part.

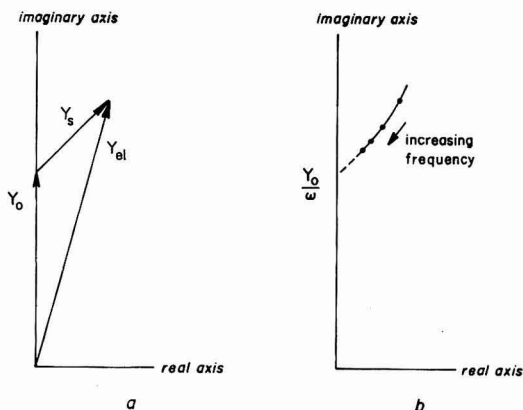


Fig. 1. (a) The components of the electrode admittance, Y_{e1} ; (b) the electrode admittance plotted in the Y_{e1}/ω plane for different frequencies.

Now $Y_0 = j\omega\kappa A_0$ ($j \equiv \sqrt{-1}$; κ , differential double-layer capacitance per unit area of the electrode-solution interface; A_0 , area of the unshielded surface) changes with frequency, whereas $Y_0/\omega = j\kappa A_0$ does not. Consequently a simple graph is obtained by plotting Y_{e1}/ω , see Fig. 1b. As Y_s in general does not behave as a perfect capacitor, Y_s/ω will not be a constant in the Y_{e1}/ω plane and extrapolation to $\omega \rightarrow \infty$ will yield Y_0/ω if such an extrapolation is feasible. Consequently if A_0 can be determined, κ can be obtained for the unshielded part of the electrode surface even if shielding takes place at other parts of the same electrode. Moreover the Y_{e1}/ω plane makes it possible to verify equations derived for the effect of shielding in a given geometry.

MODELS FOR CAPILLARY RESPONSE

(a) We will assume first that the solution film has a constant thickness, d , over a length, l , within the capillary (Fig. 2a). If we neglect the admittance of its end, such a film behaves (ref. 10, eqn. (10)) as a pore with admittance

$$\begin{aligned}
 Y_s &= \frac{1}{\sqrt{ZR}} \tanh l \sqrt{\frac{R}{Z}} = (1 + j)\pi r \sqrt{\left(\frac{2\omega\kappa d}{\rho}\right)} \tanh \left[(1 + j)l \sqrt{\frac{\omega\kappa\rho}{2d}} \right] = \\
 &= \pi r \sqrt{\left(\frac{2\omega\kappa d}{\rho}\right)} \frac{(\sinh u - \sin u) + j(\sinh u + \sin u)}{\cosh u + \cos u} \quad (1)
 \end{aligned}$$

$R = \rho/2\pi r d$, the solution resistance per unit length along the axis of the capillary; $Z = 1/2\pi r j\omega\kappa$, the double-layer impedance per unit length along the axis of the capillary;

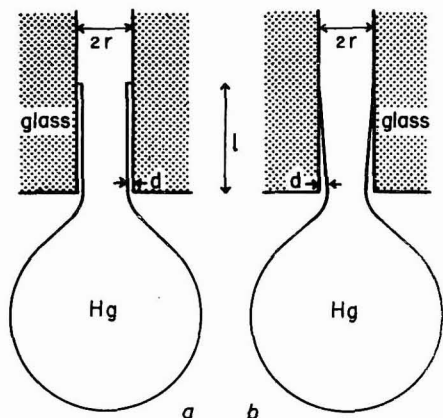


Fig. 2. Cross-sectional view of a mercury drop at the orifice of a capillary; drawing not to scale.

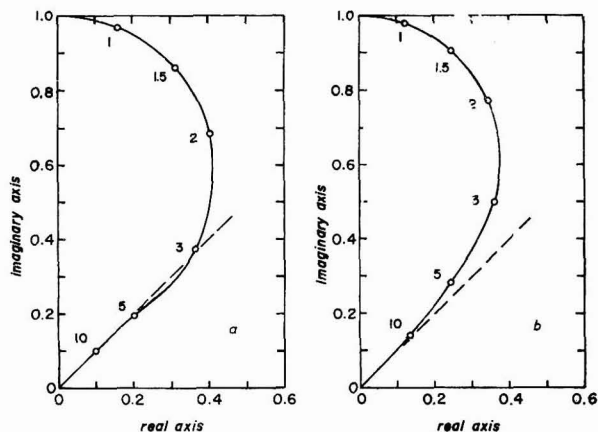


Fig. 3. (a) The function $\{(\sinh u - \sin u) + j(\sinh u + \sin u)\}/u(\cosh u + \cos u)$ appearing in eqn. (2), a few values of the parameter $u = l\sqrt{(2\omega\kappa\varrho/d)}$ are indicated; (b) the function $(2M_1/zM_0)(\cos\theta + j\sin\theta)$ appearing in eqn. (5), a few values of the parameter $z \approx 2l\sqrt{(\omega\kappa\varrho/d)}$ are indicated. The high frequency approximation, eqn. (3), is given by the broken lines.

- d = film thickness;
- $j \equiv \sqrt{-1}$;
- $2r$ = internal bore of the capillary;
- $u \equiv l\sqrt{(2\omega\kappa\varrho/d)}$;
- κ = differential double-layer capacitance per unit area of the Hg-solution interface;
- ϱ = specific solution resistance;
- ω = angular frequency used.

As we will use the Y_{e1}/ω plane (section 2) the more useful quantity is

$$\frac{Y_s}{\omega} = 2\pi r \kappa l \frac{(\sinh u - \sin u) + j(\sinh u + \sin u)}{u(\cosh u + \cos u)} \quad (2)$$

see Fig. 3a. It is clear that for $u \equiv l\sqrt{(2\omega\kappa\rho/d)} \geq 3$ or $l \geq 3\sqrt{(d/2\omega\kappa\rho)}$ we have

$$\frac{Y_s}{\omega} = (1 + j) \frac{2\pi r \kappa l}{u} = (1 + j) \pi r \sqrt{\frac{2\kappa d}{\omega\rho}} \quad (3)$$

which is the simple result for a semi-infinitely long film, compare ref. 10.

(b) We will now assume that the thickness of the solution film decreases linearly with increasing distance from the orifice of the capillary (Fig. 2b). The film then behaves (ref. 8 eqn. (17)); note that we have the analogue of half a groove) as a linearly-tapered transmission line with admittance

$$Y_s = \frac{\pi r d}{\rho l} \frac{z M_1}{M_0} (\cos \vartheta + j \sin \vartheta) \quad (4)$$

$$z \equiv 2\sqrt{\left\{\frac{\omega\kappa\rho l\sqrt{(l^2 + d^2)}}{d}\right\}} \approx 2l\sqrt{\frac{\omega\kappa\rho}{d}} \text{ for } l \gg d$$

For the derivation of this result and the notation used, see ref. 8. In the Y_{e1}/ω plane we have

$$\frac{Y_s}{\omega} = 2\pi r \kappa l \frac{2M_1}{z M_0} (\cos \vartheta + j \sin \vartheta) \quad (5)$$

see Fig. 3b. For $z \approx 2l\sqrt{(\omega\kappa\rho/d)} \geq 10$ or $l \geq 5\sqrt{(d/\omega\kappa\rho)}$ we find as before

$$\frac{Y_s}{\omega} \approx (1 + j) \frac{4\pi\kappa l}{z/2} = (1 + j) \pi r \sqrt{\frac{2\kappa d}{\omega\rho}} \quad (3)$$

(c) It is useful to estimate the order of magnitude of the calculated effects. Let us take as typical values for a dropping mercury electrode in a solution of an inert electrolyte

$$r = 0.003 \text{ cm}; A_0 = 0.03 \text{ cm}^2; \kappa = 25 \mu\text{Fcm}^{-2}; \rho = 10 \Omega \text{ cm}.$$

If we now assume that $l \gg \sqrt{(d/\omega\kappa\rho)}$ so that the film behaves as a semi-infinite one, in which case the effect is maximal, we have for the electrode admittance

$$\frac{Y_{e1}}{\omega} = j\kappa A_0 + (1 + j) \pi r \sqrt{\frac{2\kappa d}{\omega\rho}} \approx 0.75 j + (1 + j) 23.8 \sqrt{\frac{d}{\omega}} \mu\text{F}$$

Consequently in order to observe an effect of 4% in the imaginary part of Y_{e1}/ω (the measured *electrode capacitance*) at $\omega = 10^3 \text{ sec}^{-1}$ (approximately 160 c/sec) we calculate $d \approx 1.6 \mu$.

A liquid film with a thickness of this order of magnitude is quite probable. It is obvious however that the region of solution just below the tip of the capillary, where a *shading* effect should occur, has quite different dimensions (note that a Hg drop has the shape of a pear rather than of a sphere^{17,18}), which means that the solution resistance at the bottom of the capillary is far too low to cause any measurable frequency dependence of the electrode admittance or impedance.

DISCUSSION

(a) We will first give a tentative explanation of the observed difference in behaviour^{2,4,5,9,11} between blunt and tapered capillaries. We assume that a liquid film is formed spontaneously by creeping of solution between the mercury and a wettable capillary. The formation of such a film will not depend on the dislodgement of the Hg drops, and consequently cannot be expected to show up in irregular drop times, etc.

Upon detachment of a drop, however, the mercury thread in a capillary with a straight bore will tend to retract inside the capillary in order to have as small a mercury-solution interface as possible; this effect of surface tension is of course counteracted by the pressure of the mercury column. The upward movement of the mercury thread sucks solution into the capillary. Such a sucking action can easily be observed with normal polarographic capillaries, and has been described^{17,19}. It is not yet clear why the pockets¹¹ are formed but they certainly are; we have observed them also with electrocapillary measurements in a Lippmann electrometer.

The decrease in exposed mercury-solution interface on retraction is somewhat less for tapered capillaries and, much more important, the increasing internal diameter of the capillary causes a decrease in the radius of curvature of the end of the mercury thread, thus reducing the surface pressure^{17,18}. This presumably prevents the sucking from taking place*. (This is in agreement with the observation^{20,28,29} that there is a short time delay between disengagement of a droplet and the appearance of the next one with a capillary of uniform diameter, whereas such a time delay is usually not observed²⁰ with a tapered capillary**). Hence no pockets are formed and the drop time is regular. Moreover, without suction (which clearly introduces too much solution into the film, as shown by the formation and subsequent movement of the pockets) the film is thinner, which reduces its influence on a.c. measurements of the double-layer capacitance.

(b) The graphical method outlined in section 2 does not presuppose any model, the only assumptions made being that the surface at which shielding occurs is well-defined, and that an extrapolation is feasible. The former assumption will be justifiable for a solution film inside a capillary, although there may be variations in thickness and shape of the film from one drop to another if some sucking up of solution takes place. For a tapered glass capillary the film may well be considered steady and non-changing from drop to drop.

(c) From a comparison of Fig. 4, a and b, it is clear that there are only minor differences in the admittances of the differently shaped films. For the two film geom-

* Clearly both the degree of tapering and the length of the Hg column have to be specified in a more quantitative treatment.

** NEWCOMBE AND WOODS³⁰ have plotted accurate polarographic current-time data for Cd²⁺ in 1 M KCl as obtained by various workers. In our opinion, the graphs shown clearly indicate the effect of a time delay of the order of 50–150 msec, which is constant for a given series of experiments provided the height, h , of the Hg column, and hence the mass flow rate, m , is constant (ref. 30, Fig. 2) whereas it becomes smaller if h and m increase (ref. 30, Figs. 3 and 4). Such a time delay may very well be important in the verification of the Ilkovič equation or one of its proposed modifications. Actually, from the graphs given, one obtains the original Ilkovič relation $it^{-1/6} = \text{constant}$, if the time axis is shifted 50–150 msec! However, uneven Hg flow²⁰ might also cause such apparent time delay.

eries considered, we may summarize that the film behaves as a Warburg impedance (phase angle -45°) for $\omega \gg d/\kappa \rho l^2$ and as a capacitance (phase angle -90°) for $\omega \ll d/\kappa \rho l^2$, and we believe that this will hold for other film geometries as well.

(d) In drawing any conclusion from the Y_{e1}/ω plane as to the existence of a solution film, one should carefully exclude all reducible, oxidizable and/or adsorbable substances from the solution, as they may show up in a way similar to that of the liquid film (see under c). As one can never be sure of the effectiveness of cleaning and

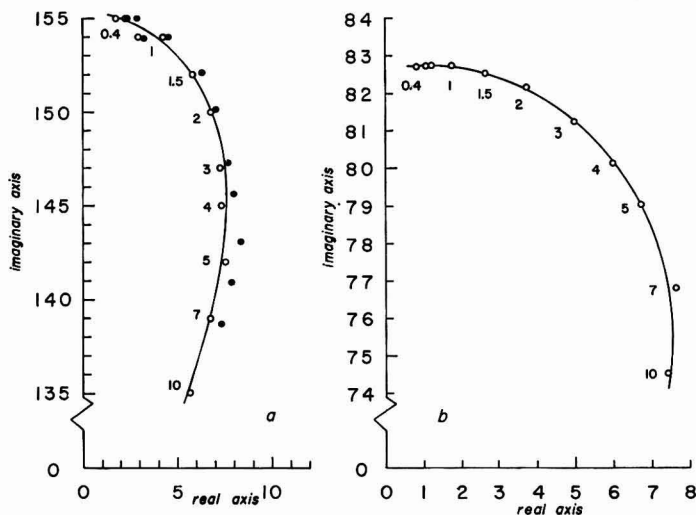


Fig. 4. Experimental data from measurements in 0.1 M KCl plotted in the Y_{e1}/ω plane at: (a) -0.5 V; (b) -1.0 V (vs. Hg pool). In (a) the effect of a correction of the bridge readings is indicated with solid points. Numbers in the graph denote the frequency in kc/sec. Units of the axes, nF.

purifying procedures, a simple but effective check should be made by making measurements at different potentials and/or drop times. Residual faradaic or adsorption admittances are usually negligibly small except in fairly narrow potential intervals, and are proportional to the surface area of the drop, whereas Y_s is not. The characteristics of the film will only slightly (but continuously) vary if one moves away from the potential of zero charge (*electrocapillary maximum*) due to the corresponding change in surface tension. Of course, κ also depends on potential.

(e) Although the present treatment has been restricted to the a.c. case, the solution film inside the capillary influences other fast-measuring techniques as well. This is obvious from the fact for example, that impedance and response to potential or current step functions are related by a Fourier transform²¹. In the present case this, moreover, is amply demonstrated by the fact that capillary response has been observed both with a.c. measurements^{1,2,3}, potential step function measurements^{4,9} and high-sensitivity polarography¹¹.

(f) It is far better to avoid the formation of the solution film by making the capillary water-repellent (or, even better, by using a Teflon capillary²²) than to correct for its existence. Moreover, a correction is extremely difficult to make if there is a faradaic current flowing also. The graphical method of section 2, however, still yields the correct value of the double-layer capacitance of the unshielded electrode surface in the presence of a faradaic admittance.¹⁶

The method presented here may be of some use for data already existing, and serve as a check on the effectiveness of siliconizing capillaries. Moreover, small cracks and crevices between glass and Pt support of hanging Hg drops²³ may cause a similar effect, and in this case a treatment with silicone is not feasible.

(g) We finally want to stress a closely connected point. Surface tension measurements (electrocapillary curves) have proved to be an extremely useful tool in the determination of specific adsorption. Until recently^{16,24} such a determination at potentials where an electrode reaction occurs, was only possible from drop-time measurements, and these were usually not considered very accurate. Now that we have a better understanding of what causes irregular dropping of the electrode and of how to prevent it, there seems to be no reason why the measurement of the drop time should not be just as accurate as (but considerably more convenient than) the determination of surface tension with a Lippmann electrometer or from capacitance data.

PRELIMINARY EXPERIMENTS

A few experiments have been performed to verify the validity of our calculations. The measurements were made with a conventional impedance bridge. The standard arms consisted of plug-in type precision components chosen to match closely the impedance of the cell (General Radio type 500-F $500\ \Omega \pm 0.05\%$ resistors in series with General Radio type 505-T $100\ \text{nF} \pm 0.5\%$ capacitors); the balancing arm consisted of a General Radio type 1432-N decade resistor box plus a series $0-1\ \Omega$ potentiometer, in series with a General Radio type 1419-K decade capacitor box plus a parallel $0-1\ \text{nF}$ variable air capacitor. The direct voltage source (lead battery and potentiometer) was blocked for a.c. with a 2.5 kHz choke. The oscillator used was a Hewlett-Packard model 200 CD, coupled to the bridge *via* a General Radio type 578-A shielded transformer. The alternating voltage across the cell was monitored on the oscilloscope before each measurement and adjusted to 10 mV peak-to-peak. The detector used was a General Radio type 1232-A, a highly sensitive frequency-selective amplifier and null detector, the output of which was displayed on a Tektronix type 533-A oscilloscope with type D plug-in amplifier. All components and cables were shielded on a single ground; the dropping mercury electrode was grounded and the oscillator, detector-amplifier and oscilloscope all had one terminal grounded. The bridge was balanced at 90% of the drop time imposed by a mechanical hammer. The time base of the oscilloscope was expanded 5 times and only the last 20% was displayed on the screen. The hammer dislodging the drops was driven by a synchronous motor and had a period of about 4 sec. The capillary used was made out of a regular Sargent S-29417 "6-12 sec" polarographic capillary, which was given a constriction so as to yield a free drop time of about 100 sec in the solution, with a Hg column of

80 cm as used in the experiments. The tip of the capillary was slightly tapered*, but not siliconized.

A large (20 cm²) Hg pool served as an auxiliary and reference electrode. The 0.1 M KCl solution was made from analytical-grade KCl and twice-distilled water and was de-aerated with tank nitrogen. The temperature was 25 ± 1°.

The measured cell impedances (no correction whatsoever applied) at two different direct voltages across the cell are given in Table I, together with calculated

TABLE I
EXPERIMENTAL AND CALCULATED RESULTS FOR 0.1 M KCl AT TWO DIFFERENT CELL VOLTAGES.

The cell impedance has been measured as series combination of R_s and C_s . The values of R_{s01} used in the calculation of Y_{ei}'/ω and Y_{ei}''/ω have been determined from the cell impedance planes as 570 ± 5 Ω, and 550 ± 5 Ω, respectively. Y_{ei}'/ω and Y_{ei}''/ω are the real and imaginary components of Y_{ei}/ω , respectively.

Frequency (kc/sec)	dummy cell		0.1 M KCl, E = -0.5 V (Hg)				0.1 M KCl, E = -1.0 V (Hg)			
	$R_s(\Omega)$	$C_s(nF)$	$R_s(\Omega)$	$C_s(nF)$	$\frac{Y_{ei}'}{\omega}(nF)$	$\frac{Y_{ei}''}{\omega}(nF)$	$R_s(\Omega)$	$C_s(nF)$	$\frac{Y_{ei}'}{\omega}(nF)$	$\frac{Y_{ei}''}{\omega}(nF)$
0.4	491	150.0	600	155	1.8	155	598	82.7	0.8	82.7
0.5	494	150.0	600	155	2.3	155	595	82.7	1.1	82.7
0.7	497	150.1	599	154	3.0	154	591	82.7	1.2	82.7
1	498	150.0	599	154	4.3	154	591	82.7	1.8	82.7
1.5	498	149.9	597	152	5.9	152	591	82.5	2.6	82.5
2	499	149.9	594	150	6.8	150	594	82.1	3.7	82.1
3	499	149.7	588	147	7.3	147	590	81.4	5.0	81.2
4	499	149.4	584	145	7.4	145	587	80.6	6.0	80.1
5	499	148.9	582	142	7.6	142	584	79.6	6.8	79.0
7	499	148.1	578	139	6.8	139	578	77.5	7.7	76.8
10	499	146.3	575	135	5.7	135	571	75.2	7.5	74.5

results for Y_{ei}/ω . Also given are measurements on a dummy cell consisting of 500 Ω in series with 150 nF (General Radio 500-F, 505-T and 505-R) which indicate the inherent errors of the bridge. The solution resistance (including that of the capillary and wiring), R_{s01} , was determined by extrapolation to infinite frequency of the measured cell impedance in a complex impedance plane ($-j/\omega C_s$ vs. R_s)^{10,25,26,27}. Owing to intermediate manipulation of the cell, R_{s01} was not the same in the two sets of measurements.

The final results are given in Fig. 4. We have also indicated in Fig. 4a what the result would be after correction of the experimental R_s and C_s data by a factor which would make the dummy cell measurements read 500 Ω and 150.0 nF at every frequency (e.g., at 5 kc/sec R_s has been multiplied by 500/499 = 1.002 and C_s by 150.0/148.9 = 1.007). It should be realized that the determination of R_s and C_s with a

* We tried several capillaries with straight tips, both with and without a constriction, to lower the mass flow rate (all capillaries were, or were made from, Sargent S-29417 polarographic capillaries). It appeared to be impossible to make accurate measurements with the capillaries with a straight bore at the orifice. When the bridge seemed to be sharply balanced, and we waited and observed the scope trace for a number of drops to see whether the reading was stable, there was always a roughly cyclic shift in the balance, with a period of 10–20 drops. We believe that this is due to the formation of pockets¹¹. The measurements on the capillary with a tapered tip were perfectly stable and reproducible.

dropping mercury electrode is less accurate than with a dummy cell, owing to the practical difficulty of balancing a time-dependent impedance at a certain fixed moment; presumably the maximum error is $\pm 1\%$ in R_s and C_s , and such an inaccuracy would show up as a much larger one in the Y_{el}/ω plane. However such an error is a non-systematic one and consequently would result in a scatter of experimental points, which is not observed, see Fig. 4.

An inaccuracy of the same order of magnitude, but much more serious as it would lead to a systematic error, is caused by the uncertainty of $\pm 1\%$ in the extrapolated value of R_{so1} as obtained from the impedance plane. If we use the estimated extreme values of R_{so1} instead, the points in Fig. 4 change quite significantly, especially at the high frequencies; the general shape of the curves, however, remains the same. The results clearly cannot be ascribed to possible trace impurities (O_2, Cu^{2+} , etc.) as in that case the curves in the Y_{el}/ω plane would move away from the imaginary axis at lower frequencies¹⁶; moreover it would be a coincidence if faradaic admittances from impurities would be involved precisely at the two randomly chosen direct voltages. The difference between the two curves is due to the change in surface tension and double-layer capacitance with direct voltage. The direct voltage across the cell is very nearly the electrode potential *vs.* a 0.1 *N* calomel electrode, as the direct charging current and hence the resulting iR drop in the cell is negligible with the very slowly dropping electrode used. Moreover a slowly changing surface area greatly enhances the precision with which the bridge can be balanced at a certain time, and at a small surface area of the drop the effect of the liquid film is relatively important.

Although the measurements are not yet accurate enough to allow a quantitative evaluation, we feel that the present preliminary results tend to support our approach and give the following indications.

(i) The virtual absence of a variation of the double-layer capacitance with frequency over a small frequency interval does not necessarily imply the absence of capillary response. At *low* frequencies the capacitance of the solution film may be included in the measured capacitance. In our experiments this situation prevailed in 0.1 *M* KCl at frequencies up to about 1 kc/sec and one would expect this to occur in 1 *M* KCl up to about 10 kc/sec!

(ii) An extrapolation to infinite frequency to correct for the film is not possible for our measurements, partly because the accuracy of the measurements at high frequencies is insufficient (due to the inductance of the bridge and the inaccuracy of Y_{el}' which is essentially determined by the difference between two almost equal quantities).

(iii) The effect is certainly not negligible for precision measurements; it should be realized however that in our experiments the effect has been exaggerated by the use of very small droplets. One may expect that the effect is relatively even more important at high positive and negative potentials because there the low surface tension between Hg and aqueous solutions facilitates the formation of a film.

A more thorough experimental investigation, including different electrolyte concentrations and drop times, is now being made.

ACKNOWLEDGEMENTS

I wish to thank Prof. P. DELAHAY for his kind interest in this work, which has been supported by the Office of Naval Research. The author is also indebted to the

N.A.T.O. for a travelling grant, obtained through the Netherlands Organization for the Advancement of Pure Research (Z.W.O.).

SUMMARY

A solution film inside the capillary is the principal locus of shielding at a D.M.E. A graphical method for obtaining the true double-layer capacitance is presented, and a model is given which represents the electrical characteristics of the solution film.

REFERENCES

- 1 D. C. GRAHAME, *J. Am. Chem. Soc.*, 63 (1941) 1207.
- 2 D. C. GRAHAME, *J. Am. Chem. Soc.*, 68 (1946) 301.
- 3 V. I. MELIK-GAIKAZYAN, *Zh. Fiz. Khim.*, 26 (1952) 560.
- 4 G. C. BARKER AND I. L. JENKINS, *Analyst*, 77 (1952) 685.
- 5 M. VON STACKELBERG AND V. TOOME, *Leybold Polarograph. Ber.*, 1 (1953) 55.
- 6 J. O'M. BOCKRIS, W. MEHL, B. E. CONWAY AND L. YOUNG, *J. Chem. Phys.*, 25 (1956) 776.
- 7 J. O'M. BOCKRIS AND B. E. CONWAY, *J. Chem. Phys.*, 28 (1958) 707.
- 8 R. DE LEVIE, The influence of surface roughness of solid electrodes on electrochemical measurements, *Electrochim. Acta*, in press.
- 9 G. C. BARKER, *Anal. Chim. Acta*, 18 (1958) 118.
- 10 R. DE LEVIE, *Electrochim. Acta*, 9 (1964) 1231.
- 11 W. D. COOKE, M. T. KELLEY AND D. J. FISCHER, *Anal. Chem.*, 33 (1961) 1209.
- 12 D. LAFORGUE-KANTZNER AND M. MUXART, *Electrochim. Acta*, 9 (1964) 151.
- 13 D. H. GRANTHAM, *Thesis*, Iowa State Univ., 1962; *Dissertation Abstr.*, 23 (1963) 3646.
- 14 G. J. HILLS AND D. J. G. IVES, *Nature*, 165 (1950) 530; *J. Chem. Soc.*, (1951) 311.
- 15 D. J. G. IVES AND G. J. JANZ, *Reference Electrodes*, edited by D. J. G. IVES AND G. J. JANZ, Academic Press, New York, 1961, p. 131.
- 16 R. DE LEVIE, On impedance measurements: The determination of the double layer capacitance in the presence of an electrode reaction, *Electrochim. Acta*, in press.
- 17 F. CHAO-ORTEGA, *J. Rech. Centre Nat. Rech. Sci., Lab. Bellevue (Paris)*, 58 (1962) 5.
- 18 M. VON STACKELBERG, *Z. Anal. Chem.*, 173 (1960) 90.
- 19 M. VON STACKELBERG AND R. DOPPELFELD, *Advances in Polarography*, Vol. II, edited by I. S. LONGMUIR, Pergamon, Oxford, 1960, p. 68.
- 20 G. C. BARKER AND A. W. GARDNER, *Advances in Polarography*, Vol. I, edited by I. S. LONGMUIR, Pergamon, Oxford, 1960, p. 330.
- 21 W. LORENZ, *Z. Physik. Chem., Leipzig*, 205 (1956) 311.
- 22 H. P. RAAEN, *Anal. Chem.*, 34 (1962) 1714.
- 23 H. GERISCHER, *Z. Physik. Chem., Leipzig*, 202 (1953) 302.
- 24 M. SLUYTERS-REHBACH, B. TIMMER AND J. H. SLUYTERS, *Rec. Trav. Chim.*, 82 (1963) 553.
- 25 H. GERISCHER, *Z. Elektrochem.*, 58 (1954) 9.
- 26 J. EULER AND K. DEHMELT, *Z. Elektrochem.*, 61 (1957) 1200.
- 27 J. H. SLUYTERS, *Rec. Trav. Chim.*, 79 (1960) 1092.
- 28 J. J. LINGANE, *J. Am. Chem. Soc.*, 75 (1953) 788.
- 29 R. J. NEWCOMBE AND R. WOODS, *Trans. Faraday Soc.*, 57 (1961) 130.
- 30 R. J. NEWCOMBE AND R. WOODS, *Advances in Polarography*, Vol. I, edited by I. S. LONGMUIR, Pergamon, Oxford, 1960, p. 375.
- 31 R. PARSONS, *Modern Aspects of Electrochemistry*, Vol. I, edited by J. O'M. BOCKRIS, Butterworth, London, 1954, p. 160; G. KORTUM AND J. O'M. BOCKRIS, *Textbook of Electrochemistry*, Vol II, Elsevier, 1951, p. 358.
- 32 R. PARSONS, *Modern Aspects of Electrochemistry*, Vol. I, edited by J. O'M. BOCKRIS, Butterworth, London, 1954 p. 137.
- 33 R. J. JOHNSTON AND A. R. UBBELOHDE, *Proc. Roy. Soc.*, A206 (1951) 275.
- 34 B. C. SOUTHWORTH, *Dissertation Abstr.*, 21 (1960) 441.

A STUDY OF THE ANOMALOUS BEHAVIOUR OF THE GLASS ELECTRODE IN SOLUTIONS CONTAINING HYDROFLUORIC ACID

E. SØRENSEN AND T. LUNDGAARD

The Danish Atomic Energy Commission Research Establishment, Risø (Denmark)

(Received October 28th, 1964)

Although the research of recent years has brought about a considerable extension of the applicability of the glass electrode, its behaviour in solutions containing free HF has attracted little attention^{1,2} considering the special action of this acid on glass.

In this laboratory a glass electrode has been used for some time as a convenient device for controlling the addition of HF to aqueous solutions. This mode of operation was the incentive to the present work, in which we examine the variation of the glass-electrode potential when the outer glass surface is exposed to dilute solutions of HF.

EXPERIMENTS

A Radiometer glass-calomel electrode assembly, type GK 202B, is used in combination with a Radiometer pH-meter, model 22, and a Varian graphic recorder. The perspex electrode vessel is made so as to allow a continuous flow of the test solutions (Fig. 1). The small volume of liquid contained in the vessel can be replaced within a fraction of a second through the two introduction holes, connected with independent feed pumps.

In order to eliminate variations in H^+ activity, all the solutions used are 0.1 *N* in HCl. The temperature is kept at 21°. A glass electrode which has been soaked in 0.1 *N* HCl overnight is placed in the cell and treated alternately with pure 0.1 *N* HCl and with 0.1 mole/l of HF in 0.1 *N* HCl, both applied at a rate of 0.5 ml/sec. During this process the potential difference is registered by the recorder as shown in Fig. 2. The potential drop caused by the first contact with HF is seen to be different from subsequent ones. This initial behaviour is the more marked the longer the electrode has been soaking in HF-free aqueous solution. During the periods of regeneration the potential curve shows a steep rise, which is followed by a moderately ascending part converging towards the normal electrode potential (Fig. 2, II and IV). As the data given below presupposes the sensitivity of a recently HF-treated glass electrode, the regeneration time is kept within 3 min, and reproducible results are obtained by introducing the HF solution at the same stage every time.

Experiments with varying [HF] gave a series of potential *vs.* time curves. A selection of these is shown in Fig. 3. They are seen to be composed essentially of two

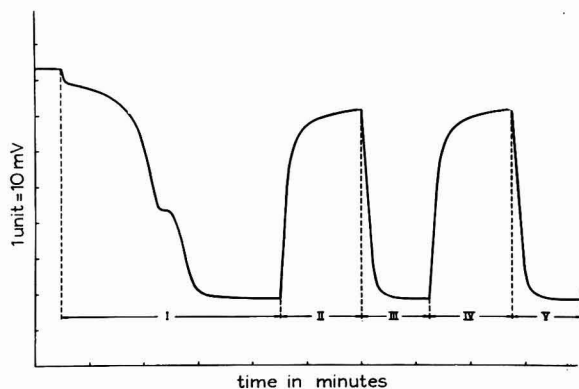
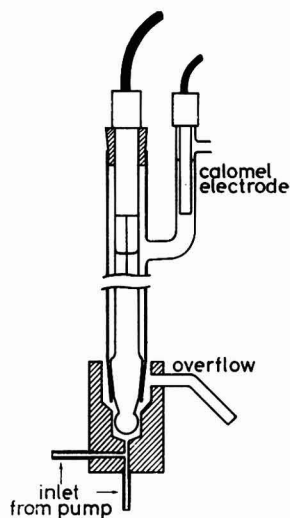


Fig. 1. Glass-calomel electrode assembly and electrode vessel.

Fig. 2. Graph of potential vs. time during pre-treatment of a glass electrode which has been kept overnight in 0.1 N HCl. Periods I, III and V, flow of 0.1 mole/l of HF in 0.1 N HCl; periods II and IV, regeneration with pure 0.1 N HCl.

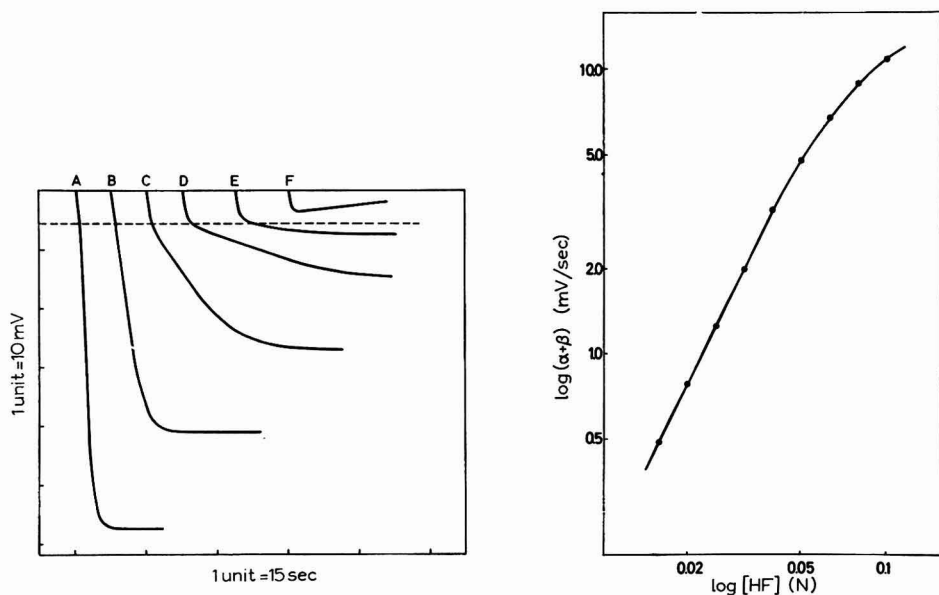


Fig. 3. Potential change of a pre-treated and regenerated glass electrode on contact with a series of HF in 0.1 N HCl solutions. The starting points correspond to the beginning of periods III and V in Fig. 2. (A), 0.1 N; (B), 0.04 N; (C), 0.02 N; (D), 0.0125 N; (E), 0.0078 N ~ 156 p.p.m. HF; (F), 0.0039 N ~ 78 p.p.m. HF. The dashed line indicates the approximate limit of the initial drop.

Fig. 4. $\log(\alpha + \beta)$ vs. $\log [HF]$ ($[HF] > 0.01 N$).

parts, namely a rapid drop, which is nearly 5.5 mV for the curves representing [HF] above 0.01 *N*, and a further decrease. The latter dominates at higher [HF], where it is almost linear. At lower [HF] the slope declines while the linearity becomes less pronounced. If the slope expressed in mV/sec is denoted by α , a constant, β , can be determined in such a way that the plot of $\log(\alpha + \beta)$ vs. \log [HF] is strictly linear in the lower part of the concentration range (Fig. 4). The meaning of β will be discussed later.

It appears that for each [HF] above 0.01 *N* a new constant potential is established. If the difference between the normal glass-electrode potential in 0.1 *N* HCl and the HF-depressed potential is called ΔE_{HF} and plotted against \log [HF], a curve is obtained which deviates little from a straight line (Fig. 5). This result formally corresponds to an HF-electrode function:

$$E_{\text{HF}} - E_0 = -\frac{RT}{Fz} \log [\text{HF}],$$

where $z = 1.4$.

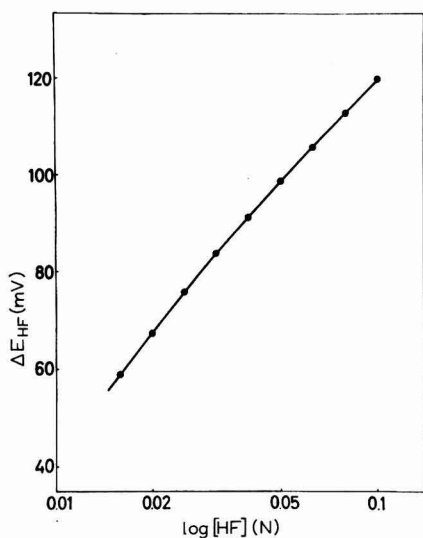


Fig. 5. ΔE_{HF} vs. \log [HF] ([HF] > 0.01 *N*).

At [HF] below 0.01 *N* the potential does not seem to attain a definite value, but after a rapid drop, ΔE_{HF} , it continues the slow climb of the preceding regeneration curve (Fig. 3F). The relation $\Delta E_{\text{HF}} = k [\text{HF}]^n$ is here found to be obeyed fairly well. Figure 6 shows the plot of $\log(\Delta E_{\text{HF}}) = n \log [\text{HF}] + \text{const.}$, whence $n = 0.6$.

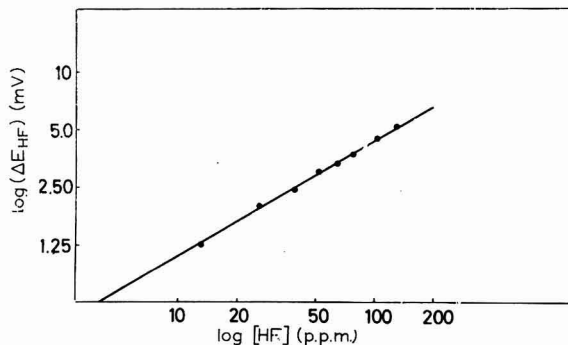


Fig. 6. $\log (\Delta E_{\text{HF}})$ vs. $\log [\text{HF}]$ ($[\text{HF}] < 0.01 \text{ N}$).

DISCUSSION

According to BOKSAY *et al.*³ it is assumed that practically only protons participate in the electrode processes taking place in the hydrated surface layer. Voltage anomalies may then arise from the exchange of some of the proton acceptors for others to which the protons are bound with altered forces.

When a hydrated glass surface is exposed to dilute hydrofluoric acid, a reaction takes place which can be expressed in the simplified form



where x and y represent average numbers.

If we assume that the voltage deviation of the electrode is proportional to the degree of surface fluorination, dE/dt will be closely related to the reaction rate. The terms, α and β , of Fig. 4 are interpreted as the rates of the initial net reaction and the reverse reaction, respectively. This is confirmed by the fact that the magnitude of β is very similar to the average slope of the regeneration curve after the steep rise. Thus $(\alpha + \beta)$ represents the forward reaction rate. It is seen from Fig. 4 that $(\alpha + \beta)$ is proportional to $[\text{HF}]^2$ in the lower concentration range as the slope of the linear curve part equals 2.0. This can be explained by supposing that the observed change of the glass-electrode potential follows upon the uptake of 2 F per Si-atom, where the second step is the rate-determining step.

Finally the reverse reaction rate reaches a magnitude equal to that of the forward reaction rate (compare the steep rise of the regeneration curve), and a stationary state is established corresponding to the constant value of the glass-electrode potential.

The negative deviation is in agreement with the assumption that the substitution of F^- for OH^- increases the dissociation constant of silicic acid.

The relation presented in Fig. 6 shows a formal similarity with a Freundlich adsorption isotherm. It may well be assumed that the potential drop in question is due to adsorption of HF by the glass surface. This is supported by the low $[\text{HF}]$ sufficient to produce the effect, and the instantaneous character of the latter.

APPENDIX

In a routine chemical operation a 70% solution of HF was added to a uranium leach liquor containing chiefly Na_2SO_4 , $\text{Al}_2(\text{SO}_4)_3$ and SiO_2 . aq. When the formation of fluoride complexes ceased, the potential of an immersed glass electrode underwent a characteristic change, indicating a slight excess of free HF. However, the amount added did not agree with calculations based upon an analysis of the liquor and certain stoichiometric assumptions. It was therefore decided to perform similar experiments with separate compounds of elements known to form fluoride complexes.

To 50 ml of each of the following solutions, contained in a polystyrene beaker equipped with a magnetic stirrer, 2 M HF was added at a rate of 5 ml/min:

- (a) 0.2 M $\text{Fe}(\text{ClO}_4)_3$;
- (b) 0.2 M H_3BO_3 in 0.1 N HCl;

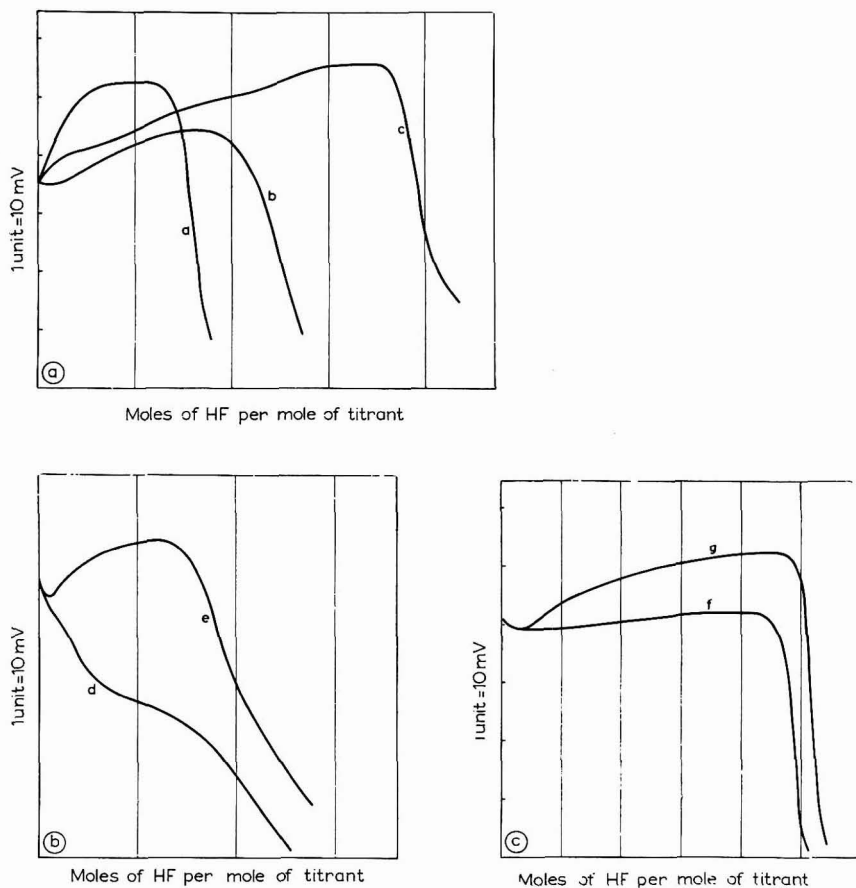


Fig. 7. (a), 0.2 M $\text{Fe}(\text{ClO}_4)_3$; (b), 0.2 M H_3BO_3 in 0.1 N HCl; (c), 0.2 M ZrOCl_2 in 0.1 N HCl; (d), 0.2 M AlCl_3 in 0.1 N HCl; (e), 0.1 M $\text{Al}_2(\text{SO}_4)_3$ in 0.1 N HCl; (f), silicic acid in 0.1 N HCl (0.75% SiO_2); (g), (f) + 2 KCl per 1 SiO_2 . See text.

- (c) 0.2 M $ZrOCl_2$ in 0.1 N HCl;
- (d) 0.2 M $AlCl_3$ in 0.1 N HCl;
- (e) 0.1 M $Al_2(SO_4)_3$ in 0.1 N HCl;
- (f) silicic-acid solution (0.75% SiO_2) in 0.1 N HCl;
- (g) (f) + 2 KCl per SiO_2 .

Figures 7(a, b, c) show the variations of the glass-electrode potential as a function of the amount of HF added. The initial rise is due to liberation of H^+ during the complex formation. The drop later is indicative of free HF in the mixture. A semi-quantitative determination can be made on comparison with Fig. 3.

It should be noted, however, that when the $[HF]$ exceeds 0.05 mole/l, no further details can be obtained by this method.

In Fig. 7a Fe^{3+} is introduced in the form of perchlorate in order to avoid complexing competition from anions other than F^- . In the presence of ZrO^{2+} the HF concn. is negligible until the stoichiometric amount has been added. This property of ZrO^{2+} makes it the preferred titrant for F^- .

In Fig. 7b the difference between (d) and (e) is probably due to the formation of a mixed complex of Al^{3+} , SO_4^{2-} and F^- . In fact this agrees with experience from the manufacture of synthetic cryolite, where sulphate in the raw materials inevitably gets into the product.

In Fig. 7c the effect of K^+ is a low $[SiF_6^{2-}]$ ensured by the solubility product of K_2SiF_6 . Even then a considerable surplus of HF is needed to convert SiO_2 . aq. entirely into SiF_6^{2-} .

ACKNOWLEDGEMENT

The authors have benefited greatly from discussions, particularly with C. U. LINDERSTRØM-LANG and the late T. ROSENBERG.

SUMMARY

A defined surface hydration of the glass electrode is secured by pre-treatment with 0.1 N HF followed by rinsing with pure 0.1 N HCl for a few minutes. On subsequent contact with 0.1 N HCl containing HF, the electrode potential shows a change which is determined by the $[HF]$.

The immediate reaction is an adsorption of HF by the glass surface. This is followed, at $[HF]$ higher than 0.01 N, by the substitution of two F^- for OH^- per Si atom.

With increasing HF the attack on the Si-O-Si bonds becomes severe, but it can be tolerated to a considerable degree because the newly formed surface is identical with the previous one.

Some applications of the glass electrode in titrations with HF are suggested in an appendix.

REFERENCES

- 1 M. DOLE, R. M. ROBERTS AND C. E. HOLLEY, JR., *J. Am. Chem. Soc.*, 63 (1941) 725.
- 2 D. HUBBARD AND G. F. RYNDERS, *J. Res. Natl. Bur. Std.*, 39 (1947) 561.
- 3 Z. BOKSAY, B. CSÁKVÁRI AND B. LENGVEL, *Z. Physik. Chem., Leipzig*, 207 (1957) 223.

POLAROGRAPHIC REDUCTION OF NITRATE IONS IN THE PRESENCE OF ZIRCONIUM SALTS

H. WHITNEY WHARTON

Procter and Gamble Company, Miami Valley Laboratories, Cincinnati 39, Ohio (U.S.A.)

(Received September 14th, 1964)

The polarographic determination of nitrate ions usually involves a catalytic reduction of the nitrate in the presence of uranium². The U(III) produced by polarographic reduction of the U(V) ion probably catalyzes the nitrate reduction. This method is somewhat limited in that i_d/C_{NO_3} is constant only between 0.05 and 0.4 mM nitrate. A wider concentration range of nitrate reductions has been reported using 0.1 M zirconyl chloride as supporting electrolyte⁴. Nitrate in the range 0.007–1.7 mM is satisfactorily reduced but the nitrate wave is barely resolved from the hydrogen discharge wave of the supporting electrolyte. Iron(II) removes the nitrate wave and the amount of nitrate is taken as the difference between the polarographic wave before and after the addition of the iron(II). MECHELYNCK AND MECHELYNCK-DAVID³ made an extended study of the nitrate reduction in zirconium solutions. Zirconium was used in the concentration range 10^{-3} – 10^{-7} M in 0.1 M sodium chloride supporting electrolyte. A wave attributed to the irreversible reduction of nitrate was found in the range 10^{-2} – 10^{-7} M nitrate and could be used analytically in the range $5 \cdot 10^{-3}$ – 10^{-5} M; 10^{-3} M zirconium in 0.1 M sodium chloride was used as supporting electrolyte. These authors stated that the reduction was catalyzed by the zirconium.

This work has been extended to provide a reliable polarographic system for determining nitrate ions in the concentration range $2.4 \cdot 10^{-5}$ – $2 \cdot 10^{-2}$ M using 0.1 M zirconyl chloride as supporting electrolyte. In addition, a study of the reduction itself has been made which indicates an irreversible reduction of a distinct Zr–NO₃ complex; the particular complex depends on the relative and absolute concentrations of each ion. The effect of ageing of the zirconium supporting electrolyte solutions on the character of the polarographic reduction wave of nitrate ion was also investigated.

EXPERIMENTAL

Reagents, apparatus and procedures

Reagent-grade chemicals were used as received. All solutions were prepared using de-ionized water. Tank nitrogen was used for de-aeration without further purification.

Standard nitrate solutions were prepared by weight from dried potassium nitrate. The 0.2 M zirconium solutions were prepared from zirconyl chloride octahydrate and standardized by titration with ethylenediaminetetraacetate using SPADNS as

indicator. These zirconium solutions were allowed to age for at least two weeks prior to use as supporting electrolytes for analytical purposes and for the studies regarding the Zr-NO₃ species present in solution.

For studying the effect of the age of the zirconium solutions on the shape of the polarographic reduction wave, freshly prepared solutions of zirconyl chloride were mixed with appropriate amounts of nitrate and diluted to final zirconium concentrations of 0.1, 0.05, 0.01 and 0.001 *M*. The latter was made 0.1 *M* in potassium chloride as added supporting electrolyte. In addition, similar solutions were prepared from 0.2 *M* zirconium solutions which had been allowed to age for appropriate times. The pH of all solutions containing zirconium was maintained below pH 2.5 to prevent precipitation of hydrated zirconyl oxide.

All polarograms were obtained using the Sargent Model XXI recording polarograph and the dropping mercury electrode. Values for $m^3t^{\frac{1}{2}}$ were maintained at about 1.6. All solutions were de-aerated for 10 min with nitrogen passed through a fritted-glass gas dispersion tube. No maxima suppressor was required. The rate of application of the impressed potential was about 75 mV/min. Half-wave potentials were determined from plots of the maximum current of the undamped recorder oscillations *vs.* the applied potential, using the equal area method. Diffusion current values were extrapolated and measured at the half-wave potential, as the slopes of the residual current and the diffusion current were not the same.

RESULTS AND DISCUSSION

The ratio of diffusion current to concentration, i_a/C_{NO_3} , was constant at a value of 15.2 μA per mmole/l in 0.1 *M* zirconyl chloride supporting electrolyte over the concentration range $2.4 \cdot 10^{-5}$ – $2.0 \cdot 10^{-2}$ *M* nitrate. The reduction wave was well-defined when aged zirconium solutions were used. Linear diffusion current *vs.* nitrate concentration plots were also obtained with less concentrated zirconium solutions (0.05, 0.01 and 0.001 *M*) as supporting electrolyte, but only over reduced nitrate concentration ranges.

Characteristics of the polarographic reduction of nitrate ions

As the nitrate concentration increased from 10^{-4} to 10^{-2} *M*, in 0.1 *M* ZrOCl₂ supporting electrolyte, the half-wave potential shifted from about -0.8 V *vs.* the S.C.E. to about -1.0 V. Although both anodic and cathodic scanning produced identical wave forms, half-wave potentials and diffusion currents, a plot of $\log i/(i_a - i)$ *vs.* *E* gave a straight line, the slope of which gives an apparent *n* value of 0.310 electrons.

Plots of *h vs.* $i_a/h^{\frac{1}{2}}$, where *h* is the height of the mercury head, indicate that the reduction process is not entirely diffusion-controlled. Table 1 shows the values for $i_a/h^{\frac{1}{2}}$ at three different mercury column heights for NO₃/Zr ratios in each region wherein distinct Zr-NO₃ species exist in the 0.00676 *M* Zr supporting electrolyte. The constancy of i_a/C_{NO_3} , however, indicates that the reductions are nearly diffusion-controlled and that any kinetic factors are secondary.

Influence of the age of the zirconium solutions on the reduction of nitrate ions

The influence of the age of the zirconium solution on the reduction of the nitrate ion is shown in Fig. 1 and Table 2 for 0.1 *M* zirconium and $2.4 \cdot 10^{-3}$ *M* nitrate. Curve A

TABLE 1

VARIATION OF $i_a/h^{1/2}$ WITH CHANGES IN THE HEIGHT OF THE MERCURY COLUMN AT DIFFERENT NO_3/Zr RATIOS

Height of Hg column h (cm)	Ratio NO_3/Zr	$i_a/h^{1/2}$ ($\mu\text{A}/\text{cm}^{1/2}$)
25.0	0.12	2.34
45.5	0.12	2.16
60.5	0.12	2.08
25.0	0.47	7.20
45.5	0.47	6.53
60.5	0.47	5.76
25.0	0.77	10.08
45.5	0.77	9.02
60.5	0.77	8.41

TABLE 2

DIFFUSION CURRENT (i_a) AND HALF-WAVE POTENTIAL ($E_{1/2}$) OF 2.4 mM KNO_3 FRESHLY MIXED WITH 0.1 M ZrOCl_2

Age of ZrOCl_2 (days)	Slope of i_a plateau ($\mu\text{A}/v$)	i_a (μA)	$E_{1/2}$ vs. S.C.E. (v)
0	54	31.2	-1.00
2	26	38.4	-0.90
5	18	40.0	-0.89
7	14	41.2	-0.89
12	10	42.8	-0.86
15	10	44.4	-0.86

TABLE 3

SUMMARY OF $\text{Zr}-\text{NO}_3$ SPECIES PRESENT IN SOLUTION AS DETERMINED FROM THE MOLE RATIO STUDY

Zr. concn. (M)	NO_3 concn. range (M)	Species present (NO_3/Zr)
0.00343	$5 \cdot 10^{-5}$ - $6 \cdot 10^{-3}$	1.00/4.0 3.00/4.0
0.00676	$4 \cdot 10^{-4}$ - $9 \cdot 10^{-3}$	1.00/4.0 2.99/4.0
0.00686	$1 \cdot 10^{-4}$ - $1 \cdot 10^{-2}$	1.00/4.0 3.04/4.0
0.01014	$5 \cdot 10^{-4}$ - $1.5 \cdot 10^{-2}$	1.98/3.0

and curve B of Fig. 1 suggest that the ageing of freshly prepared zirconium solutions is inhibited by the presence of the nitrate ion. Curve C, the envelope of values obtained from freshly mixed solutions of zirconium and nitrate (the zirconium having been aged as indicated) further supports this conclusion. Figure 2 shows the appearance of waves of solutions of fresh zirconium, and of zirconium allowed to age for

two weeks in the absence of nitrate. The general result of ageing the zirconium is that the diffusion current plateau of the polarographic reduction wave of the nitrate ion becomes more pronounced and horizontal while the half-wave potential shifts in an anodic direction. This is highly favorable and increases the usefulness of the wave

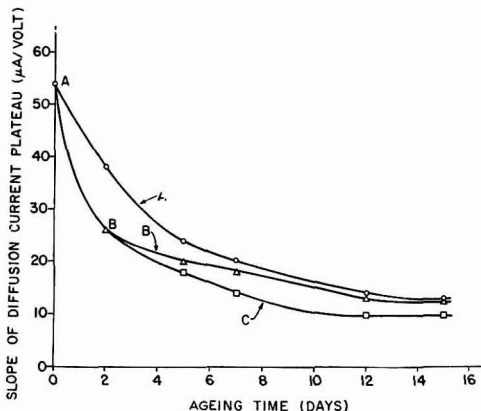


Fig. 1. Effect of ageing of the supporting electrolyte on the slope of the diffusion current plateau; all solutions are 0.1 M ZrOCl_2 and 2.4 mM KNO_3 . (A), ZrOCl_2 and KNO_3 mixed, and aged as shown; (B), KNO_3 added to two-day old ZrOCl_2 ; ageing continued; (C), Envelope of variously aged 0.1 M ZrOCl_2 freshly mixed with 2.4 mM KNO_3 .

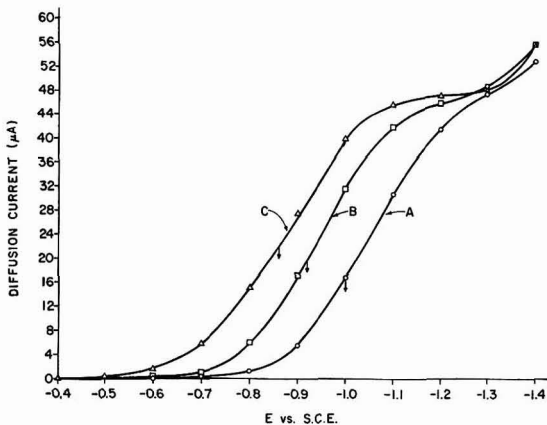


Fig. 2. Polarograms of the nitrate reduction (2.4 mM KNO_3) with fresh and aged supporting electrolyte (0.1 M ZrOCl_2). (A), 2 h old; (B), 2 days old; (C), 2 weeks old.

for analytical purposes. This effect of ageing is less noticeable as the concentration of zirconium decreases, and is negligible below 0.05 M . Thus the method of RAND AND HEUKELEKIAN should require aged zirconium, which should also eliminate the need for the addition of iron(II), while the method of MECHELYNCK AND MECHELYNCK-DAVID would not require aged zirconium. The change in characteristics of zirconium

solutions on ageing has been reported previously in connection with the use of zirconium and an azo dye for the spectrophotometric determination of fluoride⁵.

The examination of the reduction process suggests that, depending on the relative and absolute concentrations of zirconium and of nitrate, distinct Zr-NO₃ species are

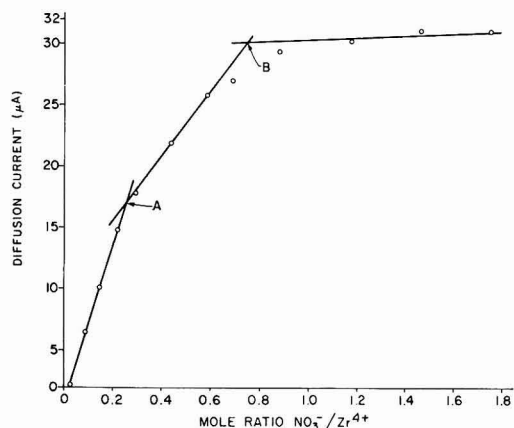


Fig. 3. Mole ratio plot, 0.00343 *M* Zr. (A), 0.250 NO₃⁻/Zr⁴⁺ or 1.00 NO₃⁻/4.00 Zr⁴⁺; (B), 0.750 NO₃⁻/Zr⁴⁺ or 3.00 NO₃⁻/4.00 Zr⁴⁺.

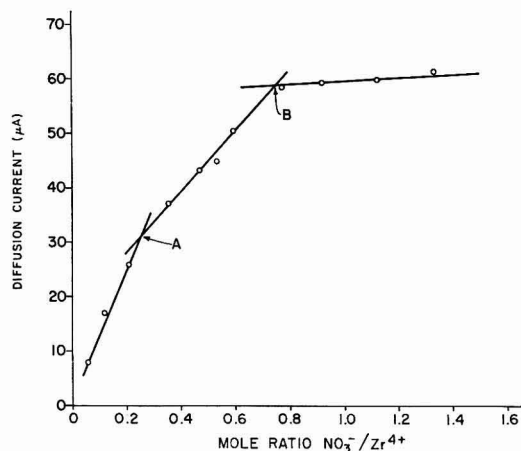


Fig. 4. Mole ratio plot, 0.00676 *M* Zr. (A), 0.250 NO₃⁻/Zr⁴⁺ or 1.00 NO₃⁻/4.00 Zr⁴⁺; (B), 0.747 NO₃⁻/Zr⁴⁺ or 2.99 NO₃⁻/4.00 Zr⁴⁺.

present in solution and are apparently the reducible species. Figures 3–5 show typical plots of diffusion current vs. the mole ratio of nitrate to zirconium at three concentrations of zirconium and the indicated ranges of nitrate concentration. Table 3 summarizes the species present as shown by repeated application of this mole ratio method.

These polarographic observations are further supported by the spectrophotometric work of KOLIKOV¹. He reported that, as the concentration of nitrate increased, the absorptions due to Zr-NO₃ complexes increased in intensity while the intensity of those absorptions attributed to Zr-OH complexes diminished.

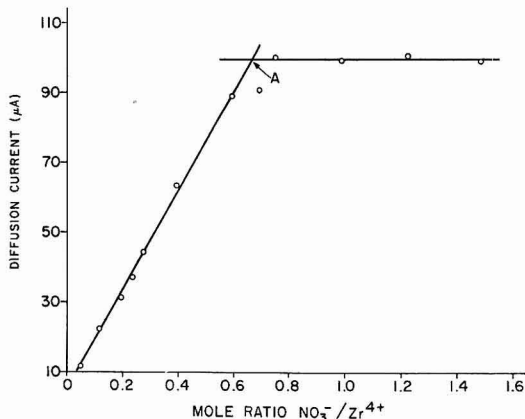


Fig. 5. Mole ratio plot, 0.01014 *M* Zr. (A), 0.660 NO₃⁻/Zr⁴⁺ or 1.98 NO₃⁻/3.00 Zr⁴⁺.

SUMMARY

The present study has shown that the irreversible polarographic reduction of the nitrate ion in the presence of 0.1 *M* zirconium as supporting electrolyte is not catalytic, but rather involves the reduction of distinct Zr-NO₃ complexes. The nature of the reducible species is dependent on the relative and absolute concentrations of the zirconium and nitrate ions. It is also apparent that the age of the solution of zirconium used as supporting electrolyte affects the character of the nitrate polarographic wave. Freshly prepared solutions of zirconium give nitrate waves which are poorly resolved from the hydrogen discharge wave of the supporting electrolyte. Zirconium solutions aged for at least two weeks give well-defined, completely resolved waves ideally suited for analytical use. Using aged 0.1 *M* zirconyl chloride solutions as supporting electrolyte, a constant i_d/C_{NO_3} ratio is obtained over a wide range of nitrate ion concentration ($2.4 \cdot 10^{-5}$ to $2 \cdot 10^{-2}$ *M*).

REFERENCES

- 1 Y. M. KOLIKOV, *Zh. Prikl. Khim.*, 34 (1961) 248; *C.A.*, 55 (1961) 14036e.
- 2 I. M. KOLTHOFF, W. E. HARRIS AND G. MATSUYAMA, *J. Am. Chem. Soc.*, 66 (1944) 1782.
- 3 P. MECHELYNCK AND C. MECHELYNCK-DAVID, *Anal. Chim. Acta*, 21 (1959) 432.
- 4 M. C. RAND AND H. HEUKELEKIAN, *Anal. Chem.*, 25 (1953) 878.
- 5 H. W. WHARTON, *Anal. Chem.*, 34 (1962) 1296.

POLAROGRAPHIC BEHAVIOUR OF CHROMIUM AROMATIC COMPOUNDS: CYCLOPENTADIENYL-CYCLOHEPTATRIENYLCHROMIUM(o) AND (I+)

C. FURLANI, A. FURLANI AND L. SESTILI

*Chemical Institutes of the Universities of Trieste and Rome (Italy)**Centro per la Chimica dei Composti di Coordinazione, Consiglio Nazionale delle Ricerche, Rome (Italy)*

(Received August 1st, 1964)

FISCHER AND BREITSCHAFT¹ reported recently the preparation of $(C_5H_5)Cr^0-(C_7H_7)$ and of salts of $[(C_5H_5)Cr^I(C_7H_7)]^+$, a redox couple of π -sandwich complexes very similar to dibenzenechromium(o) and (I+), and gave evidence of close similarity of chemical behaviour between these two systems. Since we have previously^{2,3} investigated the polarographic behaviour of dibenzenechromium(o) and (I+) and its homologues, we have extended our investigations to the system $(C_5H_5)(C_7H_7)Cr(o)$ and (I+). It will be seen from the following discussion that the latter redox couple strongly resembles the former one in its almost complete polarographic reversibility, thus giving further proof of their similarity.

Even the fact that cyclopentadienyl-cycloheptatrienylchromium has a small but definite dipole moment¹, whereas dibenzenechromium is fully apolar, does not afford any significant difference in the observed polarographic characteristics. The present polarographic investigation was carried out under exactly the same conditions as our previous works^{2,3} on the chromium aromatic complexes, *viz.*, both in non-aqueous media (CH_3OH/C_6H_6 , 4:1) and in aqueous alkaline solutions (only for the $Cr(I+)$ species).

Conventional polarographic measurements were supported and integrated by oscillographic measurements. Our previous unpublished results on the oscillographic polarography of dibenzenechromium(I+), are also reported for comparison.

EXPERIMENTAL RESULTS

Apparatus and techniques

Conventional polarograms were taken with a photographic recording polarograph model AME, and oscillograms with a single sweep AMEL-488 oscillographic polarograph which can be operated both with saw-tooth and isosceles triangular waveforms (the latter sweep mode also allows observation of re-oxidation in reduced solutions of the $Cr(I+)$ species). The procedure for measurements in non-aqueous medium has already been described^{2,3} and was originally used by SARTORI *et al.*^{4,5}, RICCOBONI AND PAPOFF⁶. Owing to the extreme air sensitivity of the investigated compounds (especially of the $Cr(o)$ species), all measurements were carried out in an atmosphere of carefully purified N_2 ; non-aqueous solvents were freshly distilled

in air-free conditions and collected directly in the polarographic vessels. All reported potential values are corrected for ohmic drops, and always referred to the calomel electrode (in $N/2$ LiCl for benzene-methanol solutions, and in saturated KCl for the aqueous medium). All measurements were taken at room temperature ($20^\circ \pm 1^\circ$) and the D.M.E. for conventional polarograms had the following characteristic: $m^{2/3}t^{1/6} = 2.16 \text{ mg}^{2/3} \text{ sec}^{-1/2}$.

Polarographic behaviour in non-aqueous solvents

The couple, $[(C_5H_5)Cr^I(C_7H_7)]^+ / (C_5H_5)Cr^0(C_7H_7)$, exhibits in benzene-methanol (1:4 vol.) an almost reversible one-electron cathodic-anodic wave, with $E_{1/2}$ about $-0.7 \text{ V vs. } N/2 \text{ C.E.}$, practically independent of concentration and fraction of reduced and oxidised species. The observed polarographic reversibility matches the chemical reversibility of the couple (Table 1).

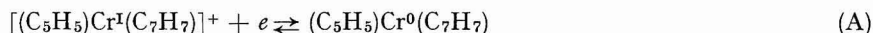
TABLE 1

POLAROGRAPHIC BEHAVIOUR OF $(C_5H_5)Cr^0(C_7H_7)$ AND $[(C_5H_5)Cr^I(C_7H_7)]I$ IN CH_3OH/C_6H_6 (4:1) WITH 0.50 M NaOH AT 19.5°

c (mmoles/l)	i_d (μA)	$E_{1/2}$ (V vs. $N/2$ C.E.)	i_d/c ($\mu A \text{ l/mmoles}$)
$[(C_7H_7)Cr^I(C_5H_5)]I$			
0.20	0.77	-0.695	3.85
0.40	1.48	-0.695	3.71
0.60	2.30	-0.695	3.83
0.80	3.07	-0.695	3.83
1.20	4.54	-0.692	3.78
1.50	5.63	-0.703	3.79
1.80	6.54	-0.695	3.68
		Average	
		-0.695	3.78
$(C_7H_7)Cr^0(C_5H_5)$			
0.73	2.48	-0.687	3.39
1.57	5.78	-0.699	3.61
2.36	8.37	-0.704	3.54
2.62	8.64	-0.699	3.29
2.88	9.47	-0.690	3.29
		Average	
		-0.696	3.43

Solutions of the Cr(0) species, showing initially only an anodic step, can be oxidised by air, when the polarographic step is gradually shifted through zero current (i_d and $E_{1/2}$ remaining constant) until it becomes entirely cathodic (see Fig. 1).

This is the same behaviour as was observed for dibenzenechromium² and corresponds therefore to the electrode reaction:



The only noticeable difference from the dibenzenechromium system is a positive

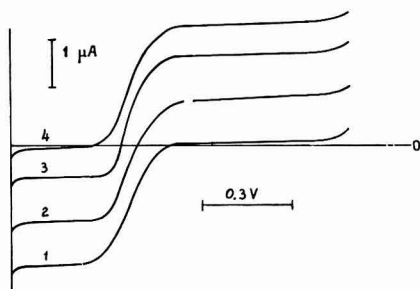


Fig. 1. Air oxidation of $0.73 \times 10^{-3} M$ $(C_5H_5)Cr^0(C_7H_7)$ in CH_3OH/C_6H_6 (4:1) with $0.50 M$ NaOH at 20° , beginning at $-0.3 V$.

TABLE 2

POLAROGRAPHIC CHARACTERISTICS OF $(C_6H_6)_2Cr(o)$ AND $(+I)$ AND OF $(C_5H_5)(C_7H_7)Cr(o)$ AND $(+I)$ IN CH_3OH/C_6H_6 (4:1) AT ROOM TEMPERATURE ($20 \pm 1^\circ$)

Substance	Supporting electrolyte (M)	$E_{1/2}$ (V vs. N/2 C.E.)	$i_d/Cm^{3/2}\tau^{1/2}$
$[(C_6H_6)_2Cr^I]I$	NaOH 0.35	-0.807	1.92
	LiCl 0.50	-0.835	1.9
$(C_6H_6)_2Cr^0$	NaOH 0.35	-0.807	1.9
	LiCl 0.50	-0.835	1.9
$[(C_5H_5)Cr^I(C_7H_7)]I$	NaOH 0.50	-0.695	1.75
	LiCl 0.50	-0.720	1.62
$(C_5H_5)Cr^0(C_7H_7)$	NaOH 0.50	-0.696	1.58
	LiCl 0.50	-0.720	1.52

shift of $\sim 0.1 V$ in $E_{1/2}$ of the C_5 - C_7 - Cr compounds (see Table 2). Other similarities are (i) slight variations in $E_{1/2}$ according to the composition of the supporting electrolyte (see Table 2); (ii) the slope of the waves, which is very close to the value for reversible one-electron steps ($\Delta E_{1/2}/\Delta \log [i/(i_a - i)] \sim 62 mV$ for $1.0 \times 10^{-3} M [(C_5H_5)Cr^I(C_7H_7)]^+$ in NaOH); (iii) the diffusion control (i_d being proportional to $h^{1/2}$); (iv) the diffusion current constant, which points to a value for the diffusion coefficient of the order of $8 \cdot 10^{-6} cm^2 sec^{-1}$.

Oscillopolarograms taken in the same medium confirm the simple, one-electron, diffusion-controlled nature of the redox electrode process (A). Thus $[(C_5H_5)Cr^I(C_7H_7)]I$ exhibits a single, well-defined cathodic peak, with E_p very close to $E_{1/2}$, and i_p proportional to both the concentration of electro-active substance, and $v_{1/2}$, (v = rate of potential sweep in V/sec), as expected for diffusion peaks (Figs. 2 and 3).

The oscillopolarographic behaviour of the $Cr(o)$ species has been investigated by means of re-oxidation during the descending part of triangular sweep wave forms (see Fig. 2) where a regular anodic peak appears, which corresponds closely to the reduction peak of the $Cr(I+)$ species. Direct observation of the anodic peak in non-aqueous solutions of $(C_5H_5)Cr^0(C_7H_7)$ does not lead to reproducible results, and the peak intensity is, at least with fresh solutions, anomalously high. This is the only

part of our researches in which the investigated couple deviates from reversibility, and it becomes evident only under special conditions (higher current density, high rate of potential change) of oscillographic electrolysis. Similar behaviour has been reported³ for the anodic polarographic waves of $(C_6H_6)_2 Mo^0$.

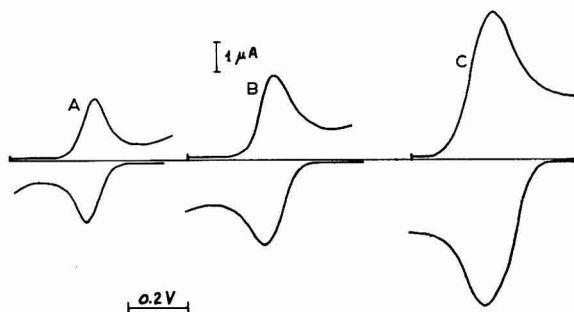


Fig. 2. Oscillographic reduction and subsequent oxidation peaks at various rates of potential sweep, v : (A), 0.4; (B), 1.0; (C), 2.5 V/sec. $[(C_5H_5)Cr^I(C_7H_7)]I$, $0.2 \times 10^{-3} M$ in CH_3OH/C_6H_6 with 0.50 M NaOH, beginning at $-0.4 V$.

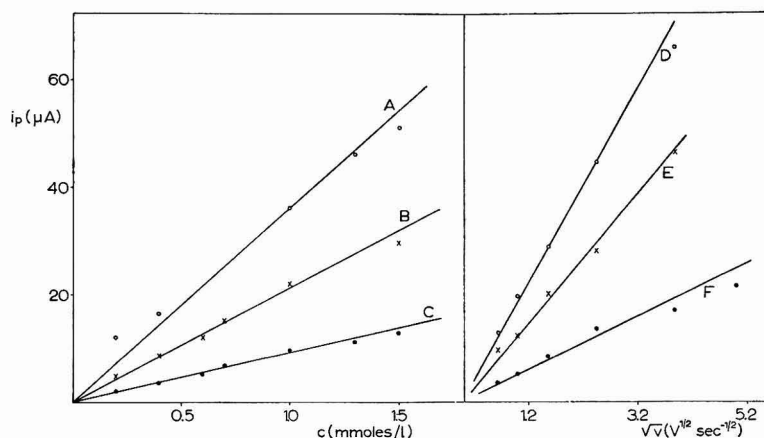


Fig. 3. Peak intensity in oscillograms of $[(C_5H_5)Cr^I(C_7H_7)]I$ in CH_3OH/C_6H_6 (4:1) with 0.50 M NaOH. (A), 15.0; (B), 2.5; (C), 0.4 V/sec. (D), 1.5; (E), 1.0; (F), 0.4 mmoles/l.

Polarographic behaviour in aqueous solutions

As in the case of dibenzenechromium³, polarographic investigations in aqueous medium have been confined to the $Cr(I+)$ species in basic solutions, where $[(C_5H_5)Cr^I(C_7H_7)]^+$ is more stable. Also, the observed polarographic behaviour is conditioned by complete insolubility of the reduced form, which causes a sharp (not S-shaped) rise of the polarographic wave (Fig. 4). Again, as in non-aqueous medium, reduction potentials of $[(C_5H_5)Cr^I(C_7H_7)]^+$ are approximately 0.1 V more positive than those of

$[(C_6H_6)_2Cr^{I+}]$. Other similarities with the polarographic behaviour of $[(C_6H_6)_2Cr^{I+}]$ in water include the occurrence of two adsorption steps (one pre-wave and one post-wave). The pre-wave precedes the main step by ~ 0.2 V in dibenzenechromium(I+); the post-wave is less evident, except in oscillographic polarography, since it is often accompanied by a rounded maximum (suppressible by gelatine) at about -1.3 V, where a

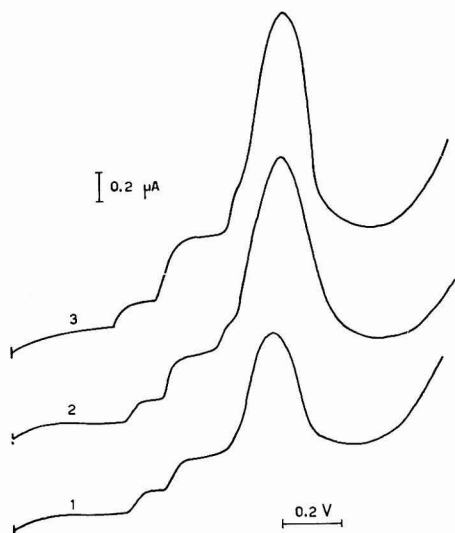


Fig. 4. Typical polarograms of $[(C_5H_5)Cr^I(C_7H_7)]I$ in aq. medium (0.50 M NaOH) at $20^\circ \pm 1^\circ$; beginning at -0.4 V; no maximum suppressor added. Concn. of reducible substance: (1), 0.165×10^{-3} M; (2), 0.198×10^{-3} M; (3), 0.264×10^{-3} M.

TABLE 3

POLAROGRAPHIC BEHAVIOUR OF $[(C_5H_5)Cr^I(C_7H_7)]I$ IN AQUEOUS SOLUTION (0.50 M NaOH) AT 20° ; NO MAXIMUM SUPPRESSOR ADDED

Concn. (mmoles/l)	$i_{dI}(\mu A)$	$i_{dII}(\mu A)$	$E_{iI}(V)$	$E_{iII}(V)$	$\frac{i_{dI} + i_{dII}}{c}$ ($\mu A l/mmoles$)
0.099	0.11	0.10	-0.790	-0.903	2.12
0.132	0.12	0.14	-0.789	-0.902	1.96
0.165	0.12	0.20	-0.768	-0.886	1.93
0.198	0.12	0.28	-0.760	-0.870	2.02
0.264	0.12	0.40	-0.755	-0.860	1.98
0.330	0.11	0.59	-0.740	-0.858	2.12
0.462	0.12	0.86	-0.745	-0.848	2.12
0.792	0.12	1.48	-0.755	-0.840	2.03
0.924	0.12	1.76	-0.750	-0.835	2.03
1.060	0.12	2.02	-0.745	-0.840	2.03
1.650	—	3.30	—	-0.825	2.02
					Average 2.03

distinct irregularity occurs in the electrocapillary curve. This is again analogous to the curve reported³ for $[(C_6H_6)_2Cr^I]^+$. The steps obtained with $[(C_5H_5)Cr^I(C_7H_7)]^+$ show the expected regularities; *i.e.*, proportionality between total i_d and concentration (Table 3); linear shift of E_{red} with log concentration (Fig. 5); proportionality

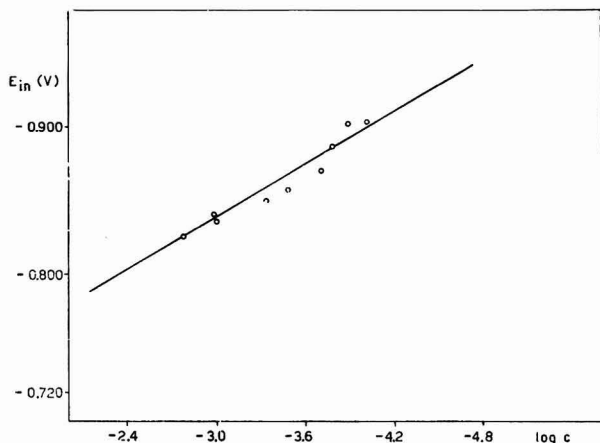


Fig. 5. Plot of E_{in} (potential of the initial rise of the polarographic diffusion) vs. log concn. $[(C_5H_5)Cr^I(C_7H_7)]^I$ in 0.50 *M* aq. NaOH at 20°. $\Delta E_{in}/\Delta \log c \approx 0.06$ V.

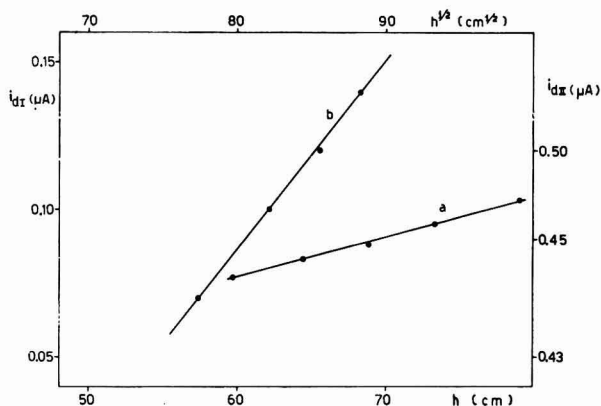


Fig. 6. Plots of limiting currents of the polarographic steps of 0.297×10^{-3} *M* $[(C_5H_5)Cr^I(C_7H_7)]^I$ in 0.50 *M* aq. NaOH at 20° as function of the Hg pressure of the dropping capillary, h : (a), pre wave (adsorption-controlled) vs. h ; (b), main wave (diffusion-controlled) vs. $h^{1/2}$.

between limiting current and h for adsorption pre-wave, and $h^{1/2}$ for the main wave, which is diffusion-controlled (Fig. 6). The oscillographic behaviour of $[(C_5H_5)Cr^I(C_7H_7)]^+$ in the same medium is rather complicated, no less than four different peaks being observed (Fig. 7). The first peak has a triangular shape, with $\Delta \log i_p/\Delta \log v$

> 0.5 and i_p nearly independent of concentration. These features point to the adsorption-controlled nature of the peak, which therefore corresponds to the pre-wave in conventional polarography. The second peak increases proportionally with the concentration of reducible substance, and with $v^{1/2}$; it is therefore diffusion-controlled and corresponds to the main polarographic waves. The third and fourth peaks are

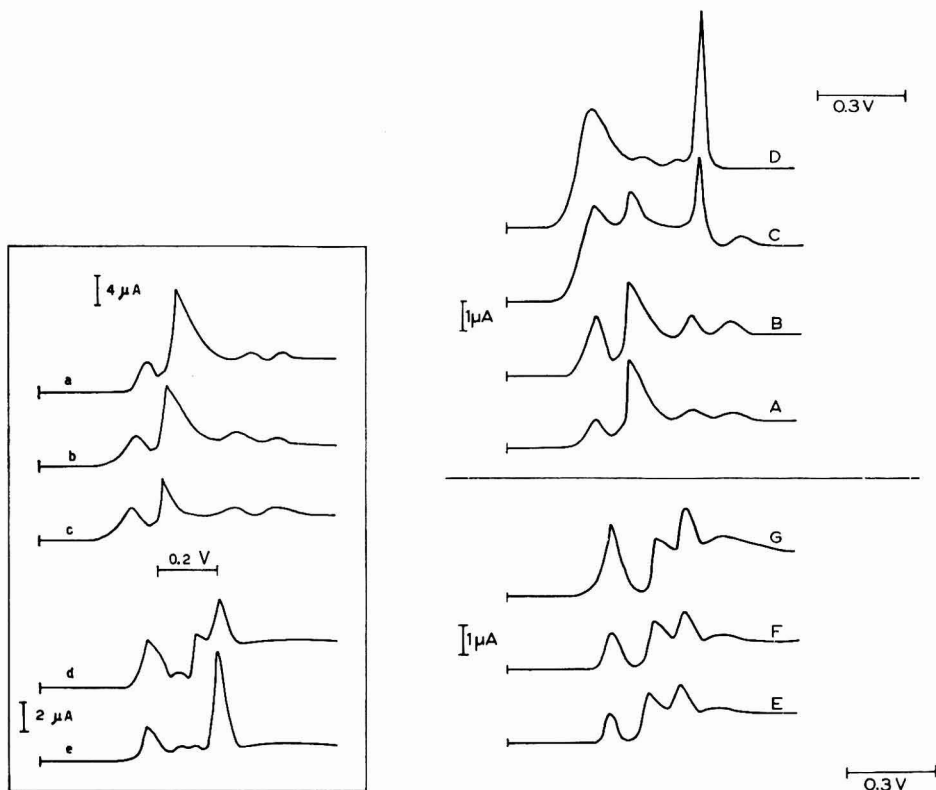


Fig. 7. Oscillopolarograms in $0.50 M$ aq. NaOH at 20° , $v = 1.0$ V/sec, beginning at -0.4 V vs. S.C.E. (a), $[(C_5H_5)CrI(C_7H_7)]I$: Concn. $1.00 \times 10^{-3} M$; (b), $0.80 \times 10^{-3} M$; (c), $0.60 \times 10^{-3} M$. Concn. $[(C_6H_6)_2CrI]I$: (d), $0.48 \times 10^{-3} M$; (e), $0.24 \times 10^{-3} M$.

Fig. 8. Effect of sweep rate v (V/sec), on the peak intensity of the oscillopolarograms of $0.40 \times 10^{-3} M$ aq. soln. of $[(C_5H_5)CrI(C_7H_7)]I$ in $0.50 M$ NaOH at 20° , beginning at -0.4 V vs. S.C.E. (A), 0.15 ; (B), 0.25 ; (C), 1.00 ; (D), 2.50 V/sec. Lower part: $0.48 \times 10^{-3} M [(C_6H_6)_2CrI]I$ under the same conditions. (E), 0.25 ; (F), 0.40 ; (G), 1.00 V/sec.

less well-defined, not always present and less regularly dependent on c and on v , although there are indications that the third one is at least partially adsorption-controlled (Figs. 8 and 9). These peaks probably correspond to the same successive electrode processes which lead in conventional polarography to the observed post-wave and maximum, and are revealed also by the already mentioned irregularity in the electrocapillary curve³.

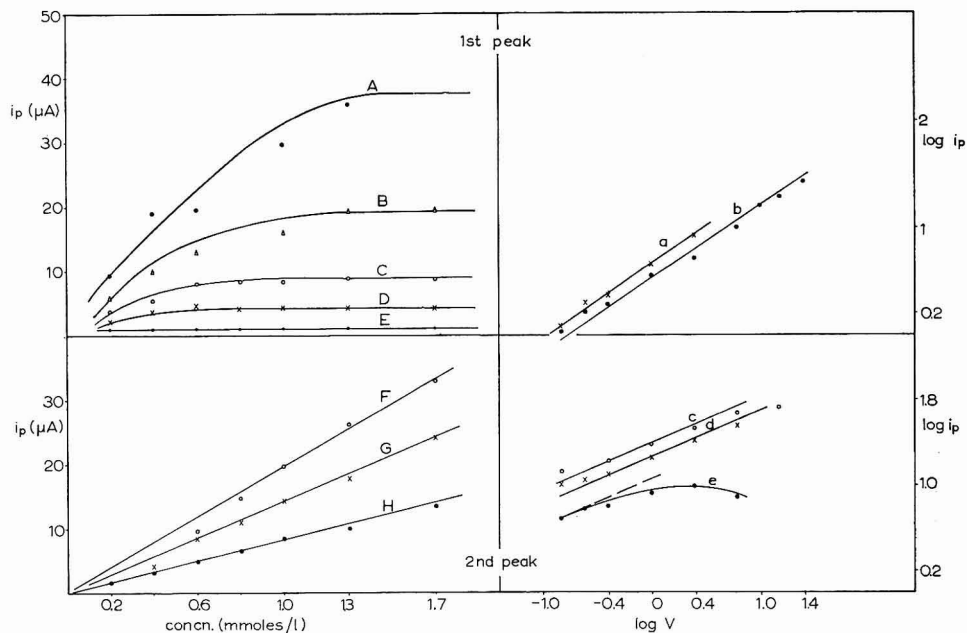


Fig. 9. Effect of concn. (mmoles/l) and of sweep rate v (V/sec), on the intensities of the 1st ($\Delta \log i_d / \Delta \log v \approx 0.7$) and 2nd ($\Delta \log i_d / \Delta \log v \approx 0.49$) oscillopolarographic peaks of $[(C_5H_5)Cr-(C_7H_7)]I$ in aq. 0.50 M NaOH at 20°. (A), 15; (B), 6; (C), 2.5; (D), 1; (E), 0.15; (F), 25; (G), 1; (H), 0.15 V/sec. (a), 0.6; (b), 0.4; (c), 1.7; (d), 1.3; (e), 0.6 mmoles/l.

For comparison, we have also run oscillopolarograms of $[(C_6H_6)_2Cr]I$ under the same conditions (aqueous alkaline medium), and found again that it behaves in the same way as $[(C_5H_5)Cr(C_7H_7)]I$, *i.e.*, there are four peaks, the first of which is certainly adsorption-controlled, and the second diffusion-controlled, which thus correspond, respectively, to the pre-wave and main wave previously reported for $[(C_6H_6)_2Cr^+I]$. Like all the other investigated polarographic conditions, the peak potentials of reduction are slightly more negative for $[(C_6H_6)_2Cr^+]$ than for $[(C_5H_5)-Cr^+(C_7H_7)]^+$.

DISCUSSION

The polarographic and oscillopolarographic behaviour of the system $[(C_5H_5)-Cr^+(C_7H_7)]^+ / (C_5H_5)Cr^0(C_7H_7)$ reveals a very close similarity to the system $[(C_6H_6)_2Cr^+ / (C_6H_6)_2Cr^0]$ previously investigated, and thus confirms the parallelism of their physical and chemical properties. The observed similarity includes the practically equal adsorbability of the two cations at mercury-water interfaces; the latter point is rather significant, since it shows that the dipole moment observed for the $(C_5H_5)Cr-(C_7H_7)$ system¹ does not basically affect the characteristics of its electrochemical behaviour.

The only relevant difference between the polarographic behaviour of dibenzenechromium and cyclopentadienyl-cycloheptatrienylchromium is the shift of the half-wave or peak potentials already mentioned (approximately 0.1 V more positive in the latter system). This shift is not very large (*e.g.* it is comparable with the difference of $E^{1/2}$ between ditoluenechromium and dibenzenechromium³), and it could possibly be explained on the basis of the hypothesis involved in the latter case³, *i.e.*, assuming that as a result of the net balance of electron-releasing and -repelling powers of C_5H_5 and C_7H_7 groupings, the electron density in the valence shell of the chromium atom in the $(C_5H_5)Cr(C_7H_7)$ system is slightly lower than in the $(C_6H_6)_2Cr$ system. In both instances, however, the electron transfer between Cr(0) and Cr(I+) species is very rapid, and attains almost full polarographic reversibility.

Our polarographic results give also some useful hints about analytical applications, *i.e.*, in the detection and determination of π -sandwich complexes. For example, although the redox potentials of the C_5-C_7-Cr system are separated by as little as 0.1 V from those of the dibenzenechromium system, the steepness of the waves makes possible the separation of $[(C_6H_6)_2Cr^I]I$ and $[(C_5H_5)Cr^I(C_7H_7)]I$. In non-aqueous medium, it is also possible to determine the percentages of the reduced and oxidized components of the couple, as shown in Fig. 1.

ACKNOWLEDGEMENT

We thank Prof. E. O. FISCHER of Munich, whose researches have led to the discovery of the substances investigated in the present work, and who has kindly supplied us with pure samples of $[(C_5H_5)Cr^I(C_7H_7)]I$ and $(C_5H_5)Cr^0(C_7H_7)$.

SUMMARY

The couple, $(C_5H_5)Cr^0(C_7H_7)/[(C_5H_5)Cr^I(C_7H_7)]^+$, exhibits in non-aqueous medium (benzene:methanol 1:4) a cathodic-anodic polarographic wave at about -0.7 V *vs.* N/2 C.E. and correspondingly a single diffusion-controlled oscillopolarographic peak. $[(C_5H_5)Cr^I(C_7H_7)]^+$ in aqueous alkaline solutions has a diffusion-controlled, one-electron main reduction wave, preceded and followed by adsorption waves. This behaviour reveals a close analogy to the polarographic and oscillopolarographic behaviour of the dibenzenechromium couple, the only relevant difference being a positive shift of about 0.1 V in the redox potentials of the C_5-C_7-Cr system.

REFERENCES

- 1 E. O. FISCHER AND S. BREITSCHAFT, *Angew. Chem.*, 75 (1963) 94.
- 2 C. FURLANI AND E. O. FISCHER, *Z. Elektrochem.*, 61 (1957) 481.
- 3 C. FURLANI AND G. SARTORI, *Ric. Sci. Suppl.*, 28 (1958) 973.
- 4 G. SARTORI AND G. GIACOMELLO, *Gazz. Chim. Ital.*, 70 (1940) 178.
- 5 G. SARTORI AND E. BIANCHI, *Gazz. Chim. Ital.*, 74 (1944) 8.
- 6 L. RICCOBONI AND P. PAPOFF, *Gazz. Chim. Ital.*, 74 (1949) 573.

J. Electroanal. Chem., 9 (1965) 140-148

THE ELECTRICAL DOUBLE LAYER ON THALLIUM AMALGAM ELECTRODES

JAMES N. BUTLER

Tyco Laboratories Inc., Bear Hill, Waltham 54, Mass. (U.S.A.)

(Received November 9th, 1964)

INTRODUCTION

In connection with a study of hydrogen overvoltage on thallium amalgams¹, we have made some measurements of double-layer capacity on thallium amalgam electrodes in 0.1 *M* HClO₄ at 25°. In addition, a critical survey was made of the literature concerning the electrical double layer on thallium amalgams. In this paper, our experimental results are presented and compared with the literature values. In view of the extensive literature data available on capacity, and the difficulty of measuring accurate zero-charge potentials, a more detailed study of the double layer on thallium amalgams does not seem appropriate at present.

Measurements of the double-layer capacity of thallium amalgams have been made by DELAHAY AND KLEINERMAN², and by BOGUSLAVSKII AND DAMASKIN³. Both sets of measurements appear to be consistent, but neither investigator measured the double-layer capacity in 0.1 *M* HClO₄, the medium which we chose for our overvoltage measurements. Furthermore, one peculiarity exists in the measurements of capacity on 40% thallium amalgams in aqueous sodium fluoride solutions³. A potential-independent frequency dispersion effect was observed, which is difficult to explain by any of the current theories of the electrical double layer. We therefore thought it advisable to make some additional measurements of capacity, which we have reported here.

From the data in the literature on the electrocapillary curves of thallium amalgams⁴⁻¹⁰, together with capacity data^{2,3}, it is possible to obtain some information about the surface composition of the amalgams. The influence of surface composition on the rate of hydrogen evolution is relevant to the more general question of how alloy composition affects the rate of electrode reactions.

EXPERIMENTAL

The amalgams were prepared from triple-distilled mercury (Doe and Ingalls) and 99.999% pure thallium (American Smelting and Refining Co.) by weighing out the required quantities of mercury and thallium and combining them under an atmosphere of argon. The amalgam was allowed to stand overnight to become homogeneous, and then filtered into the dropping-electrode reservoir where it was stored. Thallium

amalgams oxidize readily on exposure to air, but the material in the reservoir was maintained free of oxide by keeping it under an atmosphere of argon.

The method of measuring capacity was essentially that of GRAHAME^{11,12} and has been described in detail previously¹³. Zero-charge potentials were measured by the streaming-electrode method¹⁴⁻¹⁶. Provided the electrode is ideally polarized, the potential at which no current flows between a rapidly dropping electrode and a reference electrode corresponds to the condition where there is no charging current, and hence no excess surface charge at the metal-solution interface; this is the zero-charge potential, or electrocapillary maximum.

However, the conditions for ideal polarization were not perfectly satisfied by a thallium amalgam electrode. At the potential where no current was observed, the capacity showed a slight frequency dispersion and the polarization resistance increased, indicating that thallium was dissolving at an observable rate. Furthermore, the measured zero-current potential was different, depending on whether it was approached from the negative side or the positive side. If the zero-current point was approached consistently from the negative side, and great care was taken to prevent any dissolution of amalgam in contact with the solution, reproducible values were obtained. On the other hand, if the dropping electrode, or the pool of amalgam at the bottom of the cell, was allowed to become even 0.1 V more positive than the zero-current potential, thallium dissolved in the electrolyte, and the zero-current potentials observed were irreproducible. The reproducible values could be restored after long cathodic polarization. We have given the zero-current potentials measured in the absence of any thallium ion in the solution as zero-charge potentials; but in fact the true zero-charge potential is probably somewhat more positive, as will be discussed later.

Extreme care was taken to eliminate impurities in the solution. Sealed water-tight joints and Teflon stopcocks were used to avoid any organic material. The cell was washed with a chromic-sulphuric acid cleaning mixture and rinsed with triple-distilled conductivity water. Solutions were made from reagent-grade perchloric acid (J. T. Baker) and conductivity water. The solution was pre-electrolyzed overnight at 1 mA/cm², using an auxiliary mercury pool as cathode. The mercury pool was discarded before any measurements were made. All measurements were made in 0.100 M perchloric acid solution at 25.0°. The electrolyte was saturated with hydrogen throughout the experiment.

RESULTS AND DISCUSSION

Zero-charge potential

In Fig. 1 is presented a summary of the available data on zero-charge potentials for thallium amalgams. The most precise measurements are those made by FRUMKIN AND GORODETZKAYA⁴, who measured the electrocapillary curves using a Lippman capillary electrometer, and determined the point where the interfacial tension between the amalgam and $N Na_2SO_4$ solution was a maximum. A similar set of measurements was made in NaCN solutions by DELAHAY AND KLEINERMAN², using the less-precise drop-time method for determining the interfacial tension. These authors were unable to obtain a clear maximum, and determined the zero-charge point from the shift of the cathodic branch of the electrocapillary curve with respect to the curve for

pure mercury. The potentials so obtained are more than 0.1 V more positive in dilute amalgams than those of FRUMKIN AND GORODETZKAYA.

FRUMKIN AND CIRVES¹⁴ measured the potential at which no current was carried by a rapid dropping electrode, adjusting the potential by changing the concentration of thallium ion in the electrolyte. These results agreed very closely with the electrocapillary maximum measurements of FRUMKIN AND GORODETZKAYA⁴.

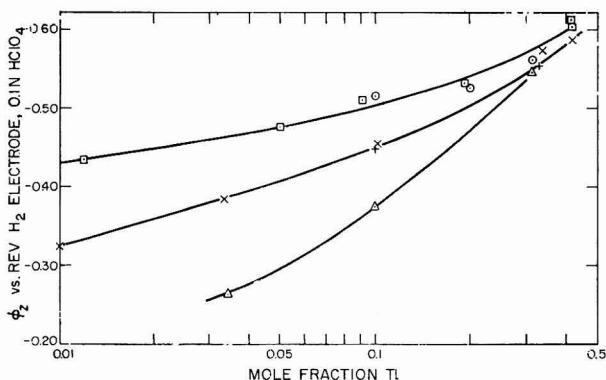


Fig. 1. Comparison of zero-charge potentials measured by various workers: ○, this work; □, BOGUSLAVSKII AND DAMASKIN³; △, DELAHAY AND KLEINERMAN²; +, FRUMKIN AND GORODETZKAYA⁴; ×, FRUMKIN AND CIRVES¹⁴.

BOGUSLAVSKII AND DAMASKIN³ measured the differential capacity of a series of amalgams in 0.01 N NaF, and identified the minimum in the capacity curve with the zero-charge point. Because they observed a frequency-dependence of the capacity at these potentials, they felt that there was some question as to whether the minimum in capacity really corresponded to the zero-charge potential. Presumably a reversible dissolution of thallium was taking place, contributing a pseudo-capacity, which distorted the shape of the capacity curve, and shifted the minimum to more negative potentials. The values obtained by this method are as much as 0.1 V more negative than those of FRUMKIN AND GORODETZKAYA⁴.

Our measurements were made by measuring the potential at which no current flowed between a reference electrode and a rapidly dropping electrode. Our experimental arrangement was essentially the same as that of FRUMKIN AND CIRVES¹⁴, except that the concentration of Tl⁺ in the electrolyte was kept as small as possible by never allowing the dropping electrode or pool of amalgam to become more positive than the zero-charge potential. Our values agree most closely with those obtained by BOGUSLAVSKII AND DAMASKIN.

In the concentrated amalgams, the results obtained by all workers are the same within 0.02 V, which can be considered adequate agreement. In more dilute amalgams, however, the discrepancy increases to as much as 0.2 V, which indicates some gross systematic difference in the results of the various measurement techniques.

The difficulty arises primarily from the dissolution of thallium. If this reaction can proceed at a finite rate, the electrode is no longer ideally polarized, and the equations derived under that assumption¹² are no longer applicable.

MOHILNER¹⁷ has treated the case where one of the components of the electrode undergoes a reversible charge exchange reaction to give one of the components of the electrolyte. At the electrocapillary maximum, he finds that the charge on the electrode is not zero, but rather that the following relation is satisfied:

$$\left(\frac{\partial\gamma}{\partial\phi}\right)_{\mu} = q - \Gamma_{\text{Tl}^+}F = 0 \quad (1)$$

where γ is interfacial tension, ϕ is electrode potential, μ is chemical potential, q is the excess electronic charge on the surface of the electrode, Γ_{Tl^+} is the surface excess of Tl^+ on the electrolyte side of the interface, and F is the faraday constant. A similar conclusion was reached by FRUMKIN AND GORODETZKAYA⁴.

This means that under reversible conditions, the maximum of the electrocapillary curve is not the same as the zero-charge point. The true zero-charge point cannot be rigorously measured under conditions where there is a reversible reaction taking place.

Capacity

In Table 1 are listed the results of our capacity measurements on three amalgams in 0.100 *M* HClO_4 at 25°. The measurements shown were made at 5 kc, but ex-

TABLE 1
CAPACITY OF THALLIUM AMALGAM ELECTRODES
0.1 *M* HClO_4 , 25°, 5 kc

Potential vs. reversible H_2 - electrode	Capacity ($\mu\text{F}/\text{cm}^2$)		
	10.1%	31.2%	40.5%
-1.26			21.5
-1.20	17.9	20.6	21.4
-1.10	18.0	20.9	21.8
-1.00	18.5	21.7	22.6
-0.90	19.5	23.8	24.3
-0.80	21.9	(26.0) ^a	27.0
-0.70	25.9	29.6	30.3
-0.60	31.0	35.4	38.7
-0.58	(32.3) ^a	(33.2) ^a	42.4 ^{b, c}
-0.55	34.5	41.8 ^b	
-0.50	39.8	52.5 ^c	
-0.45	46.6 ^b	(63.3) ^{a, c}	
-0.40	60.8 ^c	74.1 ^c	
-0.35	66.8 ^c		

^a Interpolated.

^b Zero-charge potential.

^c Contains contribution from frequency-dependent pseudo-capacity.

cept where noted (potentials more positive than the zero-charge point) the values were independent of frequency from 0.5--10 kc. The polarization resistance was always less than $0.1 \Omega \text{ cm}^2$.

The results quoted in the table represent averages of 2-4 measurements of capacity, but the data were not otherwise smoothed. The value obtained for 31.2% amalgam at -0.80 V was discarded because of a faulty measurement of balance time, and the value listed in the table at this point was interpolated from a smooth curve through the other values. These results are plotted in Fig. 2, together with a capacity curve for pure mercury in the same potential region, for comparison. The zero-charge points shown in Fig. 2 are those of FRUMKIN AND GORODETZKAYA⁴.

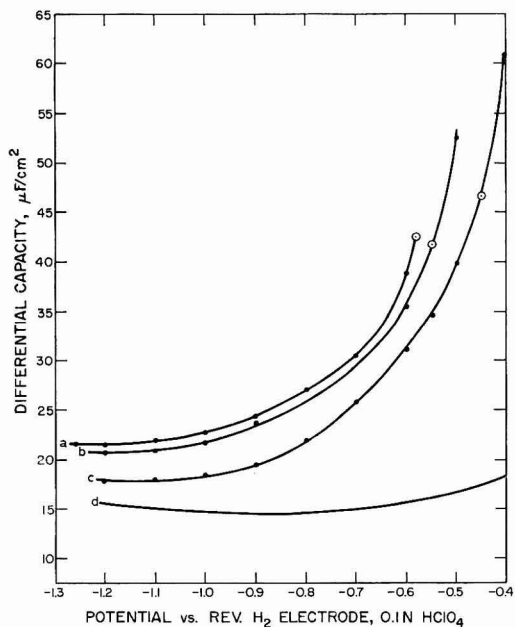


Fig. 2. Differential capacity of thallium amalgam electrodes: ●, experimental data; ○, zero-charge point (ref. 4). (a), 40.5% Tl; (b), 31.2% Tl; (c), 10.1% Tl; (d), pure Hg.

DELAHAY AND KLEINERMAN² also measured the capacity of thallium amalgams in 0.2 M NaCN at 30° . Their results for 10% and 30% amalgams agree with ours within $0.5 \mu\text{F/cm}^2$ at potentials more negative than -0.55 V in the case of the 10% amalgam, and -0.8 V in the case of the 30% amalgam. At potentials more positive than these values, DELAHAY AND KLEINERMAN'S values are higher than ours, presumably because CN^- is more strongly adsorbed at the electrode surface than is ClO_4^- .

In Fig. 3, our capacity measurements on 40.5% thallium amalgam in 0.1 M HClO_4 are compared with the measurements made by BOGUSLAVSKII AND DAMASKIN³ on 40.0% amalgam in 0.1 M KCl . Within the experimental error, our data show no

dependence on frequency from 0.5–10 kc. At those points where a detectable difference is observed between measurements at different frequencies, both the 0.5 kc and the 10 kc measurements were lower than the more accurate 5 kc measurements. These differences can almost certainly be attributed to stray capacitances and inductances in the apparatus. In contrast, BOGUSLAVSKII AND DAMASKIN's measurements at 0.5 kc are higher than those at 10 kc by $1-1.5 \mu\text{F}/\text{cm}^2$, greater by a factor of five than the scatter of their data about a smooth curve.

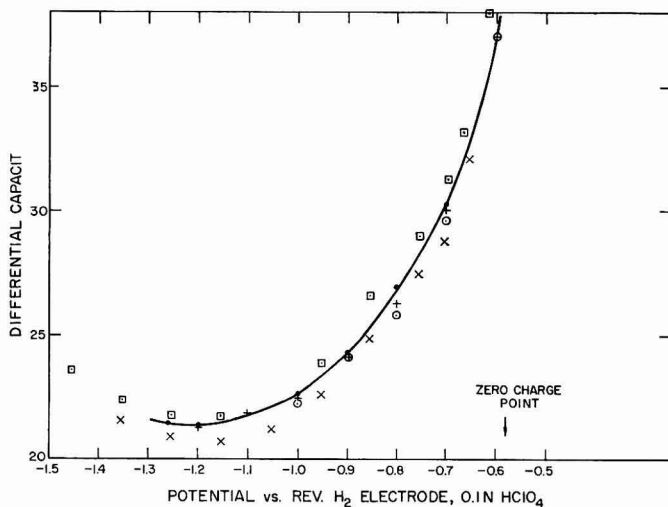


Fig. 3. Comparison of our results for frequency-dependence of capacity of 40% Tl amalgam with results of BOGUSLAVSKII AND DAMASKIN. This work (0.1 M HClO_4): O, 0.5 kc; ●, 5 kc; +, 10 kc. BOGUSLAVSKII AND DAMASKIN³ (0.1 M KCl): □, 0.5 kc; X, 10 kc.

Although an increase in capacity with decreasing frequency is expected if there is a pseudo-capacity contribution from a reversible charge-transfer or adsorption reaction, it is very difficult to imagine such a process which would be independent of potential. A much more likely explanation is a systematic instrumental error.

The diffuse double layer

Using the methods of calculation described previously^{12,13} it is possible to calculate the contribution from the diffuse and Helmholtz (compact) parts of the double layer to the capacity, under the assumption that there is no specific adsorption of ions in the Helmholtz part of the double layer. Under these same assumptions it is possible to calculate the potential drop across the diffuse part of the double layer, a quantity which enters into our overvoltage calculations.

However, one of the essential items of data required for the calculations is an accurate value for the zero-charge potential, and we have seen in our previous dis-

discussion that the values measured by various methods disagree because of the reversible dissolution of thallium from the amalgam.

MOHILNER¹⁷ has shown that it is possible to calculate the difference of potential across the diffuse double layer, even when one of the components can be reversibly transferred across the interface. He has shown that this potential drop is zero not when the surface charge is zero, but rather when the condition of eq. (1) is satisfied.

Unfortunately, under the conditions of our overvoltage experiments, the criteria for reversibility are far from satisfied. In the absence of any thallium ion in the electrolyte, the thallium amalgam electrode approximates an ideally polarized electrode at potentials more negative than the region of the zero-charge potential. Thus MOHILNER's equations cannot be used to calculate the potential drop across the diffuse double layer at the potentials where hydrogen evolution is appreciable. On the other hand, the equations for an ideally polarized electrode without specific adsorption break down in the region of the zero-charge potential, thereby making the calculated values of the potential drop across the diffuse double layer somewhat uncertain.

Since the experimental conditions of FRUMKIN AND GORODETZKAYA⁴, and FRUMKIN AND CIRVES¹⁴, approximate most closely the conditions where the potential drop across the diffuse double layer is zero, we have chosen their values for the zero-charge potential, and used the theoretical equations for the ideally polarized electrode to calculate properties of the double layer. Although such a procedure is far from rigorous, the agreement of the integrated capacity curve with the experimental electrocapillary curve (discussed later) shows that the errors introduced in the overpotential correction¹ are at most a few millivolts, approximately the same order of magnitude as the experimental errors in the overvoltage measurements.

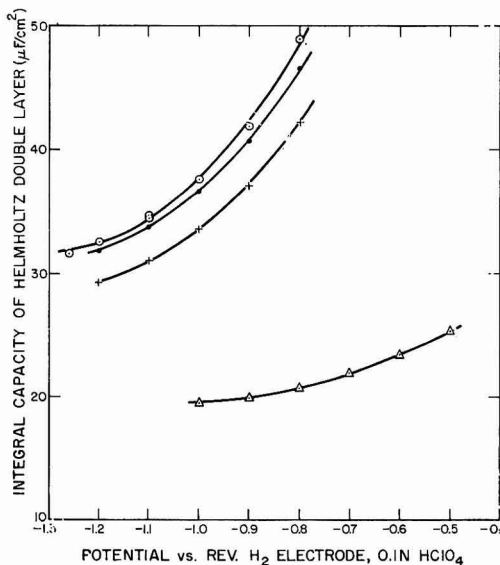


Fig. 4. Integral capacity of the Helmholtz double layer. The curves were calculated from the polynomial functions given in Table 2. \circ , 40.5% Tl; \bullet , 31.2% Tl; $+$, 10.1% Tl; Δ , Hg.

The integral capacity of the Helmholtz layer, calculated using the zero-charge potentials given in Table 1, according to the iteration method described previously¹³ are shown in Fig. 4. For ease in subsequent computations, these results were fitted by the least-squares method to a quadratic polynomial:

$$K^o = C_0 + C_1\phi_0 + C_2\phi_0^2 \quad (2)$$

where ϕ_0 is the potential with respect to the zero-charge point. The curves shown on Fig. 4 were calculated from eqn. (2) using the coefficients listed in Table 2. Note that the values for the amalgams are quite similar, but very different from those for mercury. At corresponding values of surface charge, the capacity of the thallium amalgams is essentially the same, but nearly twice the value for pure mercury. This is in agreement with our observations on indium amalgams in perchloric acid¹³.

Figure 5 shows the curves of the potential drop across the diffuse double layer, ϕ_2 , as a function of overpotential η , for mercury and the three amalgams. Note that the contribution of the diffuse double layer is an appreciable fraction of the total potential drop, approximately 100 mV at an overpotential of 1.0 V. The differences

TABLE 2

COEFFICIENTS OF QUADRATIC POLYNOMIAL EXPRESSION FOR INTEGRAL CAPACITY OF THE HELMHOLTZ DOUBLE LAYER

$$K^o = C_0 + C_1\phi_0 + C_2\phi_0^2$$

	C_0	C_1	C_2
Mercury, pure	34.31	32.98	18.17
Thallium, 10.1%	67.73	92.32	54.86
Thallium, 31.2%	65.85	92.86	62.57
Thallium, 40.5%	66.96	98.91	69.63

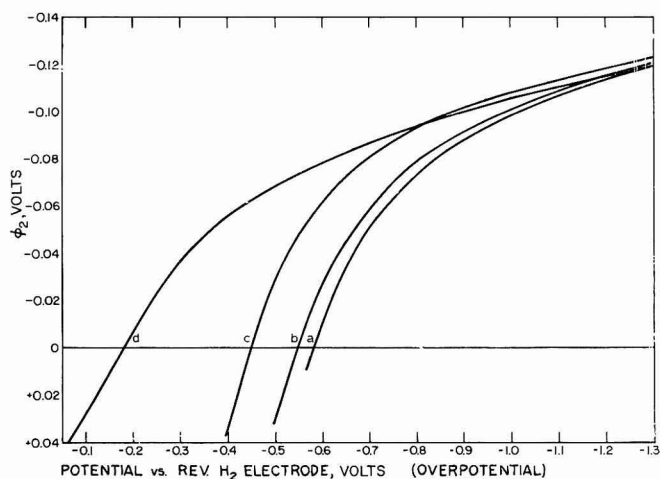


Fig. 5. Potential of the outer Helmholtz plane. Note that the curves converge at large overpotentials. (a), 40.5% Tl; (b), 31.2% Tl; (c), 10.1% Tl; (d), Hg.

between mercury and the amalgams, however, are only about 10 mV in the potential range around 1.0 V. This effect results from the cancellation of two factors; although the zero-charge potential of the amalgams is more negative (larger value of η), the capacity is larger, and hence the curve ϕ_2 rises more steeply. Fortunately, the curves for mercury and the amalgams nearly intersect in the region between 0.8 and 1.3 V.

Interfacial tension and surface concentration of thallium amalgams

One of the factors which can influence the rate of the hydrogen evolution reaction at the surface of a thallium amalgam is the concentration of thallium and mercury at the surface. This concentration need not be the same as in the bulk and the ratio of surface to bulk concentration will in general be a function both of the bulk concentration and the potential.

FRUMKIN AND GORODETZKAYA⁴ have made measurements of the interfacial tension between thallium amalgams and normal Na_2SO_4 . Since at negative potentials, the specific adsorption of both SO_4^{2-} and ClO_4^- should be negligible^{12,18}, the interfacial tension of the thallium amalgams should be essentially the same whether the electrolyte is 0.1 M HClO_4 or 1.0 N Na_2SO_4 . The most sensitive way to see any differences in the structure of the electrical double layer is to look at the differential capacity. Fortunately, FRUMKIN AND GORODETZKAYA's data are accurate enough to permit two successive differentiations to obtain the capacity

$$C = 0.1 \frac{\partial^2 \gamma}{\partial \phi^2} \quad (3)$$

where C is the differential capacity in $\mu\text{F}/\text{cm}^2$, γ is the interfacial tension in erg/cm^2 , and ϕ is the potential with respect to a reference electrode¹².

This differentiation was done in two ways. First, the simple second-differences between the interfacial tension values were used. These results are plotted as crosses on Fig. 6, and show considerable scatter. The other method used was to fit a least-squares polynomial to the data and to differentiate it analytically. The best fit was obtained with a 5th-order polynomial, and the values of its derivative are shown as circles on Fig. 6. The line on Fig. 6 represents our experimental measurements of the differential capacity (Table I). Except for a slight increase at potentials more negative than -1.0 V, the values obtained from the polynomial fit to FRUMKIN AND GORODETZKAYA's data agree with our experimental capacity within the experimental error.

On the other hand, when our capacity data is integrated to obtain the interfacial tension, the results shown in Fig. 7 are obtained. The interfacial tension was obtained by integrating the capacity twice, fixing the position of the integrated curve to coincide with FRUMKIN AND GORODETZKAYA's measurement at the electrocapillary maximum. In Fig. 7, their experimental data are shown as circles, and the result of integrating our capacity data is shown as a line. Even though the capacity is essentially the same in both cases (Fig. 6), our integrated interfacial tension is about 1% higher than FRUMKIN AND GORODETZKAYA's in the negative potential region. This is due in part to their slightly higher capacity values (which make the curve bend more steeply) but is primarily due to a shift in the zero-charge potential.

The integrated curve can be made to agree within 0.2% with the data of FRUMKIN AND GORODETZKAYA if the electrocapillary maximum point is taken to be

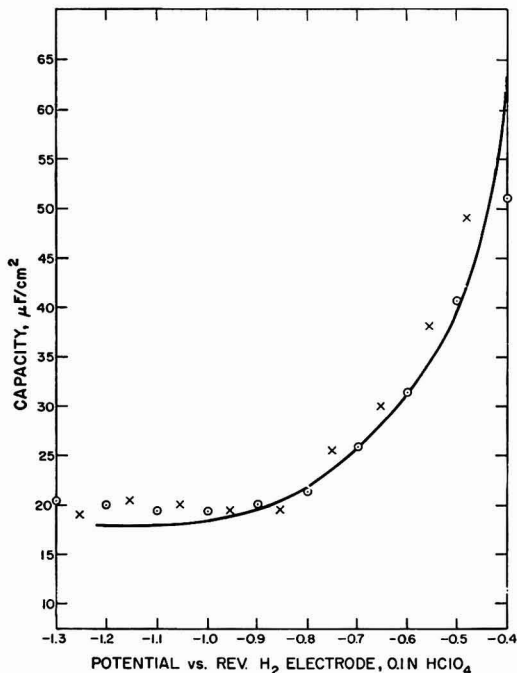


Fig. 6. Comparison of differential capacity of 10% Tl amalgam calculated by differentiating the electrocapillary curve with experimental differential capacity: —, differential capacity (this work); x, 2nd difference of experimental points; o, 2nd derivative 5th-order polynomial⁴.

approximately 15 mV more positive in 0.1 M HClO₄ than in 1 N Na₂SO₄. One explanation for this is that the incipient dissolution of thallium at potentials near the electrocapillary maximum introduces uncertainties of this order of magnitude. As we saw in our discussion of the zero-charge potential, this is quite a reasonable explanation. The other possibility is that the sulfate ion is slightly more strongly adsorbed than the perchlorate ion at positive potentials. This would cause a shift in the electrocapillary maximum, but would also imply that the capacity in Na₂SO₄ should be higher than in HClO₄ at the positive end of the curve. As can be seen from Fig. 6, this is not the case. The question of specific adsorption of anions on thallium amalgams has been briefly touched by FRUMKIN^{4,14} and by BOGUSLAVSKII AND DAMASKIN³, but detailed measurements and calculations have been carried out only for mercury¹⁸.

Being thus convinced that only minor differences exist between the directly measured interfacial tension and the integrated interfacial tension, we can use the concentration dependence of interfacial tension to obtain the surface excess of thallium. The form of the Gibbs adsorption isotherm which applies to this case is^{21,22}

$$\Gamma_{\text{Tl}} = -\frac{1}{RT} \left(\frac{\partial \gamma}{\partial \ln a_{\text{Tl}}} \right)_{\phi} \quad (4)$$

where γ is the interfacial tension, a_{Tl} is the activity of thallium in the amalgam, and Γ_{Tl} is the surface excess of thallium, with respect to mercury. The activity of thallium

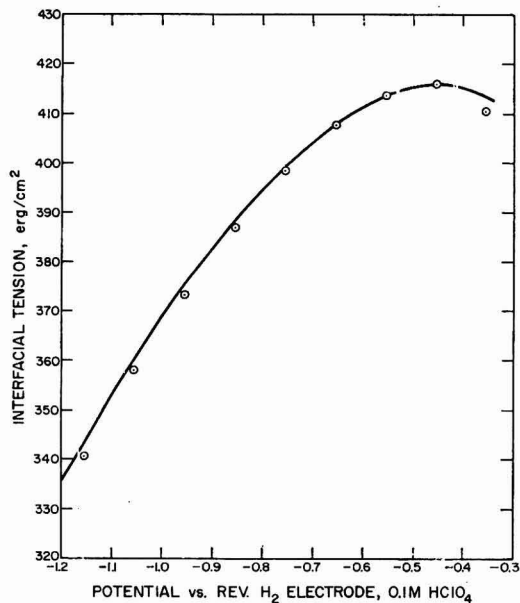


Fig. 7. Comparison of experimental interfacial tension measurements with values for 10% Tl amalgam obtained by integrating the capacity curve. The two sets of values were made to coincide at the electrocapillary maximum: —, integrated capacity curve (this work); ○, experimental interfacial tension⁴.

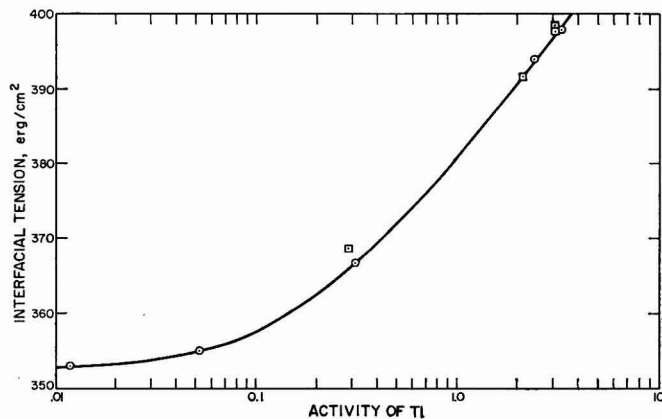


Fig. 8. Interfacial tension as function of log activity. $\phi = -1.00$ V vs. rev. H₂ electrode, 0.1 N HClO₄; ○, FRUMKIN AND GORODETZKAYA⁴; □, this work. The slope of the curve gives Γ_{Tl} .

in its amalgams is known, having been calculated by LEWIS AND RANDALL¹⁹ from the E.M.F. measurements of RICHARDS AND DANIELS²⁰.

The surface excess can be obtained from the concentration dependence of interfacial tension in two complementary ways. The first is to make use of eqn. (4) in the form given; to plot γ as a function of $\log a_{Tl}$, and measure the slope directly. Such

a plot is shown in Fig. 8. Note, however, that the slope at small values of the activity is very small, and unless an expanded scale is used, difficult to measure accurately.

The second method is to use eqn. (4) in the form

$$\Gamma_{Tl} = - \frac{a_{Tl}}{RT} \left(\frac{\partial \gamma}{\partial a_{Tl}} \right)_{\phi} \quad (5)$$

and to measure the slope of a plot of γ as a function of a_{Tl} . Such a plot is shown in Fig. 9. Note that the slope of the curve in Fig. 9 is greatest in the region where the slope of the curve in Fig. 8 is smallest. Thus the two methods complement each other, the first being more accurate in the high-concentration region, and the second being more accurate in the low-concentration region.

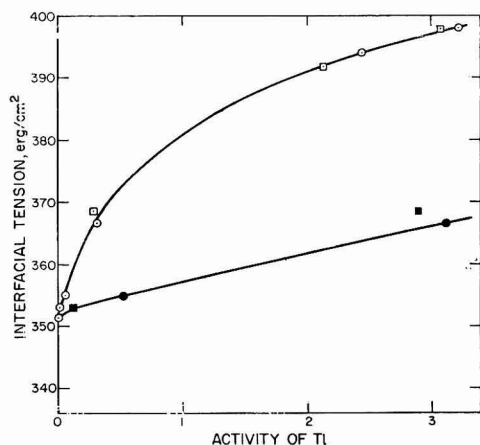


Fig. 9. Interfacial tension as a function of activity. $\phi = -1.00$ V vs. rev. H_2 electrode, 0.1 N $HClO_4$; ○, FRUMKIN AND GORODETZKAYA⁴; □, this work; ● and ■, activity scale expanded 10 times. The slope of the curve gives Γ_{Tl}/a_{Tl} .

The values of Γ_{Tl} obtained by the two methods are shown on Fig. 10, for several values of potential in the region where hydrogen overvoltage measurements¹ have been made. Note that the values of Γ_{Tl} are negative; the surface concentration of thallium is lower than the bulk concentration if the concentration of mercury is assumed to be uniform out to the interface.

The ratio of Γ_{Tl} to the bulk concentration is of interest, since it is relatively independent of concentration, as can be seen from Fig. 11. If the variation of concentration with distance from the surface were the same for all the amalgams, then Γ_{Tl}/x_{Tl} would be independent of concentration. The decrease of Γ_{Tl}/x_{Tl} as the concentration increases shows that in the higher-concentration amalgams the surface concentration is probably closer to the bulk concentration than in the dilute amalgams.

Although the surface excess Γ_{Tl} is known, the absolute value of the surface concentration cannot be obtained without prior knowledge of the shape of the concentration profile in a direction perpendicular to the surface. A close-packed monolayer of 3 Å diameter spheres gives a surface concentration of $21 \cdot 10^{-10}$ moles/cm²

and Γ_{Tl} in a 40% thallium amalgam is $-8 \cdot 10^{-10}$ moles/cm². Thus, if all the thallium were removed from the first atomic layer, this would almost precisely account for the observed value of Γ_{Tl} . Of course, a concentration profile which is uniform up to one atomic layer from the surface, and zero for that single layer is absurd, but if one assumes that the surface deficiency arises primarily in the first four or five atomic layers, one finds that the surface concentration is one-half to three-fourths of the bulk concentration, depending on the concentration profile chosen.

Thus it is rather unlikely that the observed similarity in hydrogen overvoltage

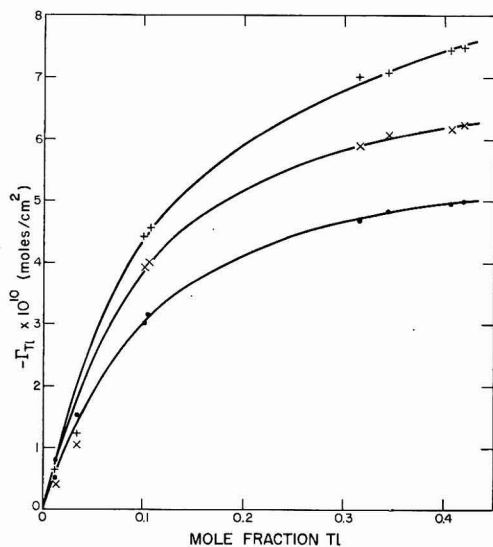


Fig. 10. Surface excess of thallium with respect to mercury: +, $\eta = 1.20$; x, $\eta = 1.00$; ●, $\eta = 0.80$.

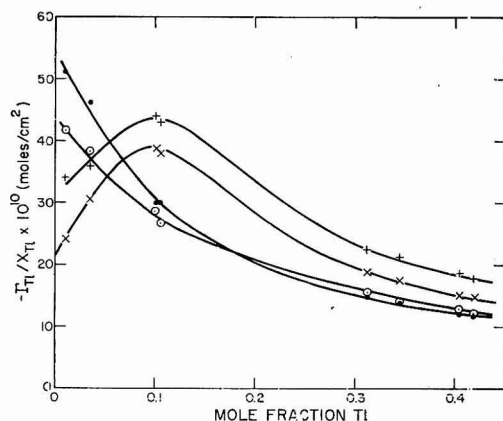


Fig. 11. Surface excess of thallium compared to the bulk concn. of thallium. The relative depletion of the surface concn. is greater at the lower concns. +, $\eta = 1.20$; x, $\eta = 1.00$; ○, $\eta = 0.90$; ●, $\eta = 0.80$.

between mercury and the thallium amalgams¹ is due entirely to a depletion of thallium at the surface. Although the surface concentration of thallium is certainly lower than the bulk concentration, the ratio of surface to bulk concentration is probably greater than 0.5, and is not very different for the different amalgams.

ACKNOWLEDGEMENTS

This work was supported by the U.S. Office of Naval Research, Materials Sciences Division, Contract No. NONr-3765(00), ARPA Order No. 302-62. The author thanks Mrs. EVELYN A. BARRON-APPS for her competent assistance with the experimental work, Dr. A. C. MAKRIDES for his penetrating criticism and helpful suggestions, and Mrs. MARY L. MEEHAN for assisting with the experiments and calculations.

SUMMARY

Measurements of double-layer capacity and zero-charge potential have been made on 10, 30, and 40% thallium amalgams. These results have been compared with existing literature data. The integrated capacity curves agree with literature values for experimental electrocapillary curves. The surface concentration of thallium, at potentials where overvoltage measurements have been made, is one-half to three-fourths of the bulk concentration. In contrast to results reported in the literature, the double-layer capacity of 40% thallium amalgam shows no dependence on frequency, within experimental error in the range from 0.5–10 kc.

REFERENCES

- 1 J. N. BUTLER, E. A. BARRON-APPS AND M. L. MEEHAN, *Trans. Faraday Soc.*, in press (Tech. Memo # 17).
- 2 P. DELAHAY AND M. KLEINERMAN, *J. Am. Chem. Soc.*, 82 (1960) 4509.
- 3 L. I. BOGUSLAVSKII AND B. B. DAMASKIN, *Zh. Fiz. Khim.*, 34 (1960) 2099.
- 4 A. FRUMKIN AND A. GORODETZKAYA, *Z. Physik. Chem., Leipzig*, 136 (1928) 451.
- 5 S. V. KARPACHEV AND A. G. STROMBERG, *Zh. Fiz. Khim.*, 7 (1936) 754.
- 6 S. V. KARPACHEV AND A. G. STROMBERG, *Zh. Fiz. Khim.*, 13 (1939) 1831.
- 7 S. V. KARPACHEV AND A. G. STROMBERG, *Acta Physicochim. URSS*, 12 (1940) 523.
- 8 A. N. FRUMKIN AND A. S. TITIEVSKAYA, *Zh. Fiz. Khim.*, 31 (1957) 485.
- 9 A. N. FRUMKIN AND N. S. POLYANOVSKAYA, *Zh. Fiz. Khim.*, 32 (1958) 157.
- 10 A. N. FRUMKIN, *Surface Phenomena in Chemistry and Biology*, edited by J. F. DANIELLI, K. G. A. PANKHURST AND A. C. RIDDIFORD, Pergamon, New York, 1958, pp. 189–94.
- 11 D. C. GRAHAME, *J. Am. Chem. Soc.*, 71 (1949) 2975.
- 12 D. C. GRAHAME, *Chem. Rev.*, 41 (1947) 441.
- 13 J. N. BUTLER, M. L. MEEHAN AND A. C. MAKRIDES, *J. Electroanal. Chem.*, 9 (1965) 237 (Tech. Memo # 15).
- 14 A. FRUMKIN AND F. J. CIRVES, *J. Phys. Chem.*, 34 (1930) 74.
- 15 D. C. GRAHAME, R. P. LARSEN AND M. A. POTH, *J. Am. Chem. Soc.*, 71 (1949) 2978.
- 16 D. C. GRAHAME, E. M. COFFIN AND J. I. CUMMINGS, *J. Am. Chem. Soc.*, 74 (1952) 1207.
- 17 D. M. MOHILNER, *J. Phys. Chem.*, 66 (1962) 724.
- 18 D. C. GRAHAME, M. A. POTH AND J. I. CUMMINGS, *J. Am. Chem. Soc.*, 74 (1952) 4422.
- 19 G. N. LEWIS AND M. RANDALL, *J. Am. Chem. Soc.*, 43 (1921) 233.
- 20 T. W. RICHARDS AND F. DANIELS, *J. Am. Chem. Soc.*, 41 (1919) 1732.
- 21 R. PARSONS AND M. A. V. DEVANATHAN, *Trans. Faraday Soc.*, 49 (1953) 404.
- 22 R. PARSONS, *Modern Aspects of Electrochemistry*, No. 1, edited by J. O'M. BOCKRIS, Butterworth, London, 1954, p. 103.
- 23 M. SLUYTERS-REHBACH, B. TIMMER AND J. H. SLUYTERS, *Rec. Trav. Chim.*, 82 (1963) 553.

SHORT COMMUNICATIONS

Thin-layer chronopotentiometric determination of reactants adsorbed on platinum electrodes

We have recently described a new electrode designed to allow electrochemical measurements to be performed on layers of solution 10–50 μ thick which are confined between two platinum electrodes mounted on a micrometer¹ (see Fig. 1). The electrode offers advantages in many electrochemical studies² but we wish to present here a particularly simple, yet highly useful, application of this electrode to the quantitative measurement of adsorbed reactants.

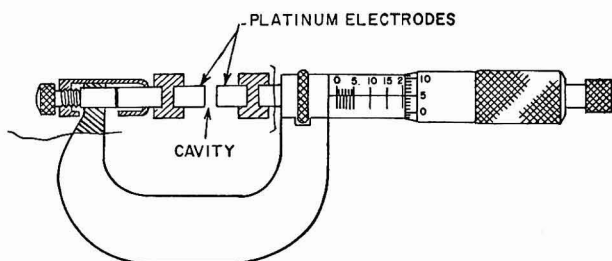


Fig. 1. Micrometer electrode for thin-layer chronopotentiometry.

It has been shown previously¹ with solutions of ferric iron in perchloric acid that the chronopotentiometric transition times obtained with the thin-layer cell could be accurately calculated from the cell geometry and Faraday's Law according to the following equation:

$$\tau = \frac{nFAiC}{i} \quad (1)$$

where τ is the transition time, $n = 1$, F is the Faraday, A the area of one of the cylindrical platinum electrodes, l the thickness of the solution layer as set with the micrometer, C the concentration of ferric iron in the solution, and i the constant current employed.

If adsorption of the reactant on the platinum electrode surfaces can occur, and the thin-layer apparatus is prepared by first bathing both electrode surfaces in excess of the reactant solution, and then closing the micrometer gap to squeeze out all the solution except for that remaining in the 10–50 μ layer, eqn. (1) will no longer be obeyed. Instead, the observed transition time will be given by

$$\tau = \frac{nFAiC}{i} + \frac{2nFAI}{i} \quad (2)$$

where I is the amount of adsorbed reactant in moles/cm² and the factor of 2 arises because adsorption occurs on both platinum pole pieces of area A .

Thus the number of coulombs in excess of those calculated from eqn. (1) which are obtained in a thin-layer experiment correspond to the quantity of adsorbed reactant.

It is not difficult to arrange the thin-layer experiment so that the contribution from the adsorbed reactant is a major fraction of the total coulombs measured. For example, if $\Gamma = 5 \cdot 10^{-10}$ moles/cm², $C = 10^{-6}$ moles/cm³, and $l = 10 \mu$, the adsorbed reactant will consume one-half of the total coulombs required to reach the transition time.

Experimental data demonstrating the utility of the technique has been obtained with solutions of iodide and tri-iodide in 1 *F* H₂SO₄. Previous work³ has shown that although both iodide and iodine are adsorbed on platinum electrodes, only the adsorbed iodine is electroactive at potentials where unadsorbed iodide and iodine are oxidized and reduced, respectively. Accordingly, one would expect eqn. (1) to describe the behavior of iodide solutions in thin-layer experiments, but eqn. (2) should be required to account for the behavior of tri-iodide solutions. The data in Table 1 confirm these expectations:

TABLE 1

Solution	$i\tau$ calc. from eqn. (1) (μC)	$i\tau$ observed (μC)	$\Gamma \cdot 10^{10}$ calc. from eqn. (2) (moles/cm ²)
0.6 mM I ₂ } 1.0 mM I ⁻ }	163	287	10.1
1.14 mM I ₂ } 1.0 mM I ⁻ }	304	422	9.6
	135	134	0

$i\tau$ observed represents the average of several trials with a standard deviation of about 2%. All solutions were air-free and the experiments were conducted with the thin-layer electrode in a nitrogen atmosphere. The current was 10 μA , the solution thickness was 40 μ .

The electrodes were cleaned by the following procedure which was repeated several times before each trial: electrode oxidized with constant current in 1 *F* H₂SO₄ until a potential of 1.35 V vs. S.C.E. was attained; current interrupted and electrode washed thoroughly with air-free 1 *F* H₂SO₄; electrode reduced potentiostatically at +0.42 V vs. S.C.E. for several minutes.

The thin-layer technique appears to offer quite general utility for the study of adsorbed reactants. In addition, it has considerable advantages over most other techniques for studying reactant adsorption because one is not required to perform experiments quickly in order to minimize the contributions from unadsorbed diffusing reactant.

Other applications of this technique to the study of adsorption at platinum, as well as mercury electrodes are in progress.

Acknowledgement

This study was supported by the U. S. Army Research Office (Durham).

Gates and Crellin Laboratories of Chemistry,
California Institute of Technology,
Pasadena, California (U.S.A.)

ARTHUR T. HUBBARD
FRED C. ANSON

- 1 A. T. HUBBARD AND F. C. ANSON, *Anal. Chem.*, 36 (1964) 723.
- 2 C. R. CHRISTENSEN AND F. C. ANSON, *Anal. Chem.*, 35 (1963) 205.
- 3 R. A. OSTERYOUNG AND F. C. ANSON, *Anal. Chem.*, 36 (1964) 975.

(Received October 20th, 1964)

Formation of thick oxides on platinum electrodes

A considerable amount of literature has been devoted to discussions of platinum oxide on platinum electrodes. LAITINEN AND ENKE¹ cite numerous references and conclude that the oxide film on platinum is electron-conducting rather than ion-conducting, and therefore does not grow beyond one or two atomic layers. Others² have estimated the platinum oxide film to be no more than three atomic layers thick. When using platinum indicator electrodes, varying results have been obtained by those working in polarography², potentiometry³, chronopotentiometry⁴, and kinetic determinations⁵. The main difficulty in obtaining reproducible results apparently stems from the inability to produce and maintain a sufficient amount of surface oxide⁶.

Platinum oxides several atomic layers thick were obtained in the present study. The thickness and composition of these oxides were dependent upon the experimental conditions. Direct chemical methods described by ANSON AND LINGANE⁷ were used to examine these oxides.

EXPERIMENTAL

Two disk platinum electrodes, each with a surface area of 4.54 cm², were used throughout this study. The platinum was heated to redness and allowed to cool to room temperature before each experiment. Molten reagent-grade KNO₃ at 400° was used as the oxidant in all cases. Oxidation was carried out with and without electrolysis.

Oxidation without electrolysis was accomplished by dipping the electrode into the molten KNO₃ for varying lengths of time. The electrode was then removed and allowed to cool to room temperature before washing with distilled water.

During electrolytic oxidation, the anodic current was manually controlled by means of a rheostat and a d.c. milli-ammeter in series with a six-volt power supply. The anode was introduced and withdrawn from the oxidizing medium under conditions of an impressed current. After being withdrawn from the oxidant, the anode was allowed to cool to room temperature and then washed with distilled water before analysis.

The platinum oxide stripping solution (0.2 M HCl, 0.1 M NaCl) was prepared from reagent-grade HCl and reagent-grade NaCl. The oxide stripping procedure followed closely the method described by ANSON AND LINGANE⁷. Beckman Model DU spectrophotometer standards for determining PtO and PtO₂ concentrations were made from reagent-grade K₂PtCl₄ and reagent-grade (NH₄)₂ PtCl₆, respectively.

RESULTS AND DISCUSSION

The results of this study are summarized in Table 1.

Electrode film

The oxide film obtained without electrolysis (expts. 1, 2 and 3) does not increase in thickness after about 1 hour. The appearance of the platinum was changed by this treatment from shiny to lustreless, but no color was apparent even after 20 h.

* Presented at the 9th Meeting of the Tetrasectional American Chemical Society, Tulsa, Oklahoma (U.S.A.), March 1963.

TABLE 1
OXIDATION OF PLATINUM ELECTRODES WITH KNO_3

<i>Expt. no.</i>	<i>Time oxidized (min)</i>	<i>Film thickness (atomic layers)</i>	<i>Mole ratio PtO/PtO₂</i>	<i>Direct current (mA/cm²)</i>
1	15	12	6.3	0
2	60	15	6.3	0
3	1200	15	7.1	0
4	60	66	3.6	0.4
5	1	157	2.9	1.1
6	5	132	3.0	1.1
7	30	51	4.0	1.1

With electrolysis, a coherent oxide film was obtained much more rapidly (comparing expts. 4-7 with expts. 1-3), and the amount of PtO_2 on the electrode was approximately doubled.

The appearance of the electrodes also changed with current density. The electrodes obtained at 0.4 mA/cm^2 were light brown, while at 1.1 mA/cm^2 the electrodes were dark brown. During expts. 4 and 7, oxides (of the same composition as the electrodes) were precipitated after several minutes, which accounts for the reduced film thickness expts. 4 and 7 vs. expts. 5 and 6). With time, the films tended to stabilize at about 60 atomic layers. These films were very difficult to remove, particularly those formed at the lowest current density.

*Central Research Division,
Continental Oil Company,
Ponca City, Oklahoma (U.S.A.)*

R. L. EVERY
R. L. GRIMSLEY

- 1 H. A. LAITINEN AND C. G. ENKE, *J. Electrochem. Soc.*, 107, (1960) 773.
- 2 I. M. KOLTHOFF AND N. TANAKA, *Anal. Chem.*, 26 (1954) 632.
- 3 J. W. ROSS AND I. SHAIN, *Anal. Chem.*, 28 (1956) 548.
- 4 F. C. ANSON AND J. J. LINGANE, *J. Am. Chem. Soc.*, 79 (1957) 1015.
- 5 S. GLASSTONE AND A. HICKLING, *Chem. Rev.*, 25 (1939) 407.
- 6 F. C. ANSON, *Anal. Chem.*, 33 (1961) 934.
- 7 F. C. ANSON AND J. J. LINGANE, *J. Am. Chem. Soc.*, 79 (1957) 4901.

Received September 3rd, 1964

J. Electroanal. Chem., 9 (1965) 165-166

A contribution to the theory of the change of electrode reaction rate by adsorption of an electro-inactive substance

The adsorption of surface active substances present in low concentration in solution often exerts a striking influence on electrode reaction rates. In cases of strong adsorption, the application of the dropping electrode makes it possible to determine the relative coverage of the electrode assuming diffusion transport of the surface active substance to the electrode¹. On this assumption WEBER, KOUTECKÝ AND KORYTA² deduced the form of polarographic current-time curves for the case when the electrode reaction rate is a linear function of the coverage (*cf.* ref. 3). KŮTA, WEBER AND KOUTECKÝ⁴ attempted to explain the experimental disparity with the theory for ionic substances adsorbed by assuming that the term in the expression for the dependence of the electrode reaction rate on coverage, corresponding to the uncovered surface, depends on the potential difference in the diffuse double layer which is a linear function of coverage.

The intention of the present paper is, by means of a simple model of the compact double layer, to explain the change of the electrode reaction rate with coverage of the electrode assuming only electrostatic effects. Thus, for the irreversible reduction of an electro-active substance, the validity of Frumkin's formula

$$i = k \exp(-\alpha n F E / RT) \exp[-(z - \alpha n) F \varphi_2 / RT] \quad (1)$$

is assumed, where φ_2 is the potential difference in the diffuse double layer and the other symbols denote the well-known quantities.

According to GRAHAME AND PARSONS⁵ the potential difference in the compact double layer can be approximately expressed by the equation

$$\varphi_{M-2} = \psi^v + \psi^{02} \quad (2)$$

where ψ^{02} depends only on the charge of the electrode and ψ^v only on the surface concentration of adsorbed ions. This equation may be written as follows

$$\varphi_{M-2} = q_1 / K^n + q / K^{02} \quad (3)$$

where q_1 is the charge of adsorbed ions per cm^2 , q the charge of the electrode, K^n and K^{02} the corresponding integral capacities. K^n has an approximately potential-independent value, K^{02} an identical potential dependence in solutions of monovalent inorganic anions (this refers to anions of the same type⁶, but the difference between halides and oxyanions does not considerably influence the results in this paper).

If large organic ions are adsorbed, water molecules are squeezed out of the interface in the area covered by the adsorbed ion and K^{02} may be expressed in the following way

$$K^{02} = K_0^{02}(1 - \theta) + K_1^{02}\theta \quad (4)$$

where K_0^{02} is the original value of the integral capacity corresponding to the charge of the electrode with a water layer, K_1^{02} , the same quantity in the area covered by the organic substance which has usually a low value and is only weakly dependent on electrode potential. θ is the coverage of the electrode.

The charge of adsorbed ions is given by the expression

$$q_1 = \theta \Gamma_m z' F \quad (5)$$

where Γ_m is the maximum surface concentration and z' the charge carried by the ion. For the potential difference in the diffuse double layer it follows that

$$\varphi_2 = \frac{2RT}{F} \operatorname{arc} \sinh \frac{\theta \Gamma_m z' F + q}{2A} \quad (6)$$

where $A = 5.86 \sqrt{c}$ for aqueous solutions of a uni-univalent electrolyte at concentration c at 25° .

The electrode potential E (vs. S.C.E.) is given by the equation

$$\begin{aligned} E &= -0.472 + \varphi_{M-2} + \varphi_2 \\ &= -0.472 + \frac{\theta \Gamma_m z' F}{K^n} + \frac{q}{K_0^{0.2} + \theta(K_1^{0.2} - K_0^{0.2})} \\ &\quad + \frac{2RT}{F} \operatorname{arc} \sinh \frac{\theta \Gamma_m z' F + q}{2A} \end{aligned} \quad (7)$$

Assuming the validity of eqn. (1) we calculated the values of φ_2 as a function of θ from polarographic instantaneous current-time curves of $0.01 M VO^{2+}$ in $0.1 M HNO_3$ in the presence of 10^{-4} tribenzylammonium ion for the electrode potential $-0.917 V$ where the current is controlled merely by the electrode reaction rate without interference of diffusion. This result is plotted in Fig. 1, curve 1, as a difference

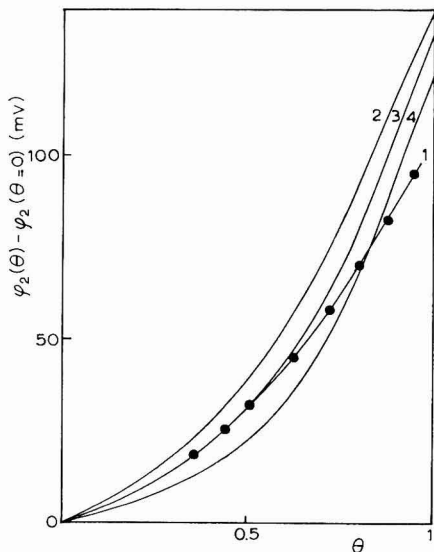


Fig. 1. Difference between φ_2 at a given θ and at $\theta = 0$ plotted against coverage. (1) Experimental dependence assuming the validity of eqn. (1). On the basis of eqns. (6) and (7): $K^n = 30 \mu F/cm^2$ (2); $20 \mu F/cm^2$ (3); $15 \mu F/cm^2$ (4).

between the value of φ_2 at a given θ and at $\theta = 0$. It was assumed that the coverage rate was controlled by diffusion according to the equation

$$\theta = \sqrt{t/\vartheta} \quad (8)$$

where ϑ is the time of full coverage. This value was determined from the current-time curve of the same system at $E = -1.317$ V.

On the basis of eqns. (6) and (7) the values of φ_2 as function of coverage were calculated for values K^n of 30, 20 and 15 $\mu\text{F}/\text{cm}^2$ using a digital computer (Fig. 1, curves 2,3 and 4). The value of $K_1^{0.2}$ was determined from differential capacity measurement⁷ as 5.7 $\mu\text{F}/\text{cm}^2$. The value of Γ_m was estimated as 1.0×10^{-10} mole/ cm^2 .

The agreement between the experimental and theoretical values is quite good for the very simple model used in the present paper. One source of discrepancy at higher coverage may be that the blocking effect⁵ of the adsorbed substance has been entirely neglected.

*J. Heyrovský Polarographic Institute,
Czechoslovak Academy of Sciences,
Prague 1 (Czechoslovakia)*

J. KORYTA
K. HOLUB

1 J. KORYTA, *Collection Czech. Chem. Commun.*, 18 (1953) 206.

2 J. WEBER, J. KOUTECKÝ AND J. KORYTA, *Z. Elektrochem.*, 63 (1959) 583.

3 R. W. SCHMID AND C. N. REILLEY, *J. Am. Chem. Soc.*, 80 (1958) 2087.

4 J. KŮTA, J. WEBER AND J. KOUTECKÝ, *Collection Czech. Chem. Commun.*, 25 (1960) 2376.

5 D. C. GRAHAME AND R. PARSONS, *J. Am. Chem. Soc.*, 83 (1961) 1291.

6 R. PARSONS, private communication.

7 L. NĚMEC, private communication.

Received October 26th, 1964

J. Electroanal. Chem., 9 (1965) 167-169

Voltammetric studies using various electrode systems

A new electrode system — mercury pool cathode and molybdenum anode, is being studied chiefly with a view to using such a system with a cathode ray polarograph with non-aqueous and mixed solvents. In the dropping mercury electrode system the drop time must be adjusted accurately to seven seconds on the cathode ray polarograph for the triggering of the sweep circuit and care must be taken so that the falling of the drop coincides with the end of the sweep voltage. With organic solvents, the capillary characteristics change considerably and the reproducibility of the result is affected.

The Hg pool cathode has a large area compared to D.M.E. and thus double-layer capacity effects, and large charging currents are minimized¹⁻³; it is therefore suitable for work with solutions of low metal ion concentration using a cathode ray polarograph. The possibility of irregular drop time is eliminated and this should lead to more reproducible results.

As far as anodes are concerned, it was thought that a Mo wire electrode should be a good reference electrode, judging from its performance in potentiometric

J. Electroanal. Chem., 9 (1965) 169-171

intrusions⁴. This electrode should be useful in non-aqueous studies, since it eliminates the bridge required for the saturated calomel electrode and also reduces the i - R drop in non-aqueous solutions. The results obtained using this electrode will be described in a later communication.

Direct and derivative cathode ray polarograms were taken on a K 1000 cathode ray polarograph manufactured by Southern Instruments Ltd., U.K. The temperature was maintained at $30 \pm 0.1^\circ$ by an electronically operated thermostat. The electrode system was also tested on a direct current semi-manual Du-Bellay polarograph.

The stationary Hg cathode was made by bending Pyrex glass tubing (0.5 cm internal diam.) into a J form, the lengths of the two arms being 7.5 and 1 cm. A cup was formed at the top of the short arm and sealed from the rest of the tube. A short Pt wire was fused into the glass so that a small portion of it was exposed in the cup as well as in the tube. Electrical contact was made by filling the tube with Hg. For comparison, polarograms were also recorded with a micro Pt cathode. A long Pt wire was tested for its anode performance. Pt and Mo wires (26 and 22 S.W.G., respectively) were fused into a Pyrex tube 0.5 cm in diameter. The lengths of the wires outside the tube were kept at 3.0 cm and a short wire in each tube made electrical contact. A commercial micro Pt electrode was used as cathode. The polarographic cell for the stationary Hg pool cathode and Mo wire consisted of a 50-ml Pyrex beaker, closed by a rubber bung, bored to take the cathode (Hg pool or micro Pt), anode (long Pt or Mo electrode) or for inserting a Pt electrode when the Hg at the bottom of the beaker forms the anode, a glass tube for passing nitrogen, and a hole for the exit of nitrogen.

TABLE 1

COMPARISON OF DIFFUSION CURRENT USING VARIOUS ELECTRODE SYSTEMS

No.	Cathode	Anode	Type of polarogram	E (peak) (V)	Current (μA)	Remarks
1	D.M.E.	S.C.E.	d.c.	-0.60	0.50	Without gelatin
2	D.M.E.	S.C.E.	d.c.	-0.60	0.48	With gelatin
3	D.M.E.	S.C.E.	d.c.	-0.60	0.48	With gelatin
4	Hg pool (J)	Large Hg pool	d.c.	-0.70	4.00	Peak obtained
5	D.M.E.	Large Hg pool	C.R. direct	-0.70	2.40	
6	D.M.E.	Large Hg pool	C.R. derivative	-0.70	0.023	
7	Hg pool (J)	Large Hg pool	C.R. direct	-0.78	20.40	Broad peak
8	Hg pool (J)	Large Hg pool	C.R. derivative	-0.70	0.32	
9	Micro Pt	Large Hg pool	C.R. direct	-0.77	0.50	S-shaped wave
10	Micro Pt	Large Hg pool	C.R. derivative	-0.75	0.0070	
11	Hg pool (J)	Long Pt	C.R. direct	-0.76	0.90	
12	Hg pool (J)	Long Pt	C.R. derivative		No wave	
13	Micro Pt	Long Pt	C.R. direct		No wave	
14	Micro Pt	Long Pt	C.R. derivative		No wave	
15	Hg pool (J)	Long Mo	C.R. direct	-0.70	20.50	Broad peak
16	Hg pool (J)	Long Mo	C.R. derivative	-0.62	0.34	
17	Micro Pt	Long Mo	C.R. direct		No wave	
18	Micro Pt	Long Mo	C.R. derivative		No wave	

Final solution contained 10 $\mu g/ml$ of Cd in 0.5 M NaCl.
Gelatin was not added to the solution from No. 3 onwards.

Comparison of diffusion or peak currents obtained by various combinations of anode and cathode are given in Table 1; the solution contained 10 μg of Cd/ml in 0.5 M sodium chloride solution (total concentration).

There is a five-fold increase in the diffusion current with D.M.E. on a cathode ray polarograph compared with a d.c. polarograph. The increase is maintained when the D.M.E. is replaced by a Hg pool cathode. However, the absolute value of current is ten times greater in the case of the Hg pool cathode for both polarographs. The Hg pool cathode is not suitable on the d.c. polarograph unless it is a recording polarograph, as the rate of change of potential does not remain constant. The results show that the micro Pt cathode or long Pt wire electrodes are unsuitable, as the currents obtained are very small.

The Mo wire electrode, however, is as good as a saturated calomel electrode or an Hg pool anode. The performance of the Hg pool cathode on the cathode ray polarograph is much more satisfactory than the conventional D.M.E. Linearity of current with concentration is excellent up to 0.1 $\mu\text{g}/\text{ml}$ of cadmium, and is also obtained much below this concentration but this will be dealt with after considering parameters such as the effect of area of the electrode, rate of change of sweep voltage, the nature of the electrode reaction, etc., on the diffusion current and peak potential in aqueous as well as mixed and non-aqueous solvents. Investigations are also being carried out on the reproducibility of the surface area of the Hg pool, different types of cells containing the Hg pool cathode and Mo anode and analytical applications of this electrode system. A variety of applications based on the use of this electrode system is expected.

*Analytical Division,
Atomic Energy Establishment Trombay,
Bombay-28 (India)*

V. T. ATHAVALE
S. V. BURANGEY
R. G. DHANESHWAR

- 1 J. E. B. RANGLES, *Trans. Faraday Soc.*, 44 (1948) 333.
- 2 W. W. ULLMANN, B. H. PFEIL, J. D. PORTER AND W. W. SANDERSON, *Anal. Chem.*, 34 (1962) 213.
- 3 C. A. STREULI AND W. D. COOK, *Anal. Chem.*, 25 (1953) 1691; 26 (1954) 963.
- 4 V. P. APTE, R. G. DHANESHWAR AND M. S. VARDE, in preparation.

Received October 12th, 1964

Announcement

16th MEETING OF THE 'COMITÉ INTERNATIONAL DE THERMODYNAMIQUE ET DE CINÉTIQUE ELECTROCHIMIQUES', BUDAPEST (HUNGARY), SEPTEMBER, 1965

The 16th Meeting of CITCE will be held in Budapest (Hungary), September 5-10, 1965. The Meeting will be restricted to the theme *The structure of and transport processes in electrolytes and electrolyte solutions*. In addition, there will be two general discussions on topics associated with the general theme; the first, *The behaviour of electrolyte junctions* and the second, *Ionic solvation*.

Correspondence regarding attendance or presentation of papers should be addressed to Professor S. LENGYEL, ELTE Fizikai-Kémiai és Radiológiai Tanszek, Pushkin u. 11-13, Budapest VIII (Hungary), or to Dr. M. FLEISCHMANN, Secretary General of CITCE, Department of Physical Chemistry, University of Newcastle upon Tyne, Newcastle upon Tyne 1 (England).

Extended abstracts of papers (750 words maximum) should be received before April 1, 1965. Application forms will be available from January 1964.

There will also be a Colloquium held jointly by CITCE Commission 5 and Cebelcor in Brussels in June 1965. The subject will be *Electrochemical methods of studying corrosion: Practical applications*. This will be organized by Professor M. POURBAIX enquiries to whom should be addressed to the University of Brussels, 50 Avenue F. D. Roosevelt, Brussels (Belgium).

J. Electroanal. Chem., 9 (1965) 172

Correction

A recent paper on the voltammetric determination of carbon monoxide by JULIAN L. ROBERTS, JR. and DONALD T. SAWYER, published in this Journal [7 (1964) 315-319] included the statement "... the direct electroanalytical determination of this gas has not been reported previously." The authors and the editors inadvertently overlooked a paper published in 1961 by Dr. P. J. OVENDEN [2 (1961) 80-87] entitled *The Electrolytic Determination of Carbon Monoxide*. This earlier work clearly indicated the potential and possibility for the electroanalytical determination of dissolved carbon monoxide and presented data for its determination in phosphate and borate solutions with a vibrating palladium electrode. Drs. ROBERTS AND SAWYER and the editors regret the oversight.

J. Electroanal. Chem., 9 (1965) 172

24ms 10 .

CONTENTS

The mechanism of step propagation and pyramid formation on the (100) plane of copper from <i>in situ</i> Nomarski-optical studies A. DAMJANOVIC, M. PAUNOVIC AND J. O'M. BOCKRIS (Philadelphia, Pa., U.S.A.)	93
Trace analysis by anodic stripping voltammetry. IV. The determination of copper in steels S. GOTTESFELD AND M. ARIEL (Haifa, Israel)	112
Capillary response at a dropping mercury electrode R. DE LEVIE (Baton Rouge, La., U.S.A.)	117
A study of the anomalous behaviour of the glass electrode in solutions containing hydrofluoric acid E. SØRENSEN AND T. LUNDGAARD (Risø, Denmark)	128
Polarographic reduction of nitrate ions in the presence of zirconium salts H. W. WHARTON (Cincinnati, Ohio, U.S.A.)	134
Polarographic behaviour of chromium aromatic compounds: cyclopentadienyl-cycloheptatrienylchromium(0) and (1+) C. FURLANI, A. FURLANI AND L. SESTILI (Trieste and Rome, Italy)	140
The electrical double layer on thallium amalgam electrodes J. N. BUTLER (Waltham, Mass., U.S.A.)	149
<i>Short Communications</i>	
Thin-layer chronopotentiometric determination of reactants adsorbed on platinum electrodes A. T. HUBBARD AND F. C. ANSON (Pasadena, Calif., U.S.A.)	163
Formation of thick oxides on platinum electrodes R. L. EVERY AND R. L. GRIMSLEY (Ponca City, Okla., U.S.A.)	165
A contribution to the theory of the change of electrode reaction rate by adsorption of an electro-inactive substance J. KORYTA AND K. HOLUB (Prague, Czechoslovakia)	167
Voltammetric studies using various electrode systems V. T. ATHAVALE, S. V. BURANGEY AND R. G. DHANESHWAR (Bombay, India)	169
<i>Announcement</i>	172
<i>Correction</i>	172

RODD'S CHEMISTRY OF CARBON COMPOUNDS

Second Edition

edited by S. COFFEY, M.Sc. (London), D.Sc. (Leyden). Formerly of I.C.I. Dyestuffs Division, Blackley, Manchester. Assisted by an Advisory Board of prominent scientists.

This completely revised edition of this standard work has been undertaken to take into account the important advances in theoretical and experimental organic chemistry recorded since the appearance of the first edition.

The treatment has remained largely unchanged although the sheer extent of new material has made it necessary to create further subdivision in order to reduce publication delay.

VOLUME IA - GENERAL INTRODUCTION, HYDROCARBONS, HALOGEN DERIVATIVES

General Introduction

1. The saturated or paraffin hydrocarbons. Alkanes. 2. Unsaturated acyclic hydrocarbons. 3. Halogen derivatives of the aliphatic hydrocarbons.

6 × 9" xx + 569 pages, 1964, subscription price £7.0.0.

non-subscription price £8.0.0.

VOLUME IB - MONOHYDRIC ALCOHOLS, THEIR ETHERS AND ESTERS, SULPHUR ANALOGUES; NITROGEN DERIVATIVES; ORGANOMETALLIC COMPOUNDS

4. Monohydric alcohols, their ethers and esters. 5. Sulphur analogues of the alcohols and their derivatives. 6. Nitrogen derivatives of the aliphatic hydrocarbons. 7. Aliphatic organometallic and organometalloidal compounds.

6 × 9" xvi + 313 pages, 16 tables, 1964, subscription price £4.8.0.

non-subscription price £5.0.0.

VOLUME IC - MONOCARBONYL DERIVATIVES OF ALIPHATIC HYDROCARBONS; THEIR ANALOGUES AND DERIVATIVES

8. Aldehydes and ketones. 9. Monobasic carboxylic acids. 10. Carbon monoxide, isocyanides and fulminic acid. 11. Carbonic acid and its derivatives.

6 × 9" xvi + 432 pages, 17 tables, April 1965, subscription price £6.0.0.

non-subscription price £7.10.0.

VOLUME ID - DIHYDRIC ALCOHOLS, THEIR OXIDATION PRODUCTS AND DERIVATIVES

12. Dihydric alcohols or glycols and their derivatives. 13. Hydroxyaldehydes and ketones and related compounds; dicarbonyl compounds. 14. Aliphatic hydroxycarboxylic acids and related compounds. 15. Nitro- and amino-acids and their derivatives. 16. Aldehydic and ketonic carboxylic acids and related compounds. 17. Dicarboxylic acids.

VOLUME IE - TRI- AND TETRA-HYDRIC ALCOHOLS, THEIR OXIDATION PRODUCTS AND DERIVATIVES

18. Trihydric alcohols and carbonyl compounds derived from them. 19. Phospholipids and glycolipids. 20. Dihydroxycarboxylic and tricarboxylic acids and their derivatives. 21. Tetrahydric alcohols and their oxidation products.

VOLUME IF - PENTA-, HEXA- AND HIGHER POLYHYDRIC ALCOHOLS, THEIR OXIDATION PRODUCTS AND DERIVATIVES; SACCHARIDES

22. Penta-, hexa- and higher polyhydric alcohols. 23. Monosaccharides. 24. Oligosaccharides and polysaccharides.

VOLUME IG - ENZYMES; MACROMOLECULES; CUMULATIVE INDEX TO VOLUME I A-G

25. Enzymes. 26. Synthetic macromolecules. 27. Rubber.

To follow

Volume II Alicyclic Compounds; Volume III Aromatic Compounds; Volume IV Heterocyclic Compounds; Volume V Miscellaneous; General Index

Multi-volume works such as Rodd's Chemistry of Carbon Compounds represent a considerable outlay for the purchaser. In order to alleviate this to a certain extent, the publishers offer a discount of 15% on the publication price. Subscribers to the complete series will thus be able to acquire the work for only 26s. (approx.) per 100 pages.



ELSEVIER PUBLISHING COMPANY

AMSTERDAM

LONDON

NEW YORK